## Science and Mathematics: Theory, Methodology and Practice

Editor Prof. Hüsniye Sağlıker, Ph.D.

# Science and Mathematics: Theory, Methodology and Practice

### Editor Prof. Hüsniye Sağlıker, Ph.D.

### **Publisher**

Platanus Publishing®

### **Editor in Chief**

Prof. Hüsniye Sağlıker, Ph.D.

### **Cover & Interior Design**

Platanus Publishing®

### The First Edition

October, 2025

### **ISBN**

978-625-6517-52-3

### **©copyright**

All rights reserved. No part of this publication may be reproduced or transmitted in any form or by any means, electronic or mechanical, including photocopy, or any information storage or retrieval system, without permission from the publisher.

### Platanus Publishing®

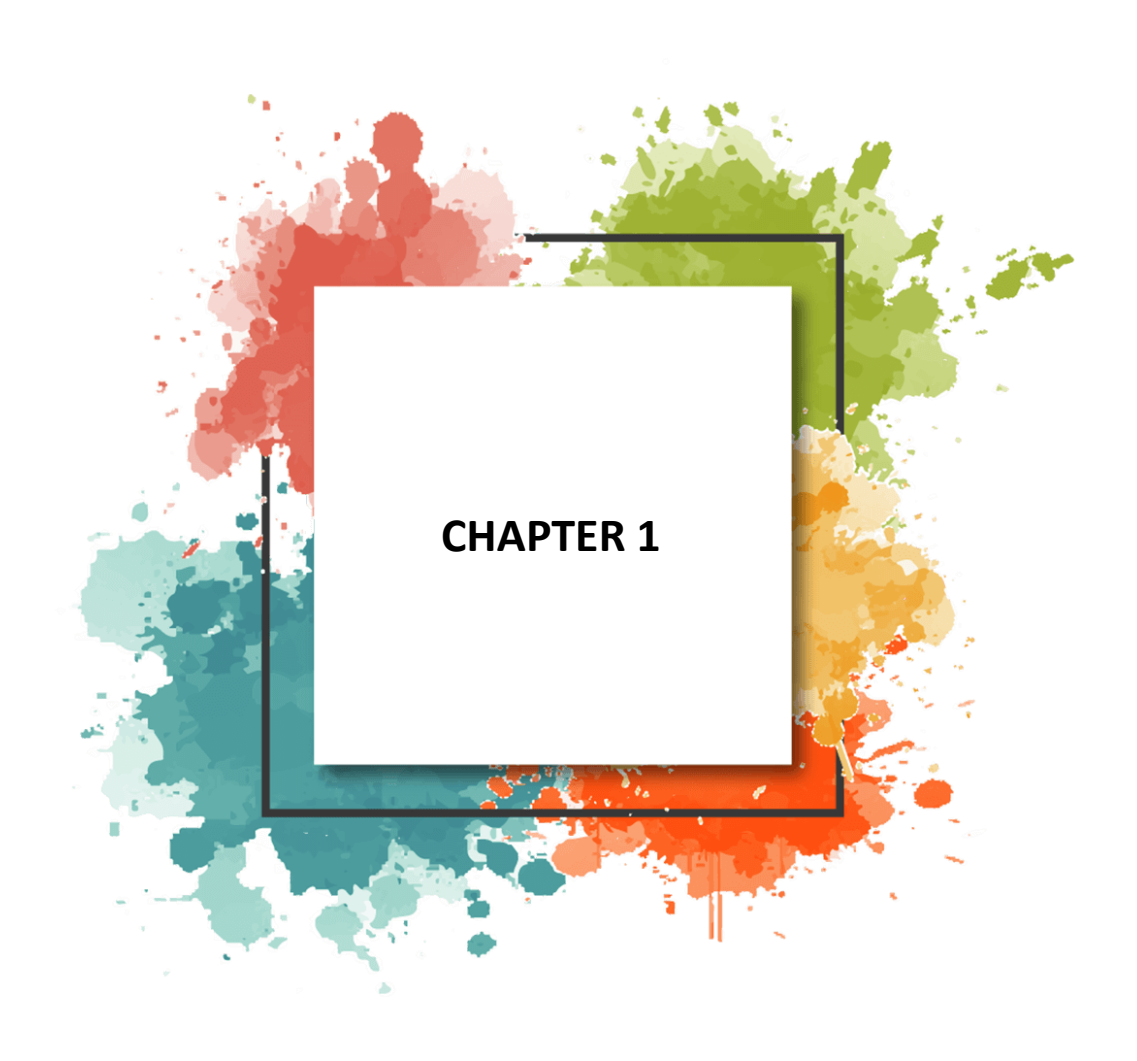
**Address:** Natoyolu Cad. Fahri Korutürk Mah. 157/B, 06480, Mamak, Ankara, Turkey.

**Phone:** +90 312 390 1 118 **web:** www.platanuspublishing.com **e-mail:** platanuskitap@gmail.com



### **CONTENTS**

CHAPTER 1 5
Explanation of Teacher Candidates' Thoughts on the World's Human Population Through Drawing  Nurcan Özkan
CHAPTER 2 39
Integrated Water Resources Management (IWRM) Approaches and Applications  Ertan Karahanlı & Cengiz Mutlu
CHAPTER 3 51
Interactions Between Biochar Applications and Soil Urease Activity: A  Synthesis of Current Knowledge  Aysu Koç & Gizem Yaman & Burak Koçak
CHAPTER 4 65
Inference for Weibull Expected Shortfall From Record Data Çağatay Çetinkaya
CHAPTER 5 77
The Role of Dampening Solution in Offset Printing Technology: Its Effects On Print Quality and Productivity Aslı Boztemir Tiftik
Bölüm 6 97
On Pseudo-Slant Submanifolds of Kähler-Norden Manifolds Süleyman Dirik & Ramazan Sarı



# **Explanation of Teacher Candidates' Thoughts on the World's Human Population Through Drawing**

Nurcan Özkan<sup>1</sup>

#### 1. INTRODUCTION

The world's human population refers to the number of people living on Earth. According to the statement made by the United Nations in November 2022, the world population has exceeded 8 billion. It took more than 200.000 years after the emergence of modern humanity for the world's human population to reach 1 billion, and only 219 years for it to reach 8 billion (Kight and Lysik, 2022; URL 1). In the last 70 years of the 20th century, the world population showed its fastest growth in history.

One of the common characteristics of all living things is their ability to reproduce. However, the growth of non-human populations is controlled by ecosystems. Thanks to her/his intelligence and technology, humans have managed to stay out of such control. Although humans are one of the least reproductive living creatures, world population growth is one of the important problems of our day (Çamurcu, 2005).

While the population growth rate increases by around 0.5-1% in developed countries, it increases at high rates such as 2-3% in developing countries. This development causes significant changes and problems in the demographic structure of the world. A small portion of the world's population lives in developed countries, while the majority lives in developing countries. Rapid population growth causes insufficient resources in developing countries, slowing down development rates and increasing economic and social problems. Developed countries, on the other hand, are concerned that this increase may disrupt the socio-economic balance and stability of the world (Çamurcu, 2005).

The rate of food production increases in parallel with the rate of human population growth. Due to the rapidly increasing food production, there is an increase in the amount of agricultural waste, which also causes the consumption and pollution of limited natural resources. In this context, high waste amounts, especially of stakeholders who do not adopt sustainable food production policies, cause serious damage to economic costs, environment and food safety issues (Özkan et al., 2022).

-

<sup>&</sup>lt;sup>1</sup> Prof. Dr., Trakya University, Education Faculty, Mathematics and Science Education Department, ORCID: 0000-0001-5045-6186

Although interest in the link between population and environmental effects has a long history, this link was first comprehensively examined as a subject of scientific research with Thomas Malthus's work (Essay on the principle of population) published in 1798 (Carr et al., 2005; de Sherbinin et al., 2007). In his work, Malthus (1998 [1798]) states that while food production increases arithmetically, population tends to increase geometrically. Therefore, he argued that food production could not keep pace with the increase in population and that further increase would result in natural checks such as starvation. More recently, the neo-Malthusian view that improving people's living standards is not possible without limiting population growth is also based on the assumption of a fixed resource base and hence ultimately a "carrying capacity" (Pimentel et al., 1998). Thus, Malthus's claim that uncontrolled population growth would lead to food insufficiency was expanded over time and turned into a dynamic discussion about the world's population carrying capacity, the deteriorating quality of the earth's surface, and environmental problems. In this context, the debate was revived by new studies in the 1960s, when the annual growth rate of the world population reached 2% and the time it took to add a new billion people to the existing population fell below 15 years (Ehrlich and Ehrlich, 1990; Ehrlich et al., 1993; Meadows et al., 1972). Perhaps the most important of these studies was the study by Meadows et al. (1972) titled "The Limits to Growth", which simulated the end of the 21st century with five parameters including population, agricultural production, natural resources, industrial production and pollution. As Bartlett (1994) stated, the findings of this research were important in terms of suggesting the sustainability of life by pointing to the "collapse of the world population in the mid-21st century."

Population dynamics affect consumption and the availability of natural resources and, together with consumption levels and productivity, determine environmental sustainability. Although in some cases human numbers have a direct impact on the environment, the relationship between population and environment is not easily understood (United Nations Population Fund-UNFPA, 2013). Population is a multidimensional concept related to the size, growth, distribution, density and characteristics of the number of people living in an area. The environment is at least as complex as the population; it includes the qualities of air, water and soil on which humans and other species depend (Hunter, 2000). In addition to these, there are also intermediary factors including scientific, technological, political, institutional and cultural contexts that complicate and ultimately shape the relationship between the population and the environment (Özgür, 2017).

Today, more than three billion people are undernourished, and most of our planet's 7 billion people consume poor-quality diets. At the same time, the world's

population is growing rapidly. It is estimated that there will be around 10 billion people on our planet by 2050. When considering sustainable food development, the goal is to ensure that this large population has both enough food to eat and access to high-quality, nutritious foods in the future (Hidalgo et al., 2022; Parsons and Hawles, 2018; Saygı, 2024).

It is known that population growth has been very slow throughout a long period of human history (Peters and Larkin, 2005). However, advances in public health and hygiene, which emerged thanks to the scientific-technological-economic revolution, began to change the course of the world population by leading to a decrease in mortality from the mid-18th century onwards and led to an increase in the population growth rate (Newbold, 2014). In this way, the world population has tended to grow dramatically over the last three centuries (Özgür, 2017).

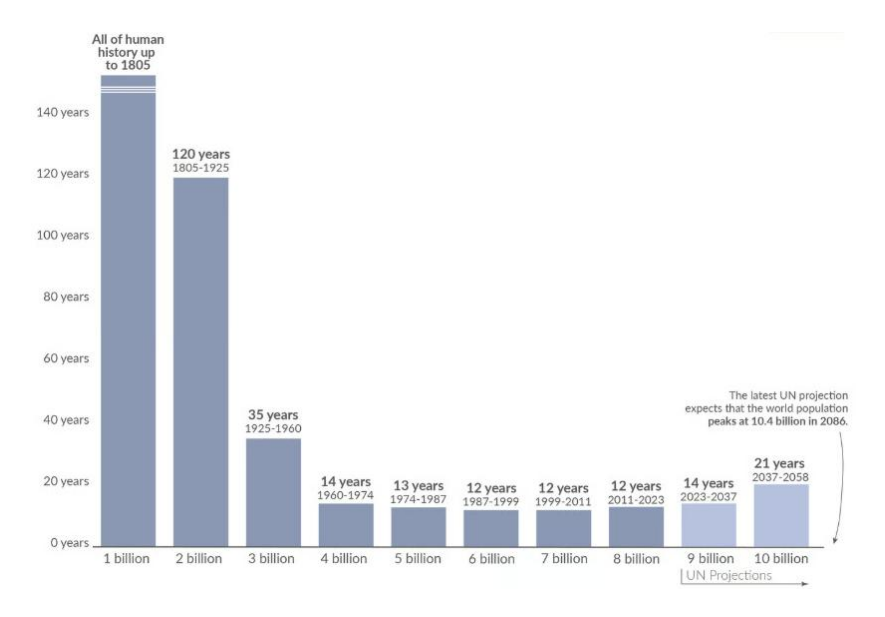
The fastest doubling of the world's population occurred between 1950 and 1987: from 2.5 billion to 5 billion in just 37 years-the population doubled in just over a generation. This period was marked by peak population growth of 2.1% in 1962.

Since then, population growth has been slowing down and the doubling time has been increasing accordingly. This visualization uses UN projections to show how the doubling time is predicted to change by the end of this century. By the 2080s, it will take approximately another 100 years for the population to double to the estimated 10.4 billion (Roser and Ritchie, 2023).

The world has now surpassed this peak growth rate and is expected to continue increasing between each billionth period. It is estimated that it will take approximately 14 years to reach nine billion in 2037 and 21 years to reach 10 billion in 2058.

According to the UN's latest medium-term forecast, the world population will not reach 11 billion this century. The population is projected to peak at 10.4 billion in 2086, then decline again (Table 1).

Table 1. The duration of each billion increase in the world's population from past to



Source: Time for the World population to increase by one billion (Roser and <u>Ritchie</u>, 2023)

Population distribution indicates the spatial distribution and concentration pattern of the population, and changes in this distribution are based on natural increase and migration. Over the past 50 years or so, two trends have significantly influenced the distribution of populations worldwide. The first of these is the global fertility pattern that emerges from the combination of high and medium fertility in underdeveloped and developing countries and low fertility in developed countries. This trend has altered natural population growth, causing the share of the population living in low- and middle-income countries in the global population to increase. UN estimates show that 83% of the world's population lived in developing and least developed countries in 2015, and this proportion is expected to reach 87% by mid-century (Table 2).

Table 2. Population and percentage distribution of the world and regions by year

	Population (millions)				%			
Years	1950	2015	2030	2050	1950	2015	2030	2050
World	2519	7350	8500	9725	100,0	100,0	100,0	100,0
Developed Regions	814	1252	1284	1286	32,3	17,0	15,1	13,2
Underdeveloped Regions	1508	5144	5891	6542	59,9	70,0	69,3	67,3
Least Developed Regions	197	954	1325	1897	8,8	13,0	15,6	19,5
Africa	221	1186	1679	2477	8,8	16,1	19,8	25,5
Asia	1399	4393	4923	5267	55,5	59,8	57,9	54,2
Europe	548	739	734	707	21,8	10,1	8,6	7,3
North America	172	358	396	433	6,8	4,9	4,7	4,5
Latin America and the Caribbean	167	635	721	784	6,6	8,6	8,5	8,1
Oceania	13	39	47	57	0,5	0,5	0,6	0,6

Source: United Nations, 2001 and 2015

It is predicted that the population density, which was 23 people per square kilometer at the beginning of the 21st century in developed and rich countries, will not change until the middle of the century; whereas the population density, which was 59 people per square kilometer in underdeveloped and poor countries, will increase to 93 (Cohen, 2003). It is highly likely that this increase in density will create unprecedented problems in land use and conservation in underdeveloped countries, increase human impacts on the natural environment, especially in Africa, and create migration pressure from this region to Europe (Cohen, 2003; Özgür, 2017).

This study was conducted with senior prospective teachers studying at the Department of Science Education at Trakya University Faculty of Education. Teacher candidates were asked to express and explain their thoughts on the world's human population, which has decreased compared to previous years but is still increasing, through drawings, and their thoughts were examined.

### 2. MATERIAL AND METHODS

This research was conducted as a phenomenological design (Yıldırım and Şimşek, 2006) study. In the research, students' drawings explaining their thoughts on the human population theme in our world and their explanations about their drawings were used as data collection tools. While using student drawings is a powerful tool, it is not sufficient on its own. Therefore, explanations of the drawings are needed (Ersoy and Türkkan, 2009).

Data were collected from 27 senior students at Trakya University, Department of Science Education, taking the environmental education course in the fall semester of the 2024-2025 academic year. In the course with the teacher candidates, the human population in the world and its ecological effects were evaluated mutually. They were then asked to express and explain their thoughts on this subject through drawings. Then, each prospective teacher was given a code between 1-27 and their pictures and explanations were arranged according

to these codes. Among these codes, teacher candidates with codes 3, 15, 16 and 19 are male, and the others are female. They were asked to draw on an A4 size paper so that they could express themselves. A free study was done in terms of crayon type. Prospective teachers were asked to draw their thoughts on world population in the classroom and to explain their drawings with open-ended semi-structured questions. This allows the researcher to more easily handle the drawings. The data were then analyzed using content analysis techniques (Cohen and Manion, 1994).

### 3. RESULTS AND DISCUSSION

In this section, the drawings of 27 science teacher candidates reflecting their thoughts on the human population of our world and their statements explaining their drawings are included.

The teacher candidate coded 1 expressed her views that resources would be insufficient if the world population increased at this rate (Figure 1): "In the picture, the rapid increase in the world population will cause people to no longer have a place to live and shelter, and people will now establish living space stations separate from Earth and enter into competition and struggle to survive there. Experts are conducting research and searching for habitats and other planets because, as the world's population grows, there is a quest for hope of rediscovering the vanished nature."

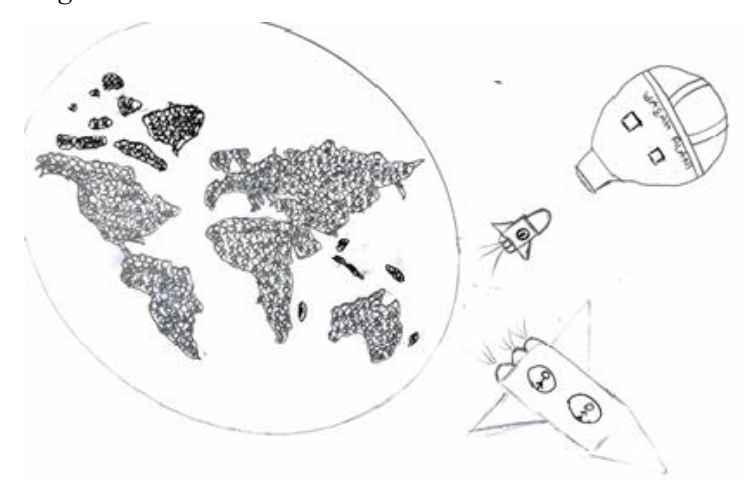


Figure 1. With the increase in the human population, efforts are being made to find new living spaces.

The teacher candidate coded 2 expresses the difficulties that will be caused by the acceleration of population growth (Figure 2). "What is meant to be explained in the picture is that population growth has accelerated from past to present and the average lifespan of the person has also increased. Today, the average growth

rate of the world's population is 1.7%. If it continues to increase at this rate, life in cities will become uninhabitable and there will be no clean water to drink. As consumption increases so much, the world's resources will not be sufficient."



Figure 2. Resource deficiencies due to the increase in the world's human population

The teacher candidate with code 3 examines the old and new situation of the population. (Figure 3). "What I want to convey in the picture is that in times when the human population was small, the resource and settlement problems were much less than today. For this reason, human damage to the environment was less. Our environmental impact wasn't significant, but as the human population grew, our resource and settlement needs increased. Humanity's environmental impact has increased. We've begun to inflict excessive damage. We've opened production facilities for resources. Urbanization has begun, and the balance has begun to shift."



Figure 3. The status of resources and the environment in the past and present, depending on the human population

The candidate with code 4 drew the world by comparing it to a seesaw (Figure 4). "The world on a seesaw is thrown off balance by the weight of so many people on the other side. It shows how population growth affects the world. In short, it explains how resources are struggling to support so many people as the world's population grows."

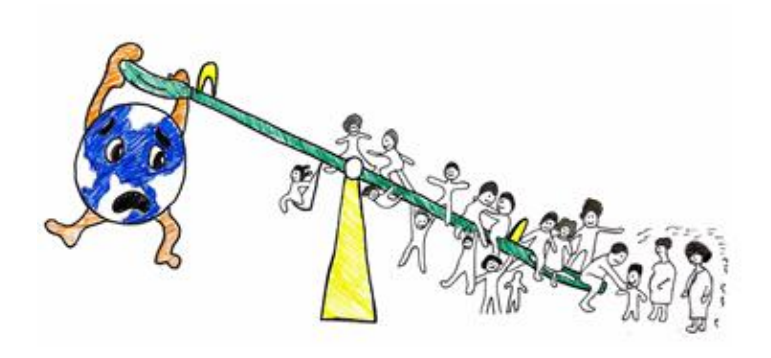


Figure 4. The destabilization of the world by human population

The teacher candidate with code 5 also compared the world to a scale with equal arms and discussed the ratio and distribution of the human population (Figure 5). "In the example given in the picture, the number of births and migrations is higher. On the other hand, the elderly population is smaller. Therefore, population growth in this region will be very high. Since the number

of young people, babies and migrants is higher in the arms of the scale, the scales are weighted in that direction. It symbolizes the dense population in cities and the crowding that comes with it."

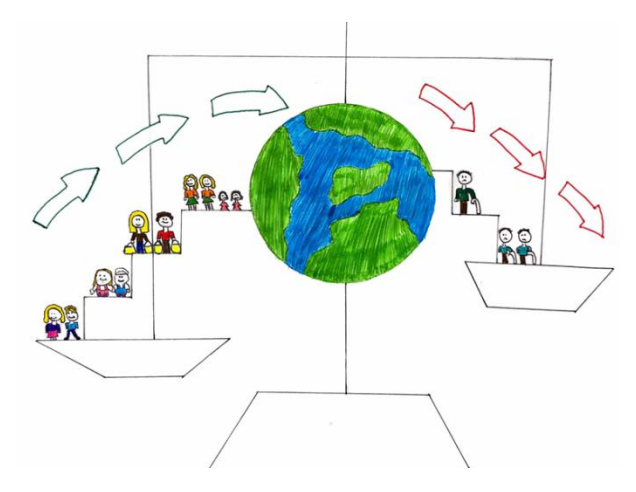


Figure 5. Distribution of human population in the world

The teacher candidate with code 6 expressed the increase in the world population from past to present graphically (Figure 6). "We see in this graph that the world population has exploded since 1830. While it increased by 1 billion in 100 years between 1830 and 1930, in the following period it increased by 1 billion in just 15 years. Population growth and increasing nutritional and development needs have put significant pressure on natural resources. As a result, environmental problems are increasing. One of these is air pollution. Increasing industrial activities along with the rapidly growing population cause increased air pollution. Another pollutant is the exhaust gases of motor vehicles. In Graph 2, the improvement in air quality in Wuhan, China, was observed as human activities decreased during the pandemic. In other words, a direct relationship can be established between population and environmental problems."

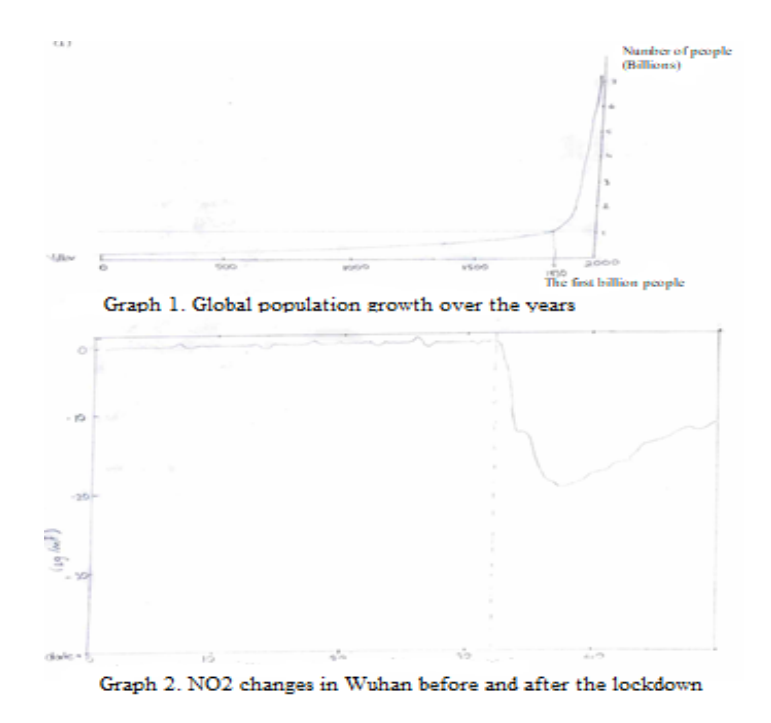


Figure 6. The world population growth from past to present and its relationship with the environment

The teacher candidate with code 7 explains the world population with the age pyramids of women and men (Figure 7). "The number of people living in certain areas may change over the years. Its number increases over the years. The number of people living in a defined area at a given time is called population. This visual shows the distribution of the population by age groups. There is a decrease in mortality rates and high fertility continues. That's why we see that more people are being transferred from the child age groups to the young, mature and elderly age groups, and the concave triangular pyramid is slowly turning into a regular triangular pyramid. More people have joined the upper age groups, meaning life expectancy has increased. The population growth rate is very high. This is due to the decreasing mortality rate."

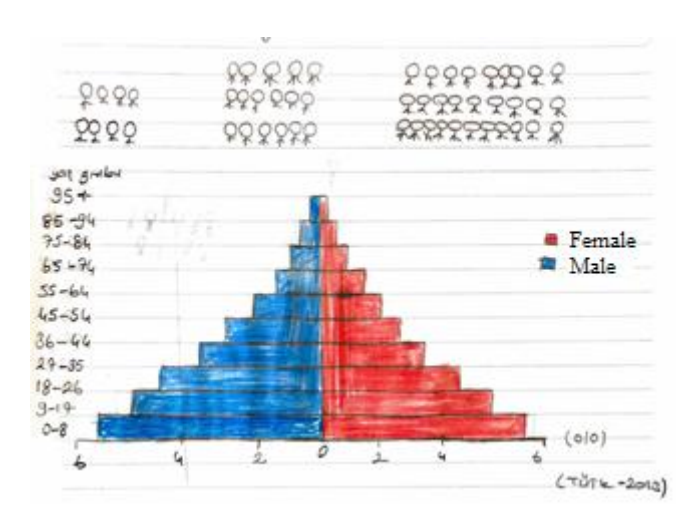


Figure 7. Explaining the world's male and female population with age pyramids

The teacher candidate with code 8 again tried to explain the increase in the world population with a graph (Figure 8). "The image I drew emphasizes that the world population is increasing rapidly and will continue to increase in the future. This increase draws attention to global issues such as resource use, environmental impacts and sustainability. It points out that the changes experienced with population growth will have economic, social and environmental impacts."

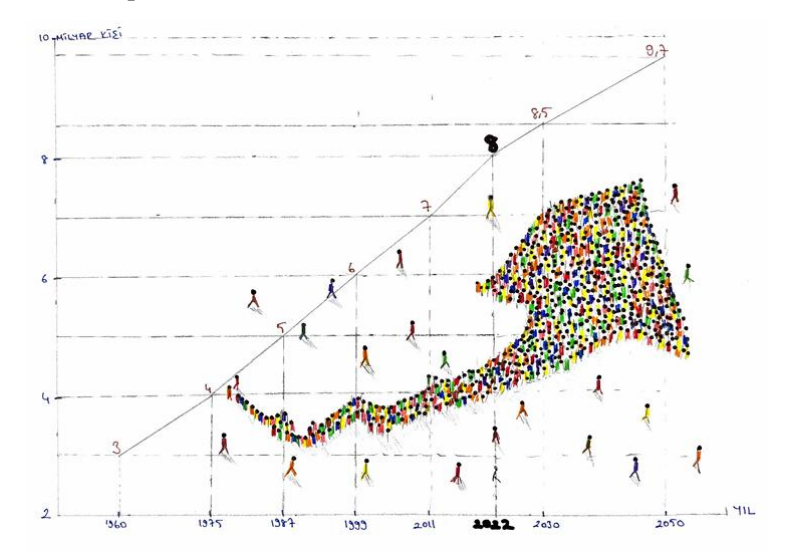


Figure 8. World population growth and its problems

The teacher candidate with code 9 states that the increase in the number of people will lead to environmental pollution and living things will be affected by

this situation (Figure 9). "In this picture, I drew what comes to my mind when I think of the human population. The human population has been increasing rapidly, especially in recent years. That's why I drew a lot of people to express the crowd in the picture. People mean shelter. The more people there are, the more houses, buildings, and workplaces there will be. In the picture, I drew shapes to represent houses, workplaces, and skyscrapers. Every person is a consumer. As the number of consumers increases around the world, so do their needs. More food to eat in the world means fewer plants and animals. Water is a basic human need. As the human population grows, water resources will gradually deplete. Excessive hunting of animals in nature and excessive consumption of plants in nature will also destroy nature. That's why I didn't include nature in my painting. Also, increasing human population means increasing pollution. Factory fumes, plastic waste, power plants, garbage disposal, waste mixing with water, and the use of pesticides are just a few of the causes of pollution. So in the picture I colored the air in gray to represent the polluted air."



Figure 9. World population growth and its negative effects

In her drawing, the teacher candidate with code 10 explains that population growth has made the world tired and sad (Figure 10). "The painting depicts the human population growing rapidly. The face of the Earth has a tired and sad expression due to the number of people it carries. This is because the rapidly

growing population consumes resources and causes environmental problems. Increasing human needs, neglecting the use of natural resources and excessive consumption, increasing the likelihood of resource depletion, environmental pollution and decreasing living standards are all contributing factors."

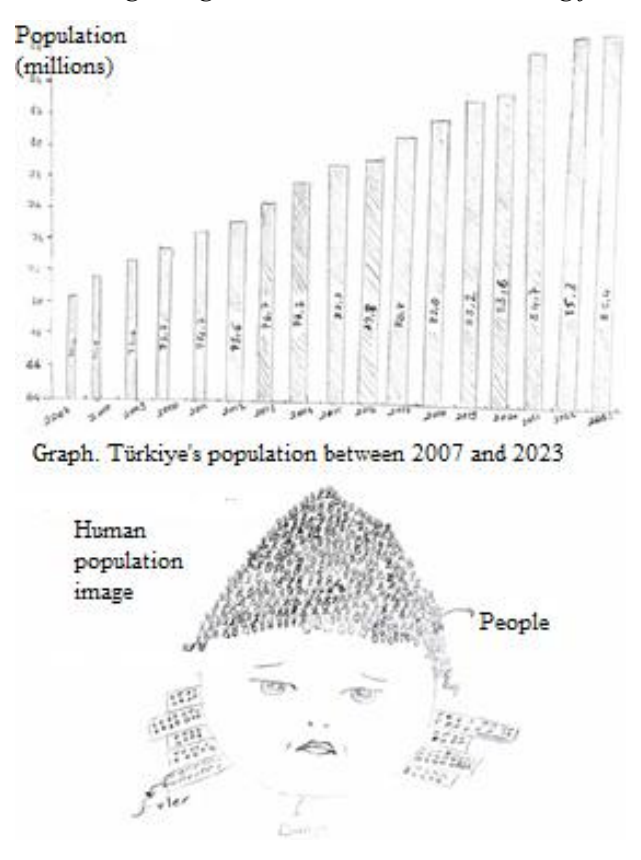


Figure 10. Dünya nüfusunun artışının yarattığı yorgunluk

In her drawing, the teacher candidate with code 11 expresses the pressure and difficulties on limited world resources (Figure 11). "The picture I drew symbolizes the increase in human population. The human community I have drawn reflects the pressure on limited resources and the challenges of population growth. It also points out that due to the increasing population, resources may be depleted further and environmental problems may increase. With this visual, I wanted to explain the excessive growth of the human population and the burden it brings. The rapid increase in the human population confronts us with the fact that resources on earth are limited. This situation may make it difficult to meet basic needs in the future. The people chained to the bowl in the picture I drew depicts the dependence and limits of the human population on nature and resources. The overflow of people also reflects the challenge of uncontrolled

population growth. It also increases the risk of competition and conflict between people as the population grows uncontrollably. Consequently, this increase can increase the likelihood of more conflict and harm between people, leading to higher crime rates."



Figure 11. Competition and conflict caused by world population

The teacher candidate with code 12 explains the human population and the needs of life with equal-arm scales (Figure 12). "What I want to convey in the picture is that our population is not balanced with our needs, and as the population increases, it becomes more difficult to meet our needs. There is an imbalance between the population and our needs. As a result, many people are left without access to their basic needs."

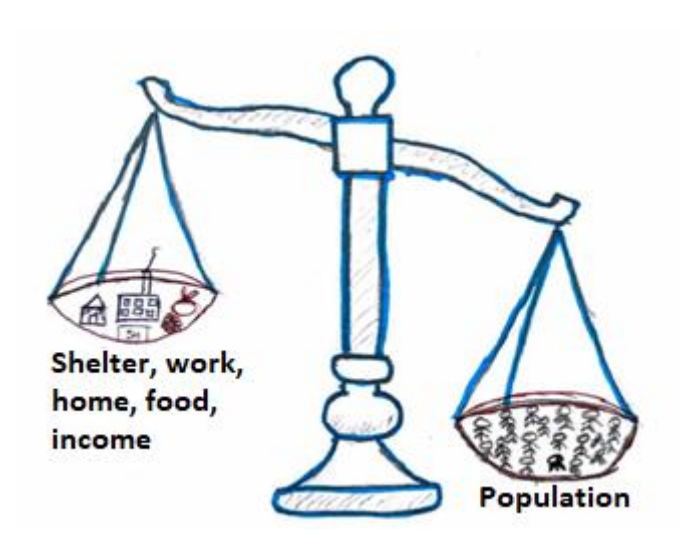


Figure 12. Imbalance between population and needs

Teacher candidate coded 13 tried to put forward the problems that await us in the future due to population growth (Figure 13). "In my drawing, I wanted to express the depletion of resources with the increase in population, the accumulation of garbage, the proliferation of buildings, and the almost extinction of clean air due to the establishment of factories. Such an unbalanced, unconscious and rapid increase in the population will bring about major problems in the future. In this painting, I thought about what kind of problems we might encounter in the future if population growth is not prevented as much as possible, researched it and put it on paper."



Figure 13. Problems that may arise from population growth

In her drawing, candidate coded 14 shows the effects of people's perspectives on the environment (Figure 14). "I wanted to explain that population growth alone does not worsen the environment, but that what really matters is people's approach to the environment. So, even if a large number of people live together, if people fail to protect the environment, use resources irresponsibly and do not manage their waste properly, the living space will quickly become polluted and disorderly. In the long run, this results in a decrease in the quality of life, depletion of natural resources and the creation of an unhealthy environment. However, even if the population is dense, life can be sustained in a clean, orderly and healthy environment if people take care to protect the environment and use resources such as energy and water properly. It is necessary to act sensitively towards the environment and manage population density consciously. The growing population increases the demand for resources. However, I wanted to emphasize that individual and societal responsibilities must be taken to prevent this demand from harming the environment. In other words, what determines the quality and order of the environment is the attitudes of people towards the environment rather than the number of people."

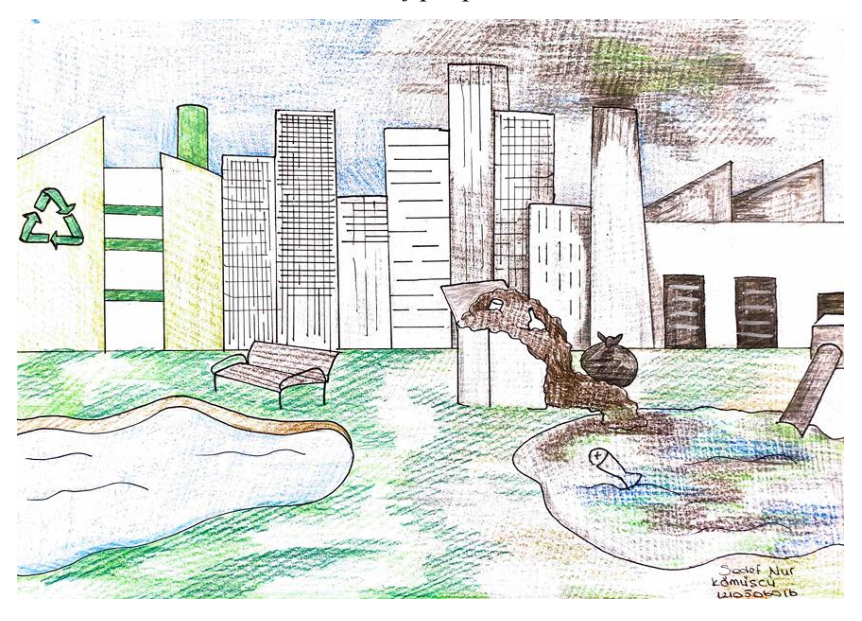


Figure 14. People's approach to the environment and its consequences

In his drawing with code 15, the candidate wanted to express the situation and effects of the world population burden (Figure 15). "In the picture, I wanted to show that the world's population is increasing uncontrollably and exponentially rapidly. I wanted to explain that this uncontrolled and exponentially rapid population growth creates a serious burden on the world and that the burden created by this increase is now unbearable and unsustainable."

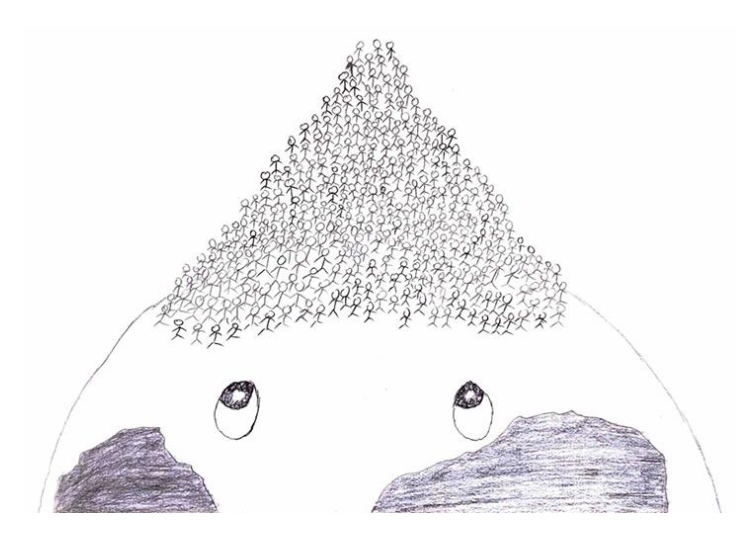


Figure 15. Uncontrolled and exponential growth of the world population

In his drawing with code 16, the teacher candidate touched upon the rapid and unsustainable use of world resources (Figure 16). "I mentioned that people are consuming resources rapidly and environmental problems are increasing, that there are too many people on the earth, and that the world is having difficulty carrying people. As the world population continues to increase, there are great difficulties in meeting basic needs such as food, water and energy. This overpopulation also leads to the destruction of ecosystems and the loss of biodiversity. Global problems like pollution and climate change are exacerbated by the impact of growing populations. For a sustainable future, human populations must be controlled."

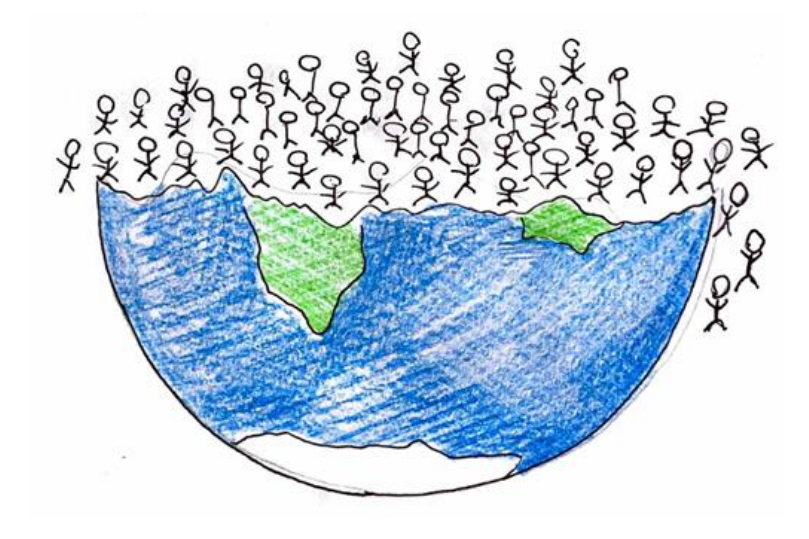


Figure 16. The world is struggling to support the growing population

The teacher candidate with code 17 touched upon the negative effects of population growth in her drawing (Figure 17). "In the picture I drew, I wanted to explain the increase and density of the world population. The diversity of human groups and crowded cities symbolize increasing population density. I also tried to draw attention to issues such as the depletion of natural resources, resource shortages and environmental impacts. Increasing population density has led to increased industrialization, which in turn has led to air pollution. The resulting air pollution has caused the decline in plant populations, which are important for the life of all living things."



Figure 17. Negative effects of population growth

In her drawing with code 18, the teacher candidate examined the changes that the human population has gone through throughout history (Figure 18). "With the picture I drew, I wanted to explain the effects of the great transformations that the human population has gone through throughout history. First, during the hunter-gatherer period, people lived in small, population-rich communities in harmony with nature. They are a part of nature and in order, so the earthly tree in the picture symbolizes this period in which they live in harmony with nature. Then, with the transition to settled life, agriculture and simple technologies begin to be developed; the wheel symbol represents the agricultural revolution and the

increasing population with this change. Although wars and epidemics slowed down population growth from time to time, industrialization resulted in large crowds in cities and increased living standards. Finally, technological and scientific developments and population pressure symbolize a period in which people turn to the search for new resources and space exploration."



Figure 18. Changes that humanity has gone through throughout history

In his drawing, the teacher candidate with code 19 examined that the human population exceeded the carrying capacity (Figure 19). "The image shows people spilling out from the earth. It's a picture of the majority of the world's population. The fact that people are falling one by one shows that if a solution is not found, people will start to suffer in the future."



Figure 19. The decline of humans from the Earth due to overpopulation

In her 20-coded teacher candidate drawing, she compared the living conditions of people in developing and developed countries (Figure 20). "In the upper part of the image I wanted to represent a family in a developing or poor country. If we look at the life there, the population of families who earn their living mostly from agriculture is high. Because women in families are often underdeveloped, children are viewed as capital. The more children, the more labor and money they bring. This is due to colonial powers. Children are viewed as caretakers who will care for them in old age. This is why we see families with many children. This, in turn, affects global population growth. They put pressure on the natural environment because they generally rely on fossil fuels to meet their needs such as food, shelter and heating.

In the lower part of the picture, I wanted to depict a family with few children in a developed country. Here, high living standards and excessive and unnecessary use of technological devices are seen. The status and development level of women in this country in the eyes of society is high. This leads women to have fewer children. However, the pressure families put on their surroundings is much greater thanks to their higher living standards and their ability to keep up with developing technology."



Figure 20. The environmental impact of people's living standards in developing and developed countries

Teacher candidate coded 21 discussed the distribution of the increasing population across all continents of the world (Figure 21). "In this picture, I wanted to express the excess human population by drawing the continents on the world. People live on every continent. I drew it with the prediction that even the continents where not many people live will increase in population after a while, and that it will increase even more in the places where there are people. If we were to take any continent from here, it would look like a crowd of people in a concert hall. After a while, it will look like a concert crowd even at a normal time."

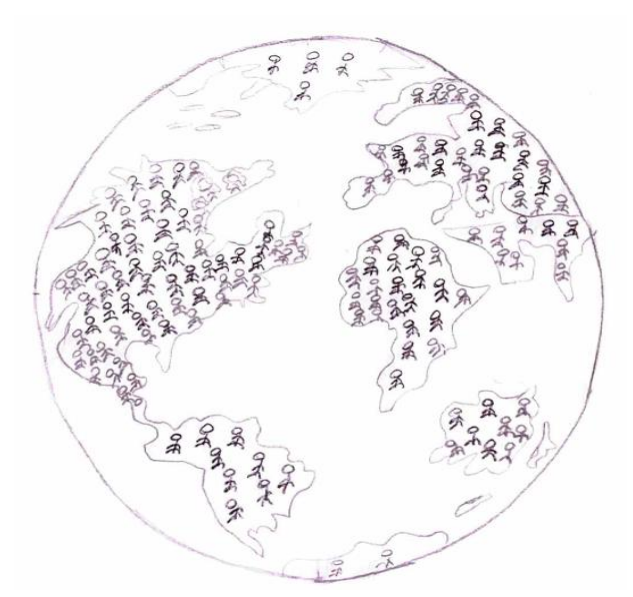


Figure 21. The spread of humans to all continents in the near future

The teacher candidate coded 22 discussed the effects of the world's human population on the environment from various aspects (Figure 22). "In the picture I drew, I tried to explain the effects of human population. Population growth brings with it social, economic, and environmental problems. Environmental problems, in particular, are directly related to population growth. The increasing population also increases the demand for basic needs such as water, energy, food and natural resources. This increase in demand leads to rapid depletion of resources and degradation of ecosystems.

In my opinion, wherever there is a large human population, there is pollution and disruption of natural life. As the population grows, marine pollution increases, significantly endangering the lives of marine life. In my drawing, I drew garbage thrown by people next to the fish on the left side of the paper. I didn't draw any garbage on the right side. I drew it this way because where the human population is high, the seas, rivers, and lakes will be more polluted.

Another factor I tried to explain in my picture is the traffic problem. The increasing human population in cities creates the need for cars. This creates traffic problems, especially in major cities. Traffic also causes noise, air pollution, and unnecessary energy consumption.

Population also has a significant impact on plants. Environmental problems arise as a result of air, water, and soil pollution. For example, in areas where industrialization is present, vegetables planted in the fields are unproductive or

trees dry out early. In short, the impacts of human populations on the environment are extensive and multifaceted. These impacts must be managed through sustainable policies and environmental protection measures."



Figure 22. The effects of increasing population on the environment

23 In her coded drawing, the prospective teacher wanted to express the environmental and social impacts of the human population in the World (Figure 23). "In this painting I wanted to highlight the increasing world population and the social and environmental impacts it brings.

### Social impacts

- 1) Need for Education Population growth increases the demand for education. More schools, teachers, and educational materials are required.
- 2) Health services Population growth increases the demand for health services.
- 3) Employment issues -A growing population can make it difficult to find employment opportunities. Unemployment rates can create social unrest.
- 4) Urbanization Increased population density in large cities can lead to housing shortages and infrastructure problems.
- 5) Cultural diversity Population growth can increase cultural diversity. However, it can also lead to conflict.

### Environmental impacts

- 1) Resource depletion An increasing population leads to increased consumption of natural resources such as water, food, and energy. This leads to resource depletion.
  - 2) Waste As the population increases, waste production also increases.
- 3) Climate change More people means more fossil fuel consumption, which increases greenhouse gas emissions and contributes to climate change.
- 4) Biodiversity loss Greater land demand for agriculture and industry can lead to habitat destruction and a decline in biodiversity."



Figure 23. Social and environmental problems created by population growth

In her drawing with code 24, the teacher candidate wanted to explain the environmental effects in connection with the population (Figure 24). "What I'm trying to convey in the picture is that as the population increases, environmental pollution increases. Furthermore, trees and flowers decrease. Urbanization is on the rise. As the number of people increases, the height of trees and their green areas decrease. Consequently, oxygen decreases and the atmosphere becomes polluted. Furthermore, as the number of people increases, the structure and shape of houses also change. When there were fewer people, the houses were more like shanty towns, but as the human population increased, the number of floors of the houses also increased. As the number of people increases, environmental pollution increases. The number of products used also increases. The number of animals is also decreasing. Because as the number of humans increases, the atmosphere becomes polluted and the struggle for survival becomes difficult."



Figure 24. Environmental impacts resulting from increasing population

The teacher candidate with code 25 wanted to express the excess human population and its consequences in her drawing (Figure 25). "I wanted to point out that the human population is very large. Considering ancient times, it has increased tremendously. As the human population increases, the number of factories and houses increases, natural areas such as forests decrease, many diseases emerge and health problems increase. Since these are the main problems, I wanted to highlight them at the top. I've drawn people in most of the world. I've left less of the rest of the world. What I'm trying to say is that as the human population grows, our resources are dwindling, and people are now moving off-world. Unfortunately, Earth is no longer as big a source of life for people as it once was."

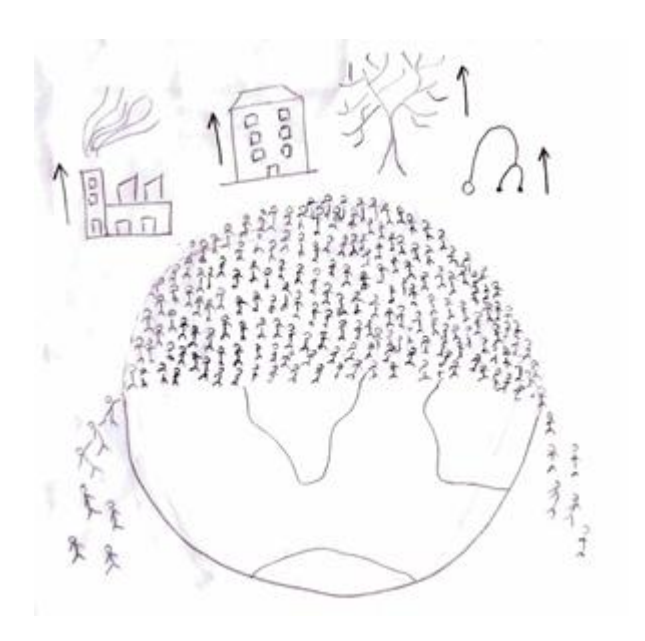


Figure 25. With the increasing population, people are overflowing from the world

In her drawing, the teacher candidate with code 26 states that the world's carrying capacity has been reached and all continents have been occupied by humans (Figure 26). "It shows that the number of people in a group is gradually increasing and that the area in which that group is located is exceeding the carrying capacity. The population is increasing not only in our country but also throughout the world and we are filling the earth allocated to us with people without leaving any space, first of all we are not giving any space to anyone, instead there is a continuous population increase without taking any precautions. If precautions aren't taken, there will be more and more people. The picture shows that the human population is increasing, and even living spaces are becoming overcrowded, and it's continuing to do so. It has a large enough population, and on top of that, it's attracting immigration. This will continue to grow day by day."



Figure 26. All continents are filled with people

In her drawing, the teacher candidate with code 27 shows that the human population has been increasing from past to present and will continue to increase (Figure 27). "The picture I drew shows that the human population is still growing. I wanted to convey that human figures are increasing in the form of a graphic curve and that further growth in the human population is expected in the future."

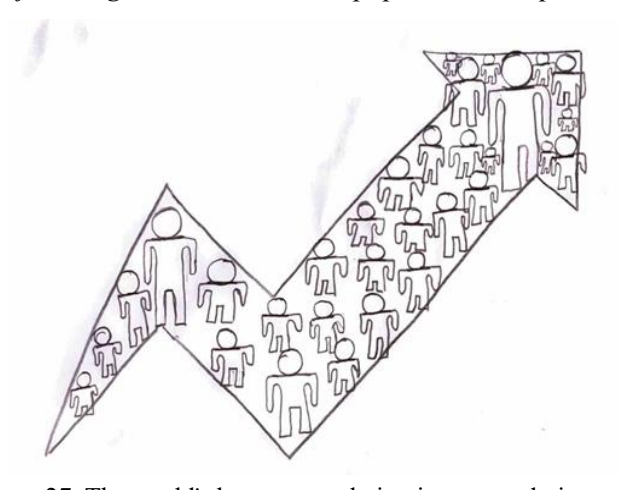


Figure 27. The world's human population is constantly increasing

### 4. DISCUSSION AND CONCLUSION

Population dynamics, which are at the heart of the developmental and environmental challenges of the 21st century, are the cumulative result of individual choices and opportunities. For example, ensuring universal access to sexual and reproductive health services, which can influence fertility rates; fiscal policies, which can influence decisions about family size; social protection and non-financial support systems such as childcare facilities; and development policies, which can alter the push and pull factors for migration, can all have an impact on this cumulative outcome. Therefore, if there is enough desire and necessary actions, these dynamics can be changed and demography can no longer be considered destiny. In this context, the sustainability and success of the development strategy to be implemented in spatial units of all sizes will depend not only on responding to population dynamics but also on producing rights-based and gender-sensitive policies and utilizing population dynamics in these policies (Özgür, 2017).

Women who lack education and economic opportunities must be empowered socially, economically and politically as they often have more children and are therefore deprived of educational and employment opportunities. Women are often the group most affected by environmental degradation and economic and social crises. Candidate coded 20 highlighted women in society and stated that in poor societies, women have more children and children are viewed as capital. Empowering women in resource-scarce, underdeveloped regions can help make development in these regions more sustainable while reducing pressure on environmental resources.

We are now living in a world that has no borders in every aspect, whether natural, social, or economic, or whose borders are being exceeded day by day. In this context, it is inevitable that the sustainability consequences of the population dynamics of a globalizing world will affect all of humanity at different levels and dimensions. Undoubtedly, underdeveloped regions that do not have a sufficient level of multiple capital structure for social and economic development, have resource shortages, rapidly growing populations and a bulge in the young generation will be more affected by these results. Because young generations will determine not only fertility and population growth trends in the future, but also more sustainable consumption and production patterns. Therefore, young generations, who now have a longer life expectancy and are the trustees of the future, deserve special attention.

Human health depends on the health of the planet. Earth's natural systems - air, water, biodiversity, and climate- are our life-support systems. However, climate change, biodiversity loss, soil and freshwater scarcity, pollution and other threats are disrupting these systems. Disruption in these systems also affects human health. Therefore, the emerging field of planetary health aims to understand how these changes threaten our health and how we can protect ourselves and the rest of the biosphere (Myers and Frumkin, 2020). It also

includes the development of multidisciplinary, intersectoral and cross-border approaches to correct and even reverse the deterioration of planetary health, so that human progress and the health and well-being of future generations can be sustained (Panorama, 2017). Most prospective teachers also share the same opinion that there are many environmental pollution problems based on the increase in resource consumption.

As the world population reaches 8 billion, scientists believe that a "civilizational collapse" may soon occur. In an article in the scientific journal World, she/he states that this large mass of people may soon face "population rectification."

Experts have been warning the world public for a long time that people are exploiting natural resources in an irreversible way. Stanford University biologist Tony Barnosky has written that the world is facing the worst global mass extinction since the dinosaurs. According to Rees, if the human population continues to grow at this rate, it may face a rude awakening. It is believed that only the richest and most resilient societies will survive a possible collapse. As stated by the teacher candidate with code 1 in her drawing, the attempts of rich people to find other planets or accommodation areas outside the world are remarkable.

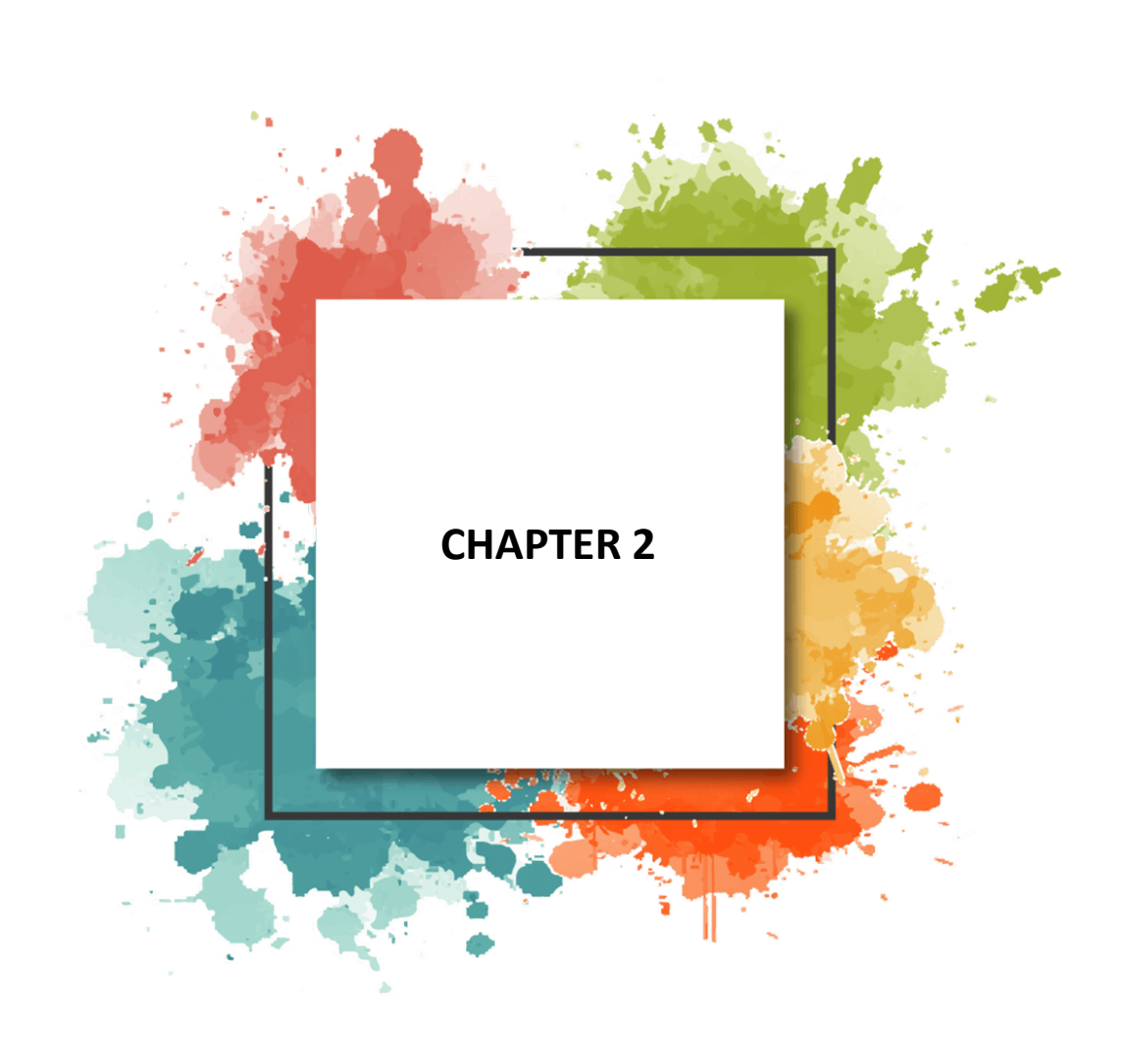
The rapid increase in the world population after the 1970s also led to an increase in the number of people who thought like Malthus. Thinkers such as Ehrlich, Meadows, and Mesarovic, called "Neo-Malthusians," argue that Malthus was wrong in the short term, but may have been right in the long term, and that the world will eventually be unable to feed its population (Çamurcu, 2005). In this study, all prospective teachers expressed that the world's population is increasing very rapidly and that natural resources are decreasing rapidly as a result. Therefore, it is inevitable that the lack of natural resources in the near future will lead to the extinction of the human race, as it has happened to other living things in the past. Unfortunately, this situation will be created by humankind's ambition to control nature and possess everything thoughtlessly. For these reasons, we must avoid excessive waste and protect our natural resources. We must also grant future generations the right to use natural resources so that they can sustain their lives.

#### REFERENCES

- Bartlett, A. A. (1994). Reflections on sustainability, population growth and the environment. *Population and Environment: A Journal of Interdisciplinary Studies*, 16(1), 5-35.
- Carr, D. L., Suter, L. & Barbieri, A. (2005). Population dynamics and tropical deforestation: State of the debate and conceptual challenges. *Population and Environment*, 27(1), 89-113.
- Cohen, J. E. (2003). Human population: The next half century. *Science*, *14*(302), 1172-1175, Doi: 10.1126/science.1088665
- Cohen, L. & Manison, L. (1994). Research methods in education. London: Routledge.
- Çamurcu, H. (2005). Dünya nüfus artışı ve getirdiği sorunlar. *Balıkesir Üniversitesi Sosyal Bilimler Enstitüsü Dergisi*, 8(13), 87 105.
- Ehrlich, P. R. & Ehrlich, A. H. (1990). *The population explosion*. Simon & Schuster: New York.
- Ehrlich, P. R. Ehrlich, A. H. & Daily, G. C. (1993). Food security, population, and environment. *Population and Development Review*, 19(1), 1-32.
- Ersoy, F. & Türkkan, B. (2010). İlköğretim öğrencilerinin çizdikleri karikatürlere yansıttıkları sosyal ve çevresel sorunların incelenmesi. *Eğitim ve Bilim Dergisi*, 35(156), 96-109.
- Hidalgo, D. M., Nunn, P. D., Beazley, H., Burkhart, S. & Rantes, J. (2022). Adaptation, sustainable food systems and healthy diets: An analysis of climate policy integration in Fiji and Vanuatu. *Taylor & Francis Online*, 22(9-10), 1130–1145.
- Hunter, L. M. (2000). *The environmental implications of population dynamics, RAND.* Santa Monica-California.
- Kight, S. W. & Lysik, T. (2022). The human race at 8 billion (https://www.axios.com/2022/11/14/global-po pulation-8-billion-data-world-humans-un).
- Malthus, T. (1998). An Essay on the principle of population (Electronic Scholarly Publishing Project), London. (<a href="http://www.esp.org/books/malthus/population/">http://www.esp.org/books/malthus/population/</a> malthus.pdf, 20.10.2016)
- Meadows, D. H., Meadows, D. L., Randers, J. & Behrens, W. W. (1972). The limits to growth: A report for the club of Rome's project on the predicament of mankind. Universe Books, New York.
- Newbold, K. B. (2014). *Population geography: Tools and issues.* (Second edition), Rowman and Littlefield Publishers, Plymounth UK.

- Özgür, E. M. (2017). Nüfus dinamikleri, çevre ve sürdürülebilirlik. *Coğrafi Bilimler Dergisi*, *15*(1), 1-26.
- Özkan, G., Gultekin Subası, B., Kamiloglu, S. & Capanoglu, E. (2022), Sürdürülebilir gıda ve tarımsal atık yönetimi. *Çevre, İklim ve Sürdürülebilirlik, 23*(2), 145-160.
- Panorama. (2017). *Planetary health 101*: Information and resources. The Rockefeller Foundation. https://assets.ctfassets.net/n0merlwkrasg/5pwyqEGQKluG81FoLybY7q/f8 5a9fa0acaa9d2772d66fd817f1519c/Planetary-Health-101-Information-and-Resources.pdf
- Parsons, K. & Hawkes, C. (2018). Connecting food systems for co-benefits: How can food systems com bine diet-related health with environmental and economic policy goals? POLICY BRIEF 31, World Health Organization (acting as the host organization for, and secretariat of, the European Observato ry on Health Systems and Policies), 36 p.
- Peters, G. L. & Larkin, R. P. (2005). *Population geography: Problems, concepts, and prospect.* (Eighth Edition), Kendal/Hunt Publishing Company, Dubuque.
- Pimentel, D., Giampietro, M. & Bukkens, S. G. (1998). An optimum population for North and Latin America. *Population and Environment*, 20(2), 125-148.
- Ritchie, H., Rosado, P. & Roser, M. (2023). Hunger and undernourishment. Published online at OurWorldinData.org. Retrieved from: 'https://ourworldindata.org/hunger-and-undernourishment'.
- Saygı, Y. B. (2024). Sürdürülebilir gıda sistemleri ve sağlıklı beslenme. *Gıda Mühendisliği Dergisi*, 55, 8-15.
- Sherbinin, A., Carr, D., Cassels, S. & Jiang, L. (2007). Population and environment. *Annual Review of Environment and Resources*, 32, 345-373. https://doi.org/10.1146/annurev.energy.32.041306.100243
- United Nations-UN. (2001). World population prospects: The 2000 revision highlights ESA/P/WP.165.
- United Nations-UN. (2015). World population prospects: The 2015 revision, Volume II: Demographic Profiles ST/ESA/SER.A/380.
- United Nations Population Fund-UNFPA. (2013). Population dynamics in the Post-2015 development agenda: Report of the global thematic consultation on population dynamics, the world we want. (<a href="http://www.unfpa.org/sites/default/files/pub-pd">http://www.unfpa.org/sites/default/files/pub-pd</a> f/Population%20D ynamics%20in%20Post-2015%20FI NAL.p df, 27.6.2016).

- URL 1. Dünya nüfusu. Vikpedi Özgür Ansiklopedi (https://tr.wikipedia.org/wiki/D%C3%BCnya n%C3%BCfusu).
- Yıldırım, A. & Şimşek, H. (2006). Sosyal bilimlerde nitel araştırma yöntemleri. 5. Baskı, Ankara: Seçkin Yayıncılık.



# Integrated Water Resources Management (IWRM) Approaches and Applications

# Ertan Karahanlı<sup>1</sup> & Cengiz Mutlu<sup>2</sup>

#### 1. Introduction

Water is not only a fundamental resource for life; it is also a strategic element for economic development, social well-being, and the sustainability of ecosystems. Today, increasing populations, rapid urbanization, industrialization, and the impacts of climate change are creating significant pressure on the water supply-demand balance. According to United Nations reports, 2.3 billion people worldwide live in regions experiencing water stress, and this number is projected to increase significantly by 2050 (UN-Water, 2021). This situation demonstrates that water is no longer just a natural resource but also a critical element for national security, international relations, and development policies (Dinar, 2024).

In light of these developments, the concept of Integrated Water Resources Management (IWRM) has come to the fore. IWRM is defined as an approach that simultaneously considers economic efficiency, social justice, and ecological sustainability in the planning, development, and management of water resources (Grigg, 2024). At its core lies the understanding that water is not merely a technical resource but also a complex system with social, economic, and environmental dimensions. Therefore, IWRM aims to reduce conflicts between different sectors, strengthen stakeholder participation in decision-making processes, and ensure long-term sustainability (Ak & Benson, 2022).

IWRM, which gained international attention at the 1992 Dublin Conference and the subsequent Rio Summit, is now included in the United Nations' Sustainable Development Goals (SDG 6.5). This goal requires all countries to "implement integrated water resources management" by 2030 (UN-Water, 2021). However, assessments reveal that many countries face various institutional, financial, and technical barriers to achieving this goal (Wang et al, 2024).

When considered specifically for Turkey, water resources management presents both opportunities and risks in the context of agricultural production, energy production, and transboundary waters. Water scarcity and groundwater

<sup>1</sup> Department of Biology, Graduate School of Natural and Applied Sciences, Giresun University, Giresun, Türkiye, ORCID: https://orcid.org/0000-0002-3202-271X.

<sup>2</sup> Department of Environmental Engineering, Faculty of Engineering, Giresun University, Giresun, Türkiye, ORCID: https://orcid.org/0000-0002-9741-4167

depletion, particularly in regions such as the Konya Closed Basin and the Gediz Basin, further underscore the importance of IWRM practices (Yilmaz & Harmancioglu, 2010). Furthermore, Turkey's harmonization process with the EU Water Framework Directive (WFD) contributes to the strengthening of the integrated approach by encouraging basin-based planning (Insight Turkey, 2022).

Therefore, the main objective of this chapter is to present the conceptual framework of IWRM, discuss its application areas and encountered problems, evaluate technological and governance innovations, and develop future policy recommendations in the Turkish context.

### 2. Theoretical and Conceptual Framework

Integrated Water Resources Management (IWRM) derives its origins from the 1992 Dublin Principles, which continue to underpin the approach today. These principles include (i) recognizing that water is a limited and fragile resource, (ii) ensuring the effective participation of all stakeholders in water management, (iii) embracing the central role of women in water planning, use, and conservation, and (iv) recognizing the economic value of water. This framework has become one of the most critical goals pursued globally within the United Nations Sustainable Development Goals (SDG 6.5) (UN-Water, 2021). Recent studies demonstrate that the success of IWRM is not limited to technical infrastructure; transparent governance, institutional coordination, stakeholder participation, digital transformation, and inclusive decision-making mechanisms are essential for its effective operation (Ak & Benson, 2022; Tuo & He, 2021; Brown et al., 2015). In this context, IWRM is considered as an interdisciplinary approach to both protecting natural resources and ensuring social equality, economic efficiency and adaptation to climate change.

### 2.1. Stakeholders in Integrated Water Resources Management

Water management is a multi-actor process. Sustainable management is impossible without the participation of central governments, local governments, farmers, industry organizations, NGOs, and the public (Dinar, 2024). Participatory governance, in particular, increases the legitimacy of decisions and ensures adaptation to local needs. For example, in the European Water Framework Directive harmonization process, stakeholder participation is emphasized as critical to achieving water quality targets (Wang, 2024).

### 2.2. IWRM and Political Frameworks

The European Union's Water Framework Directive (WFD) is one of the most comprehensive regulations that establishes IWRM principles in legal terms.

Turkey is developing similar legal regulations as part of the EU harmonization process (Insight Turkey, 2022). However, challenges remain in institutional coordination, basin-based planning, and water quality protection.

Global climate change is having multiple impacts on water resources. Rising temperatures accelerate the water cycle by increasing evaporation rates, leading to irregular precipitation patterns. This situation exacerbates droughts in some regions and increases flood and inundation risks in others (Wang, 2024).

Recent studies predict that even a 1.5°C global temperature increase will create significant pressure on groundwater reserves, lakes, and agricultural irrigation (IPCC, 2022). The Mediterranean Basin, Southern Europe, and the Middle East, in particular, are among the regions most vulnerable to water scarcity due to climate change (Iglesias et al., 2022).

Turkey is also directly affected by these risks. Increasing agricultural water demand in Central and Southeastern Anatolia is leading to falling water levels in lakes and dams. Furthermore, increased heavy rainfall in the Black Sea region brings with it disaster risks such as floods and landslides (Demircan, & Sılaydın, 2024). In this context, it can be said that the impacts of climate change on water resources encompass not only quantity but also quality and access.

### 2.3. Global Climate Change and Its Impact on Water Resources

Global climate change has multifaceted impacts on water resources. Rising temperatures accelerate the water cycle by increasing evaporation rates and leading to irregular precipitation patterns. This situation exacerbates droughts in some regions and increases the risk of floods and inundations in others (Wang et al., 2024).

Recent studies predict that even a 1.5°C global temperature increase will place significant pressure on groundwater reserves, lakes, and agricultural irrigation (IPCC, 2022). The Mediterranean Basin, Southern Europe, and the Middle East, in particular, are among the regions most vulnerable to water scarcity due to climate change (Iglesias et al., 2022).

Turkey is also directly affected by these risks. Increasing agricultural water demand in Central Anatolia and Southeastern Anatolia leads to falling water levels in lakes and dams. Furthermore, increased heavy rainfall in the Black Sea region brings with it disaster risks such as floods and landslides (Demircan, & Sılaydın, 2024). In this context, it can be said that the effects of climate change on water resources include not only quantity but also quality and access dimensions.

### 2.4. Application Areas of the Integrated Approach

Basin Management: One of the most important areas of application of Integrated Water Resources Management is at the basin level. For example, studies conducted in the Gediz Basin reveal that water pressures are increasing and groundwater resources are gradually depleting due to the imbalance between agricultural irrigation, industrial use, and domestic consumption (Kibar et al., 2023). Similarly, studies conducted in the Konya Closed Basin demonstrate that the water supply-demand balance is unsustainable, highlighting the critical role of basin-based planning (Gedik, 2021).

Urban Water Management: Increasing urban populations and the impacts of climate change are increasing the importance of smart grid technologies and water recycling practices. Smart water meters, leak detection, and real-time monitoring systems can reduce water losses by up to 20% (Lin, & Ma, 2022; Lindner, & Stamm, 2025). Furthermore, graywater reuse and rainwater harvesting stand out as complementary approaches that support the sustainable water cycle in urban areas (UN-Water, 2021). Agricultural Irrigation: As water consumption in agriculture accounts for approximately 70% of total use, innovations in irrigation technologies are critical. Drip irrigation, pressurized irrigation systems, and sensor-based smart irrigation applications can achieve water savings of up to 30–40% while simultaneously increasing crop yields (Ali et al., 2025; Ercan Oğuztürk et al., 2025). Examples from Israel and Spain demonstrate that drip irrigation and the reuse of saline/treated water can successfully manage water scarcity (Wang et al., 2024).

Industry: Water reuse and circular economy approaches are increasingly prevalent in the industrial sector. Advanced treatment technologies implemented in the textile, food, and energy sectors increase wastewater reuse, reducing costs and supporting environmental sustainability (Grigg, 2024; Deribe et al., 2024). This approach is considered critical for the sustainability of industrial activities, especially in water-stressed regions.

### 2.5. Problems Encountered in IWRM Applications

The main problems encountered in Integrated Water Resources Management (IWRM) implementations include institutional fragmentation and conflicts of authority between different ministries and institutions (Tuo, & He, 2021), financing shortcomings that hinder the sustainability of infrastructure investments (George-Williams et al., 2024), data and technology gaps associated with the lack of up-to-date monitoring systems (Brown et al., 2015), and sociocultural barriers arising from society's water use habits and low awareness levels

(UN-Water, 2021). In addition, uncertainties in drought, flood, and precipitation regimes caused by climate change (Mokrech et al., 2022), lack of cooperation in transboundary water basins (Deribe et al., 2024), insufficient administrative capacity and specialized human resources, and gaps between policy and implementation are also critical factors that reduce the effectiveness of IWRM. These problems are seen at different scales not only in developing countries but also in developed countries; This complicates the maintenance of a water supplydemand balance and the protection of ecosystems. In Turkey, IWRM implementation is hampered by difficulties in institutionalizing the basin-based management approach, persistent overlapping authority among different institutions (DSİ, the Ministry of Environment, Urbanization and Climate Change, the Ministry of Agriculture and Forestry, and local governments), and lack of coordination. Furthermore, international cooperation problems in transboundary water systems such as the Euphrates-Tigris basin and inadequate monitoring and data-sharing mechanisms in large inland river basins such as the Kızılırmak and Sakarya river basins pose obstacles to implementation. Increasing drought and flood events due to climate change also exacerbate Turkey's water management vulnerabilities, while lack of financing, awareness, and participation further complicate the process (UN-Water, 2021; Tuo, & He, 2021).

### 2.6. Technological Innovations and Digital Transformation

In recent years, artificial intelligence, machine learning, remote sensing, and Internet of Things (IoT) techniques have assumed increasingly central roles in water management. For example, LSTM, GRU, and hybrid models combined with remote sensing data for water quality prediction enable more accurate spatial and temporal monitoring of pollution levels in inland rivers (Pan et al., 2025). In irrigation management, significant advances are being made in AI-supported systems both internationally and in Turkey: AI-supported autonomous irrigation systems adaptively control irrigation rates by monitoring air and soil moisture (Ercan Oğuztürk et al., 2025); and in Turkey, particularly through the İmamoğlu Agricultural Irrigation Automation Project, many farmers are increasing irrigation efficiency and water conservation through remote control, GIS-based interfaces, and the use of real-time data (Balta & Kulat, 2024). Additionally, wireless sensor networks and real-time pressure/flow monitoring systems reduce losses by detecting problems such as blockages and low water pressure in irrigation networks early (Meric., 2025). These technological innovations, combined with decision support systems, increase the predictive capacity of basin planning and water management strategies and contribute to the sustainable use of water resources.

### 2.7. Case Studies

Integrated coastal-water management strategies implemented in the Netherlands to respond to the threat of sea level rise and increased coastal flooding have enabled risk reduction, ecosystem restoration, and balancing economic functions; the "multi-layered security approach" has set an example in long-term flood management by combining spatial planning, disaster preparedness, and protection infrastructure (de Vries et al., 2024; Lindner, & Stamm, 2025). Drip irrigation technologies, which have become widespread in Israel, have provided water savings and increased agricultural productivity; in addition, adaptation to water scarcity has been strengthened through wastewater reuse, drip irrigation in saline-alkaline soils, and groundwater recharge applications (Ak & Benson, 2022; Wang et al., 2024). In Turkey, groundwater depletion has reached serious levels, especially in the Konya Closed Basin; Hydrological analyses conducted during the period 1960–2019 clearly revealed the decline in water levels and highlighted the need for sustainable planning, institutional coordination and GIS-based monitoring at the basin scale (Gedik, 2021; Yilmaz, & Harmancioglu, 2010).

### 2.8. Future Perspectives

Future concerns about the sustainability of water resources are growing. On the one hand, there are pressures from climate change, population growth, and increasing energy, agriculture, and water demand; on the other, a lack of institutional coordination and international cooperation poses significant risks (Dinar, 2024).

At the heart of these future concerns are the following questions:

- How will the water stress situation of 50% of the world's population be managed by 2050? How will the increasing risks of conflict in transboundary water sharing be resolved?
- While digital technologies increase water efficiency, will capacity disparities in developing countries create new inequalities?

These concerns are global issues that can be overcome not only through technical solutions but also through international cooperation, public awareness, and integrated governance mechanisms. Therefore, the future of IWRM must encompass not only today's needs but also long-term perspectives on climate adaptation and global peace (Grigg, 2024).

#### 2.9. Future Concerns

Future concerns about the sustainability of water resources are growing. On the one hand, there are pressures from climate change, population growth, and increasing energy, agriculture, and water demand; on the other, a lack of institutional coordination and international cooperation poses significant risks (Dinar, 2024). Climate change scenarios indicate that water scarcity will worsen. Therefore, climate adaptation policies, green infrastructure solutions, and international cooperation will be paramount in the future of IWRM (Wang et al., 2024).

At the heart of these future concerns are the following questions:

- How will the situation of 50% of the world's population living under water stress by 2050 be managed?
- How will the increasing risks of conflict in transboundary water sharing be resolved?
- While digital technologies increase water efficiency, will capacity disparities in developing countries create new inequalities?

These concerns are global issues that can be overcome not only through technical solutions but also through international cooperation, public awareness, and holistic governance mechanisms. Therefore, the future of IWRM must encompass not only the needs of today but also long-term perspectives of climate adaptation and global peace (Grigg, 2024).

### 2.10. Conclusion and Evaluation

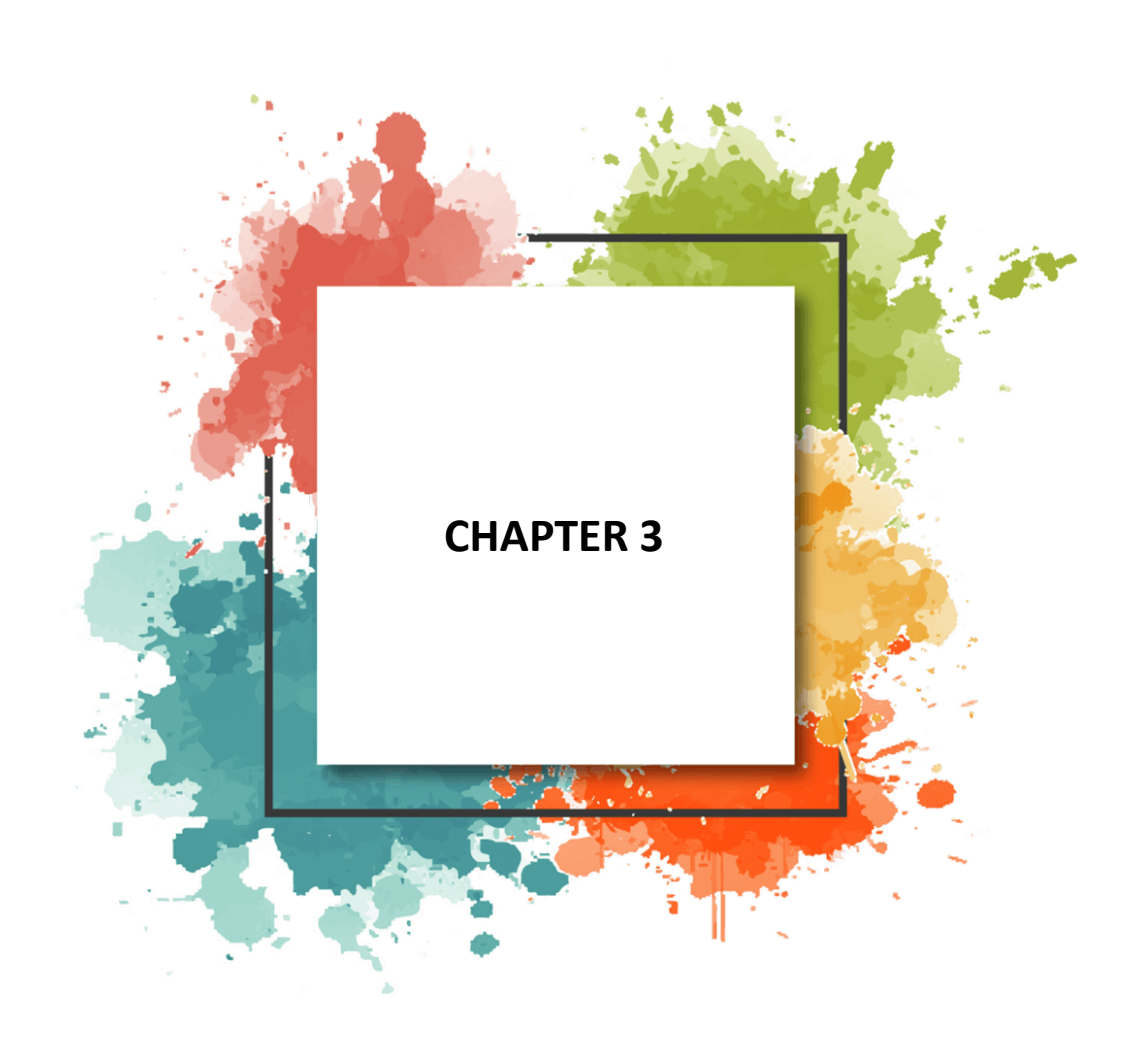
Integrated Water Resources Management (IWRM) is a holistic approach that requires not only investments in technical infrastructure but also a strong sociopolitical governance framework. Recent literature suggests that stakeholder participation, inter-institutional coordination, digital transformation, and transparent data management are key to success in sustainable water management (Tuo, & He, 2021; Brown et al., 2015). However, uncertainties in drought, flood, and precipitation regimes caused by global warming (Mokrech et al., 2022) disrupt the water supply-demand balance and make the spatial and temporal distribution of water unpredictable. This limits the effectiveness of IWRM implementations in both developing and developed countries, making cooperation challenges, particularly critical in transboundary water basins (Deribe et al., 2024). From Turkey's perspective, institutional fragmentation, inadequate funding, and data deficiencies are prominent in basin-based planning processes, while the limited participation of local people in decision-making

constitutes a significant obstacle that undermines sustainability (UN-Water, 2021; George-Williams et al., 2024). In this context, Turkey needs to shift its focus to new water management policies and practices that take into account the impacts of the global climate crisis and institutionalize a participatory, digitalized, and integrated management approach. Furthermore, progress toward SDG 6.5.1, one of the United Nations' Sustainable Development Goals, is a critical imperative not only for national water security but also for ensuring international accountability and global harmonization.

### 3. References

- Ak, M. Y., & Benson, D. (2022). Assessing the water security effectiveness of integrated river basin management: Comparative case study analysis for lesson-drawing. Frontiers in Water, 4, 1013588. https://doi.org/10.3389/frwa.2022.1013588.
- Ali, A., Hussain, T., & Zahid, A. (2025). Smart irrigation technologies and prospects for enhancing water use efficiency for sustainable agriculture. AgriEngineering, 7(4), 106.
- Balta, M. A., & Kulat, M. İ. (2024). Transforming an irrigation system to a smart irrigation system: A case study from Türkiye. İmamoğlu Tarımsal Sulama Otomasyon Projesi.
- Brown, C. M., Lund, J. R., Cai, X., Reed, P. M., Zagona, E. A., Ostfeld, A., ... & Brekke, L. (2015). The future of water resources systems analysis: Toward a scientific framework for sustainable water management. Water resources research, 51(8), 6110-6124.
- de Vries, M., Vinke-de Kruijf, J. ve Augustijn, DD (2024). Sel dayanıklılığının artırılmasına doğru: Kentsel deltalarda mekânsal planlamaya sel korumasının entegre edilmesi. 36. AESOP Yıllık Kongresi 2024: Oyunun kurallarını değiştiren bir gelişme mi? Adil ve sürdürülebilir kentsel bölgeler için planlama (s. 412). Avrupa Planlama Okulları Birliği (AESOP).
- Demircan, G., & Sılaydın, M. B. (2024). Deniz Seviyesi Yükselmesi ve Aşırı Yağış Tehditlerine Karşı Mekânsal Kırılganlık Değerlendirmesi: Küçük Menderes Alt Havzaları. *Resilience*, 8(2), 235-248.
- Deribe, M. M., Melesse, A. M., Kidanewold, B. B., Dinar, S., & Anderson, E. P. (2024). Assessing international transboundary water management practices to extract contextual lessons for the Nile river basin. *Water*, *16*(14), 1960.
- Dinar, A. (2024). Challenges to water resource management: The role of economic tools and institutional approaches. Water, 16(4), 610. https://doi.org/10.3390/w16040610.
- Ercan Oğuztürk, G., Murat, C., Yurtseven, M., & Oğuztürk, T. (2025). The effects of AI-supported autonomous irrigation systems on water efficiency and plant quality: A case study of *Geranium psilostemon*. *Plants*, *14*(5), 770. https://doi.org/10.3390/plants14050770.
- Gedik, F. (2021). Konya Kapalı Havzası'nda yeraltı suyunun değişimi ve kuraklık analizi. *Türkiye Jeoloji Bülteni*, 64(2), 145–160. https://doi.org/10.25288/tjb.2021.64.2.145.

- George-Williams, H. E., Hunt, D. V., & Rogers, C. D. (2024). Sustainable water infrastructure: visions and options for Sub-Saharan Africa. *Sustainability*, *16*(4), 1592.
- Grigg, N. S. (2024). Framework and function of integrated water resources management: Recent implementation and institutional performance. Sustainability, 16(13), 5441. https://doi.org/10.3390/su16135441.
- Iglesias, A., Garrote, L., Flores, F., & Moneo, M. (2007). Challenges to manage the risk of water scarcity and climate change in the Mediterranean. *Water resources management*, 21(5), 775-788.
- IPCC. (2022). Climate Change 2022: Impacts, adaptation and vulnerability. Contribution of Working Group II to the Sixth Assessment Report of the Intergovernmental Panel on Climate Change. Cambridge University Press. https://doi.org/10.1017/9781009325844.
- Lin, B., & Ma, R. (2022). How does digital finance influence green technology innovation in China? Evidence from the financing constraints perspective. *Journal of environmental management*, 320, 115833.
- Lindner, A., & Stamm, J. (2025). Integrating Climate Change Adaptation and Water Resource Management: A Critical Overview. *Standards*, *5*(1), 4.
- Meriç, M. K. (2025). Implementation of a wireless sensor network for irrigation management in drip irrigation systems. *Scientific Reports*, *15*(1), 14157.
- Pan, D., Deng, Y., Yang, S. X., & Gharabaghi, B. (2025). Recent Advances in Remote Sensing and Artificial Intelligence for River Water Quality Forecasting: A Review. *Environments*, 12(5), 158.
- Tuo, S., & He, H. (2021). A study of multiregional economic correlation analysis based on big data—Taking the regional economy of cities in Shaanxi Province, China, as an example. *Sustainability*, *13*(9), 5121.
- UN-Water. (2021). Progress on integrated water resources management: Global status and acceleration needs. United Nations. https://www.unwater.org/publications/progress-on-integrated-water-resources-management-2021.
- Wang, M., Wang, R., Sun, Q., Li, Y., Xu, L., & Wang, Y. (2024). Integrated drip irrigation regulates soil water–salt movement to improve water use efficiency and maize yield in saline–alkali soil. *Water*, 16(17), 2509.
- Yilmaz, B., & Harmancioglu, N. (2010). Multi-criteria decision making for water resource management: a case study of the Gediz River Basin, Turkey. *Water SA*, 36(5).



# **Interactions Between Biochar Applications and Soil Urease Activity: A Synthesis of Current Knowledge**

## Aysu Koç<sup>1</sup> & Gizem Yaman<sup>2</sup> & Burak Koçak<sup>3</sup>

### 1) Introduction

Biochar is a porous material which has a high carbon content and can be produced by burning organic biomass at high temperatures under conditions with or without oxygen. Factors such as production conditions (temperature, duration, biomass type, etc.) and the presence or absence of oxygen during pyrolysis determine the physical, chemical, and biological properties of the resulting biochar (e.g., surface area, porosity, pH, carbon content) (Khan et al., 2024).

The pyrolysis temperatures commonly used in biochar production vary across low, medium, and high ranges. Low temperatures typically range between 300 and 400 °C (Chen and Yuan, 2011); medium temperatures fall between 400 and 500 °C (Kim et al., 2012); and high temperatures exceed these values, often ranging from 500 to 700 °C (Bartoli et al., 2022). When temperature increases, the pore structure of biochar changes: higher temperatures generally result in a more aromatic structure, greater stability, and increased surface area and porosity. In contrast, pyrolysis at lower temperatures tends to retain more oxygencontaining functional groups in the biochar, such as carboxyl and phenolic groups (Zhu et al., 2025).

Biochar can be obtained and produced by various organic carbon-rich materials, including woody biomass (e.g., wood, bark, sawdust), agricultural residues (such as straw, corn stalks, rice husks), animal wastes (e.g., poultry manure), forest residues, and municipal wastes. The type of feedstock applied for biochar affects the nutrient content, pH value, stability, and microbial effects of the resulting biochar (Singh et al., 2022; Holatko et al., 2025).

In recent years, biochar has become a popular material due to its multifaceted benefits in attempts for sustainable agriculture and environmental management. Biochar can be produced by the controlled heating of organic waste—such as agricultural residues, woody materials, food and garden waste, animal manure,

 $<sup>^{\</sup>rm 1}$  Çukurova Üniversitesi Fen-Edebiyat Fakültesi Biyoloji Bölümü, 0009-0002-5400-3269

<sup>&</sup>lt;sup>2</sup> Çukurova Üniversitesi Fen-Edebiyat Fakültesi Biyoloji Bölümü, 0009-0006-1754-4567

<sup>&</sup>lt;sup>3</sup> Doç. Dr. Çukurova Üniversitesi Fen-Edebiyat Fakültesi Biyoloji Bölümü, 0000-0003-4144-6079

and industrial biological waste—under oxygen-free or low-oxygen conditions. The primary components of biochar include carbon, volatile matter, mineral content, and moisture (Antal and Gronli, 2003). Rich in carbon and environmentally friendly, biochar is considered as a potential material to enhance the physical, chemical, and biological properties of soil. Beyond enhancing soil characteristics, biochar also acts as a fertilizer that supports plant growth, facilitates long-term carbon sequestration in soil, and binds agrochemical substances to boost soil fertility. Moreover, biochar is a beneficial and important application that contributes to climate change mitigation by reducing greenhouse gas emissions, particularly CO<sub>2</sub> and CH<sub>4</sub>. In terms of waste management, it offers additional advantages such as recycling chemical pollutants, lowering material flow costs, and enabling energy production (Lorenz and Lal, 2014).

Soil quality and fertility are directly linked to biological activities and biochemical cycles occurring within the soil (Budak et al., 2023; Ergün, 2017). Among the key biological indicators of soil health, soil enzyme activities play a vital role (Singh Yadav et al., 2023). Urease (urea amidohydrolase), an enzyme that acts a crucial catalyst in the nitrogen cycle, hydrolyzes urea into ammonia (NH<sub>3</sub>) and carbon dioxide (CO<sub>2</sub>), thereby facilitating nitrogen uptake by plants. However, this process can also lead to nitrogen losses through ammonia volatilization (Kandeler & Gerber, 1988; Karaca et al., 2014). Therefore, assessing urease activity in soil is considered an important parameter for both agricultural productivity and environmental sustainability.

This study aims to review research conducted between 2014 and 2024 on the effects of increasingly popular biochar applications on soil urease enzyme activity. It focuses on the underlying mechanisms behind conflicting findings in the literature, emphasizing the role of factors such as biochar production conditions (feedstock type, pyrolysis temperature), application settings (laboratory vs. field), and dosage. This study compiles existing literature on biochar's potential to enhance, suppress, or have a neutral impact on urease activity in soil.

# 2) Effects of Biochar on the Physical, Chemical, and Biological Properties of Soil

Biochar is a highly stable soil amendment with high carbon content, large surface area, and porous structure, obtained through heating organic biomass feedstocks—such as agricultural and forestry residues (e.g., wood, crop waste, animal manure)—under oxygen-free or low-oxygen conditions through a thermochemical process known as pyrolysis (Chia et al., 2015; Gul et al., 2015;

Budak et al., 2023; Singh Yadav et al., 2023). The physical and chemical properties of biochar can vary significantly depending on production conditions such as feedstock type, pyrolysis temperature, and duration (Sakrabani et al., 2017). These factors determine biochar's potential to improve soil physical (bulk density, water retention capacity), chemical (pH, cation exchange capacity), and biological (microbial activity) properties (Singh Yadav et al., 2023).

Because it has porous structure, biochar reduces soil bulk density. For example, Zhu et al. (2025) reported that application of biochar significantly decreases soil density, with this effect being more pronounced in sandy-clay soils or under arid conditions. It enhances aggregate formation and stability, thereby improving soil structure and supporting processes such as water movement and aeration (Blanco-Canqui, 2017; Zhu et al., 2025). Additionally, its high porosity and surface area increase water retention capacity, which is particularly beneficial in arid and semi-arid regions (Zhu et al., 2025; Franco et al., 2022). Because biochar have large surface area and contains functional groups, it can enhance the retention of nutrients and water, thereby reducing losses (Günal & Erdem, 2018; Singh Yadav et al., 2023).

Biochar applications have been shown in numerous studies to improve the chemical and biological properties of soil, thereby supporting plant growth (Idbella et al., 2024; Premalatha et al., 2023). Biochar generally exhibits alkaline characteristics and has been reported to increase pH levels in acidic soils. Additionally, features such as surface functional groups and oxygen-containing terminal groups can enhance the soil's cation exchange capacity (Khan et al., 2024; Singh et al., 2022; Zhu et al., 2025). Biochar applications also contribute to increasing soil organic carbon stocks and can enrich the soil with nutrient elements derived from the feedstock (e.g., N, P, Ca, and micronutrients). However, this enrichment depends on the type of feedstock, pyrolysis temperature, and application dosage (Holatko et al., 2025; Premalatha et al., 2023). Biochar has been noted to decrease the availability of heavy metals to biological organisms, as its alkaline nature and chemical groups enable it to bind these metals. Nevertheless, in some cases, the alkaline properties of biochar may increase the mobility of other elements, and this effect is considered to be dependent on regional conditions (Liang et al., 2021; Premalatha et al., 2023).

Biochar application has been reported to enhance microbial biomass carbon and nitrogen (Li et al., 2020). It has also been shown to support microbial diversity and active microbial communities (e.g., bacteria, fungi) (Xu et al., 2023). Enzyme activities related to biogeochemical cycles in soil—such as β-glucosidase, phosphatase, and urease—are generally enhanced by biochar (Lopes

et al., 2021; Barbosa et al., 2024; Jiang et al., 2021). Because biochar has porous structure, this ability of biochar can provide microhabitats for soil microbial populations, thereby boosting microbial activity (Palansooriya et al., 2019). A meta-analysis found that the effects of biochar on soil fauna communities vary, and these differences are attributed to factors such as the feedstock type, pH, pyrolysis conditions, application rates and timing, as well as the physiological traits of the fauna organisms (e.g., body size, presence of exoskeleton) (Li et al., 2024).

### 3) Urease Activity in Soil

Urease is an enzyme that hydrolyzes urea into ammonia (NH<sub>3</sub>) or ammonium (NH<sub>4</sub><sup>+</sup>). In soil systems, urease activity is considered an important indicator for the urea cycle, nitrogen mineralization, and the utilization of nitrogen fertilizers (Koçak, 2020).

Urease activity reflects the rate of urea breakdown and, consequently, the transformation of ammonium sources in the soil. The urea-urease reaction forms a crucial link in the nitrogen cycle within soil systems. Urease is primarily produced by microorganisms, and changes in its activity are associated with the size and activity of microbial populations. Urease activity is sensitive to environmental conditions in the soil, such as pH, temperature, moisture, and the existence of microorganisms (Fisher et al., 2017).

### 4) Studies on the Effects of Biochar Applications on Soil Urease Activity

This section aims to examine studies conducted between 2014 and 2024 on the impacts of biochar applications—now popular in recent years—on urease enzyme activity in soil. It focuses on the mechanisms underlying conflicting findings in this area, emphasizing factors such as biochar production conditions (source type, the temperature of pyrolysis), application environment (laboratory or field), and dosage. The study compiles literature on biochar's potential to increase, decrease, or have a neutral effect on urease activity in soil.

In a laboratory incubation study using corn stalk biochar, it was reported that the increase in urease activity decreased as the pyrolysis temperature rose (Rahmanian & Khadem, 2024).

Zhang et al. (2023) established five treatments using biochar and urea (Control without fertilization, low and high applications of urea (LU and HU) and biocharbased urea (LBU and HBU) in a two-year field trial. They found that applications of urea increased soil urease activity but biochar-based urea significantly reduced this activity.

Yuan et al. (2022) investigated the effects on different biochar treatments (0, 5, 10, 20 and 50 t hm<sup>-2</sup>) on urease activity in a yellow soil based on field experiment. Authors reported that increase in biochar treatments led to first an increasing and then a decreasing pathway in soil urease activity. In addition, they indicated that this activity was stimulated after four months of biochar treatment

Dey and Mavi (2021) produced rice residue (RB) and poultry manure (PB) biochars at temperature 400°C and applied them on a sandy loam soil as six treatments in a 60-day incubation experiment [unamended soil as C, alone 200 kg N ha<sup>-1</sup> urea application as U, RB at 1%, PB at 1%, U+RB and U+PB]. Authors reported that U treatment was significantly highest among all treatments while RB or PB treatment didn't have any significant effect on soil urease activity compared to control. In addition, they found that co-application of biochar and urea stimulated this enzymatic activity by 24-31% and 23-33% compared to RB and PB after 60 days of incubation period, respectively.

Lopes et al. (2021) indicated that combined application of biochar produced from eucalyptus wastes at temperature 350°C and NPK fertilizer significantly stimulated soil urease activity under field conditions.

Sakin et al. (2021) treated biochar produced from different sources such as almond shell, tobacco waste, pomegranate peel, cotton waste, orange peel and wheat straw with a soil at the different doses (0, 0.5, 1 and 1.5%) to investigate their effects on soil urease activity under laboratory conditions for 37 weeks. Authors found that biochar at 0.5% was not significantly different with control and reported that biochar addition had no significant effect on urease activity in soil. Authors suggested that this may be associated with the possible changes of C/N rate on urease activity during the incubation period.

Futa et al. (2020) investigated the effects of biochar applications (0, 10, 20 and 40 t ha<sup>-1</sup>) on soil urease activity under winter rye. Authors produced the biochar from pyrolization of wheat straw at temperature 650°C and this biochar reduced this activity in each growing season in their study. Authors suggested that this effect might be associated with soil properties because of monoculture cropping and the age of biochar.

Laboratory incubation and pot experiments provide valuable data for understanding the immediate and short-term effects of biochar on enzyme activity. A global meta-analysis indicates that biochar significantly increases urease activity, particularly in short-term studies conducted within 100 days after application (Pokharel et al., 2020).

Tu et al. (2020) investigated the effects of biochar alone and bacteria loaded biochar on urease activities in a Cd and Cu contaminated soil by a pot experiment. Authors reported that biochar produced from maize straw had highly variable effects on enzymatic activities on the heavy metal contaminated soil. They found that there were generally no significant differences between control and biochar applications until 45th day of experiment but biochar treatments significantly increased soil urease activity after 45th day. Researchers in this study suggested that after heavy metals were stabilized, soil microbial functions were recovered.

Azeem et al. (2019) investigated the effects of six treatments including the combinations of biochar doses of 5 tons ha<sup>-1</sup> and 10 tons ha<sup>-1</sup> and NPK fertilizer on soil urease activity in a two-year field trial of mash bean-wheat cropping system. They reported that biochar addition significantly enhanced soil urease activity with a 20% increase compared to control in first year in mash bean but there were found no significant differences between control and treatments in the second year. They found that biochar addition reduced the urease activity in both years of study compared to control in wheat crop.

Cardelli et al. (2019) mixed the biochar produced from pruning residues of fruit trees at temperature 550°C with sandy and clay loamy soils to investigate the effects of this biochar at rate of 2% on urease activity. Authors reported that biochar treatment was significantly higher than control in sandy soil but no significant differences were found between biochar and control in clay loamy soil

Oladele (2019) conducted a two-year field study to investigate the effects of rice husk biochar at different doses (0, 3, 6, 12 t ha<sup>-1</sup>) on soil urease activity. Rice husk biochar has significantly stimulated this activity by 40% and 50% in the highest biochar rate application at soil depths 0-10 cm and 10-20 cm after two years of study.

Song et al. (2019) produced bamboo leaf biochar at temperature 500°C and applied it at different doses [0, 5(BC5) and 15 (BC15) t ha<sup>-1</sup>] in a Moso bamboo plantation within a 24-month field trial. They found that average soil urease activity was reduced by biochar treatments for 16.4% (BC5) and 20.3% (BC15) in the first year and for 15.9% (BC5) and 17.6% (BC15) in the second year.

It has been determined that the combination of hazelnut shell biochar and farmyard manure significantly increased urease activity (p<0.01) in soils where tomato plants were cultivated (Ergün, 2017).

Rizhiya et al. (2017) conducted a 90-day incubation experiment to investigate the effects of biochar produced from soft wood of broad-leaved trees at temperature 550°C on urease activity in a loamy sand soil. The treatments in their study were biochar at 10 t ha-1, NPK fertilizer at 90 kg N ha-1 and their combination. Authors reported that NPK application significantly stimulated this activity compared to control but the presence of biochar caused no significant reduction in this activity

Song et al. (2016) reported that biochar produced from maize stover at 500-600°C enhanced soil urease activity for more than 32% in upland soil and more than 50% in paddy soil under field conditions. Authors claimed that biochar was an efficient addition for stimulation of soil urease activity.

Huang et al., (2015) reported that biochar produced from rice husk at 600°C significantly reduced soil urease activity in pot experiment and no significant differences were found between the doses of biochar at 20 Mg ha<sup>-1</sup> and 40 Mg ha<sup>-1</sup>. Authors suggested that rate of biochar addition to urea fertilized paddy soils should be selected properly.

Demisie et al. (2014) incorporated the oak wood biochar and bamboo biochar, pyrolyzed at 600°C, with four different rates (0, 0.5, 1 and 2%) to a degraded red soil and investigated the effects of these biochars on soil urease activity in a pot experiment. Authors was measured this activity after 372 days and found that it was significantly higher in oak wood biochar at 0.5% and 2% doses and bamboo biochar at 0.5% than the rest of the applications. Authors suggested that higher microbial biomass in these treatments may have led to release more urease enzyme than other treatments.

### Conclusion

Soil urease activity is considered as an important parameter for modelling the nitrogen dynamics and influences the utilization rate of urea in soil. This enzymatic activity can be affected by many biotic and abiotic factors such as soil humidity and temperature, pH, nutrient availability and status and crops. It is known that this enzyme is mainly produced by soil microorganisms. Biochar can be produced from the pyrolysis of biomass including agricultural wastes or plant residues. This carbon rich material has widely used in agricultural and environmental activities. It is clear that biochar application is one of the main factors for enhancement of soil microbial biomass and soil nutrient availability. This mini-review found that biochar applications have increasing, decreasing and neutral effects on soil urease activity based on soil properties and source material of biochar.

### References

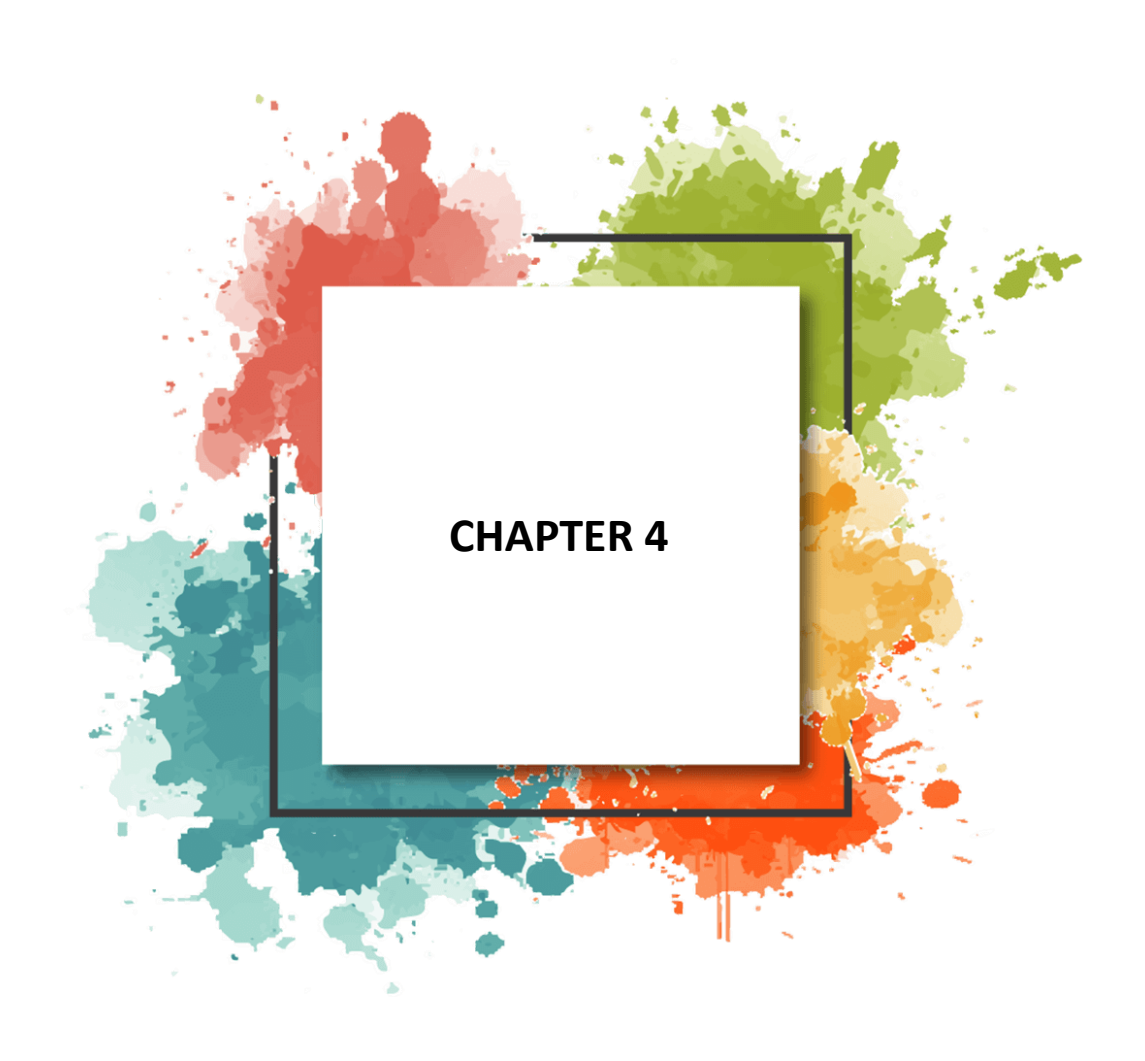
- Antal Jr, M.J. Grönli, M. (2003). The art, science, and technology of charcoal production. *Industrial and Engineering Chemistry Research*, 42(8): 1619-1640. https://doi.org/10.1021/ie0207919
- Azeem, M., Hayat, R., Hussain, Q., Tahir, M. I., Imran, M., Abbas, Z., ... & Irfan, M. (2019). Effects of biochar and NPK on soil microbial biomass and enzyme activity during 2 years of application in the arid region. *Arabian Journal of Geosciences*, 12(10), 311. https://doi.org/10.1007/s12517-019-4482-1
- Barbosa, F. L., Santos, J. M., Mota, J. C., Costa, M. C., Araujo, A. S., Garcia, K. G., ... & Pereira, A. P. D. A. (2024). Potential of biochar to restoration of microbial biomass and enzymatic activity in a highly degraded semiarid soil. *Scientific Reports*, 14(1), 26065. https://doi.org/10.1038/s41598-024-77368-9
- Bartoli, M., Troiano, M., Giudicianni, P., Amato, D., Giorcelli, M., Solimene, R., & Tagliaferro, A. (2022). Effect of heating rate and feedstock nature on electrical conductivity of biochar and biochar-based composites. *Applications in Energy and Combustion Science*, 12, 100089. https://doi.org/10.1016/j.jaecs.2022.100089
- Blanco-Canqui, H. (2017). Biochar and soil physical properties. *Soil Science Society of America Journal*, 81(4), 687-711. <a href="https://doi.org/1\_0.2136/sssaj2017.">https://doi.org/1\_0.2136/sssaj2017.</a> <a href="https://doi.org/1\_0.2136/sssaj2017">01.0017</a>
- Budak, M., Bektaş, H., & Polat, K. (2023). Biyoçar maddesinin tarımsal açıdan öneminin ortaya konulması. *Türkiye Teknoloji ve Uygulamalı Bilimler Dergisi*, 4(1), 10–19. https://doi.org/10.5281/zenodo.7950011
- Cardelli, R., Becagli, M., Marchini, F., & Saviozzi, A. (2019). Biochar impact on the estimation of the colorimetric-based enzymatic assays of soil. *Soil Use and Management*, *35*(3), 478-481. https://doi.org/10.1111/sum.12533
- Chen, B., & Yuan, M. (2011). Enhanced sorption of polycyclic aromatic hydrocarbons by soil amended with biochar. *Journal of Soils and Sediments*, 11(1), 62–71. https://doi.org/10.1007/s11368-010-0266-7
- Chia, C. H., Downie, A., & Munroe, P. (2015). Characteristics of biochar: physical and structural properties. In *Biochar For Environmental Management* (pp. 89-109). Routledge.
- Demisie, W., Liu, Z., & Zhang, M. (2014). Effect of biochar on carbon fractions and enzyme activity of red soil. *Catena*, 121, 214-221. https://doi.org/10.1016/j.catena.2014.05.020

- Dey, D., & Mavi, M. S. (2021). Biochar and urea co-application regulates nitrogen availability in soil. *Environmental Monitoring and Assessment*, 193(6), 326. https://doi.org/10.1007/s10661-021-09107-w
- Ergün, Y. A. (2017). The Effect of Biochar and Animal Manure Application on Some Enzyme Activities in Soil, CO<sub>2</sub> Production, Content of Nutrients, and the Growth of Tomato Plants. *Ordu Üniversitesi Fen Bilimleri Enstitüsü*, Ordu, Türkiye.
- Fisher, K. A., Yarwood, S. A., & James, B. R. (2017). Soil urease activity and bacterial ureC gene copy numbers: Effect of pH. *Geoderma*, 285, 1-8. https://doi.org/10.1016/j.geoderma.2016.09.012
- Franco, C. R., Page-Dumroese, D. S., & Archuleta, J. (2022). Forest management and biochar for continued ecosystem services. *Journal of Soil and Water Conservation*, 77(4), 60A-64A.
- Futa, B., Oleszczuk, P., Andruszczak, S., Kwiecińska-Poppe, E., & Kraska, P. (2020). Effect of natural aging of biochar on soil enzymatic activity and physicochemical properties in long-term field experiment. *Agronomy*, *10*(3), 449. https://doi.org/10.3390/agronomy10030449
- Gul, S., Whalen, J. K., Thomas, B. W., Sachdeva, V., & Deng, H. (2015). Physicochemical properties and microbial responses in biochar-amended soils: Mechanisms and future directions. *Agriculture, Ecosystems & Environment*, 206, 46–59. https://doi.org/10.1016/j.agee.2015.03.015
- Günal, E., & Erdem, H. (2018). Biyoçarın toprağın fiziksel, kimyasal ve biyolojik özelliklerine etkileri. *Adnan Menderes Üniversitesi Ziraat Fakültesi Dergisi*, 5(10), 29–58.
- Holatko, J., Kucerik, J., Mustafa, A., Lonova, K., Siddiqui, M. H., Naveed, M., ... & Brtnicky, M. (2025). Influence of biochar feedstock blends on soil enzyme activity, nutrient cycling, lettuce biomass accumulation and photosynthesis. BMC plant biology, 25(1), 323 https://doi.org/10.1186/s12870-025-06352-w
- Huang, M., Zhou, X., Chen, J., Cao, F., Jiang, L., & Zou, Y. (2017). Interaction of Changes in pH and Urease Activity Induced by Biochar Addition Affects Ammonia Volatilization on an Acid Paddy Soil Following Application of Urea. Communications in Soil Science and Plant Analysis, 48(1), 107–112. https://doi.org/10.1080/00103624.2016.1253725
- Idbella, M., Baronti, S., Giagnoni, L., Renella, G., Becagli, M., Cardelli, R., ... & Bonanomi, G. (2024). Long-term effects of biochar on soil chemistry, biochemistry, and microbiota: Results from a 10-year field vineyard experiment. *Applied Soil Ecology*, 195, 105217. https://doi.org/10.1016/j.apsoil.2023.105217

- Jiang, Y., Wang, X., Zhao, Y., Zhang, C., Jin, Z., Shan, S., & Ping, L. (2021). Effects of biochar application on enzyme activities in tea garden soil. Frontiers in Bioengineering and Biotechnology, 9, 728530. https://doi.org/10.3389/fbioe.2021.728530
- Kandeler, E., & Gerber, H. (1988). Short-term assay of soil urease activity using colorimetric determination of ammonium. *Biology and Fertility of Soils*, 6(1), 68–72. https://doi.org/10.1007/BF00257924
- Karaca, A., Turgay, O. E., & Şahin, F. (2014). Toprak Biyolojisi. *Ankara Üniversitesi Ziraat Fakültesi Yayınları*, 1630.
- Khan, S., Irshad, S., Mehmood, K., Hasnain, Z., Nawaz, M., Rais, A., Gul, S., Wahid, M. A., Hashem, A., Abd\_Allah, E. F., & Ibrar, D. (2024). Biochar production and characteristics, its impacts on soil health, crop production, and yield enhancement: A review. *Plants*, 13(2), 166. https://doi.org/10.3390/plants13020166,
- Kim, K. H., Kim, J. Y., Cho, T. S., & Choi, J. W. (2012). Influence of pyrolysis temperature on physicochemical properties of biochar obtained from the fast pyrolysis of pitch pine (Pinus rigida). *Bioresource Technology*, 118, 158-162. https://doi.org/10.1016/j.biortech.2012.04.094
- Koçak, B. (2020). Importance of urease activity in soil. In International Scientific and Vocational Studies Congress–Science and Health (Vol. 12, pp. 12-15). BILMES SH.
- Li, T., Jiao, Y., Liu, T., Gu, H., Li, Z., Wang, S., & Liu, J. (2024). Effects of biochar addition on soil fauna communities—A meta-analysis. *Soil Use and Management*, 40(3), e13096. https://doi.org/10.1111/sum.13096
- Li, X., Wang, T., Chang, S. X., Jiang, X., & Song, Y. (2020). Biochar increases soil microbial biomass but has variable effects on microbial diversity: A meta-analysis. *Science of the Total Environment*, 749, 141593. https://doi.org/10.1016/j.scitotenv.2020.141593
- Liang, M., Lu, L., He, H., Li, J., Zhu, Z., & Zhu, Y. (2021). Applications of biochar and modified biochar in heavy metal contaminated soil: A descriptive review. *Sustainability*, *13*(24), 14041. https://doi.org/10.3390/su132414041
- Lopes, É. M. G., Reis, M. M., Frazão, L. A., da Mata Terra, L. E., Lopes, E. F., Dos Santos, M. M., & Fernandes, L. A. (2021). Biochar increases enzyme activity and total microbial quality of soil grown with sugarcane. *Environmental Technology & Innovation*, 21, 101270. https://doi.org/10.1016/j.eti.2020.101270

- Lorenz, K., & Lal, R. (2014). Biochar application to soil for climate change mitigation by soil organic carbon sequestration. *Journal of Plant Nutrition and Soil Science*, 177(5), 651–670. https://doi.org/10.1002/jpln.201400058
- Oladele, S. O. (2019). Effect of biochar amendment on soil enzymatic activities, carboxylate secretions and upland rice performance in a sandy clay loam Alfisol of Southwest Nigeria. *Scientific African*, 4, e00107. https://doi.org/10.1016/j.sciaf.2019.e00107
- Palansooriya, K. N., Wong, J. T. F., Hashimoto, Y., Huang, L., Rinklebe, J., Chang, S. X., ... & Ok, Y. S. (2019). Response of microbial communities to biocharamended soils: a critical review. *Biochar*, *I*(1), 3-22. https://doi.org/10.1016/S1002-0160(15)30058-8
- Pokharel, P., Ma, Z., & Chang, S. X. (2020). Biochar increases soil microbial biomass with changes in extra- and intracellular enzyme activities: a global meta-analysis. *Biochar*, 2(1), 65–79. https://doi.org/10.1007/s42773-020-00039-1
- Premalatha, R. P., Poorna Bindu, J., Nivetha, E., Malarvizhi, P., Manorama, K., Parameswari, E., & Davamani, V. (2023). A review on biochar's effect on soil properties and crop growth. *Frontiers in Energy Research*, *11*, 1092637. https://doi.org/10.3389/fenrg.2023.1092637
- Rahmanian, M., & Khadem, A. (2024). The effects of biochar on soil extra and intracellular enzymes activity. *Biomass Conversion and Biorefinery*, *14*(12), 21993–22005. https://doi.org/10.1007/s13399-023-04330-6
- Rizhiya, E. Y., Mukhina, I. M., Vertebniy, V. E., Horak, J., Kononchuk, P. Y., & Khomyakov, Y. V. (2017). Soil enzymatic activity and nitrous oxide emission from light-textured spodosol amended with biochar. *Agricultural Biology (Sel'skokhozyaistvennaya biologiya)*, 52, 464.
- Sakin, E., Ramazanoglu, E., & Seyrek, A. (2021). Effects of different biochar amendments on soil enzyme activities and carbondioxide emission. *Communications in Soil Science and Plant Analysis*, 52(22), 2933-2944. https://doi.org/10.1080/00103624.2021.1971694
- Singh Yadav, S. P., Bhandari, S., Bhatta, D., Poudel, A., Bhattarai, S., Yadav, P.,... & Oli, B. (2023). Biochar application: A sustainable approach to improve soil health. *Journal of Agriculture and Food Research*, 11, 100498. https://doi.org/10.1016/j.jafr.2023.100498
- Singh, H., Northup, B. K., Rice, C. W., & Prasad, P. V. (2022). Biochar applications influence soil physical and chemical properties, microbial diversity, and crop productivity: a meta-analysis. *Biochar*, *4*(1), 8. <a href="https://doi.org/10.1007/s42773-022-00138-1">https://doi.org/10.1007/s42773-022-00138-1</a>

- Song, D., Xi, X., Huang, S., Liang, G., Sun, J., Zhou, W., & Wang, X. (2016). Short-term responses of soil respiration and C-cycle enzyme activities to additions of biochar and urea in a calcareous soil. *PloS One*, *11*(9), e0161694. https://doi.org/10.1371/journal.pone.0161694
- Song, Y., Li, Y., Cai, Y., Fu, S., Luo, Y., Wang, H., ... & Chang, S. X. (2019). Biochar decreases soil N<sub>2</sub>O emissions in Moso bamboo plantations through decreasing labile N concentrations, N-cycling enzyme activities and nitrification/denitrification rates. *Geoderma*, 348, 135-145. https://doi.org/10.1016/j.geoderma.2019.04.025
- Tu, C., Wei, J., Guan, F., Liu, Y., Sun, Y., & Luo, Y. (2020). Biochar and bacteria inoculated biochar enhanced Cd and Cu immobilization and enzymatic activity in a polluted soil. *Environment International*, *137*, 105576. https://doi.org/10.1016/j.envint.2020.105576
- Xu, W., Xu, H., Delgado-Baquerizo, M., Gundale, M. J., Zou, X., & Ruan, H. (2023). Global meta-analysis reveals positive effects of biochar on soil microbial diversity. *Geoderma*, 436, 116528. https://doi.org/10.1016/j.geoderma.2023.116528
- Yuan, F., Li, K. Y., Yang, H., Deng, C. J., Liang, H., & Song, L. H. (2022). Effects of biochar application on yellow soil nutrients and enzyme activities. Huan Jing Ke Xue= Huanjing Kexue, 43(9), 4655-4661. https://doi.org/10.13227/j.hjkx.202112155
- Zhang, S., Zhou, J., Chen, J., Ge, T., Cai, Y., Yu, B., ... & Li, Y. (2023). Changes in soil CO<sub>2</sub> and N<sub>2</sub>O emissions in response to urea and biochar-based urea in a subtropical Moso bamboo forest. *Soil and Tillage Research*, 228, 105625. https://doi.org/10.1016/j.still.2022.105625
- Zhao, R., vd. (2022). Urea hydrolysis in different farmland soils as affected by biochar application: impacts on urease activities and microbial gene abundance. Frontiers in Environmental Science, 10:950482. https://doi.org/10.3389/fenvs.2022.950482
- Zhu, Z., Zhang, Y., Tao, W., Zhang, X., Xu, Z., & Xu, C. (2025). The biological effects of biochar on soil's physical and chemical characteristics: A review. *Sustainability*, *17*(5), 2214. https://doi.org/10.3390/su17052214



# Inference for Weibull Expected Shortfall From Record Data

Çağatay Çetinkaya<sup>1</sup>

### Introduction

In modern financial and actuarial science, risk quantification at the tail of the loss distribution has gained central importance. The motivation comes from the fact that extreme events, although rare, can have catastrophic consequences for financial institutions, insurance companies and pension funds. Two important risk measures that capture negative risks are Risk Value (VaR) and Expected Shortfall (ES), also known as Conditional Risk Value (CVaR) or Tail Value at Risk (TVaR).

The Risk Value (VaR) at the confidence level  $\alpha$  is defined as the number of losses distributed at that level. Formally, it specifies a threshold for losses that exceed this level with probability  $(1-\alpha)$ . Despite its widespread use in regulatory frameworks, VaR suffers from major limitations. In particular, it does not provide information on the severity of losses beyond the quantifiable and does not satisfy the coherence property in risk theory, particularly sub-additivity. This means that VaR can underestimate the benefits of diversification and cannot capture systemic dependencies in the tail.

Expected Shortfall (ES) overcomes these drawbacks. Defined as the expected loss conditional on exceeding the VaR, ES provides a richer representation of tail risk. Mathematically, at confidence level  $\alpha$ :

$$ES_{\alpha} = E[X|X > Var_{\alpha}(X)] \tag{1}$$

where  $VaR_{\alpha}(X) = \inf\{x \in \mathbb{R}: \mathbb{P}(X \leq x) \geq \alpha\}$  and X denotes the loss variable. ES is a consistent risk measurement in the sense of Artzner et al. (1999) meets monotony, sub-additivity, translation invariance and positive homogeneity. This property has led to the preferential treatment of ES over VaR in regulatory frameworks where it is now the main standard for determining capital requirements.

The development of the expected shortfall as a risk measurement is based on a solid theoretical foundation. Acerbi and Tasche (2002) provide an axiomatic justification for ES as a coherent alternative to VaR. They showed that ES

<sup>&</sup>lt;sup>1</sup> Department of Actuarial Sciences, Kırıkkale University, Türkiye ORCID: 0000-0001-8010-4261

captures the entire tail distribution, making it more sensitive to extreme results. Embrechts, Klüppelberg, and Mikosch (1997) emphasized the importance of large-scale models in financial and actuarial risk and further highlighted the limitations of quantifiable measures such as VaR. In actuarial contexts, Goovaerts, Kaas, and Dhaene (2003) discussed risk measures under distortion functions, showing how ES naturally appears in premium principles and solvency assessments.

In many practical cases, a complete random sample is not always available for statistical analysis. Instead, observations can be collected in the form of record values, which occur when observations exceed all previous values in a sequence (Arnold, Balakrishnan, Nagaraja, 2011; Nevzorov, 2001). These records play an important role in reliability analysis, climate science, and actuarial science, where interest is often centered on behaviour of extreme results rather than the whole distribution.

The natural generalization of classical records is given by the values of k-record, and observations are considered to be records if they exceed the previous k-largest value rather than the maximum value (Dhar & Nagaraja, 2015). This concept significantly increases the data efficiency of tail modelling by providing more frequent recording points than traditional records, while still capturing extreme information. For actuarial data, such as catastrophic insurance claims or maximum lifespans, k-records can extract valuable tail information even if the data set is sparse, censored or only partially available (Ahsanullah, Nevzorov & Shakil, 2013).

The advantage of using k record values in actuarial inference is twofold. First, they offer a modest but informative way of presenting extreme observations without the need to obtain a complete dataset, which may be difficult or expensive to obtain. Secondly, the k records maintain the essential structure of the tail risk needed to evaluate measures such as the expected shortfall. Consequently, the inference based on the k record value provides a practical and effective methodology for actuaries and risk managers who must assess liquidity, price reinsurance or longevity risk in a limited or incomplete data scenario (Balakrishnan & Ahsanullah, 1994).

The aim of this study is to develop inference procedures for ES under the Weibull distribution based on k-record values. Point estimators are derived together with their asymptotic confidence intervals. Theoretical results are further validated through simulation experiments, and the practical applicability of the proposed methods is illustrated using healthcare charges dataset.

### **Expected Shortfall for the Weibull Distribution**

The Weibull distribution has the following probability density (pdf) and cumulative distribution (cdf) functions,

$$f_X(x) = \lambda \beta x^{\beta - 1} e^{-\lambda x^{\beta}}, \quad x > 0, \lambda, \beta > 0$$
 (2)

$$F_X(x) = 1 - e^{-\lambda x^{\beta}} \tag{3}$$

Where  $\lambda$  is scale and  $\beta$  is the shape parameters. Then, replacing (2) in (1), ES for the Weibull distribution is obtained as

$$ES_{\alpha} = \frac{\lambda^{-\frac{1}{\beta}}}{1-\alpha} \Gamma\left(1 + \frac{1}{\beta}, -\ln(1-\alpha)\right) \tag{4}$$

It is clear that  $ES_{\alpha}$  is strictly decreasing in  $\lambda$  (for all  $\lambda > 0, \beta > 0$ ). On the other hand, effect of  $\beta$  is ambiguous. The sign of  $\partial ES_{\alpha}/\partial \beta$  depends on the balance  $\ln \lambda$  and the truncated-gamma mean  $M(1/\beta, t)$ . In special cases, if  $\lambda = 1$ ,  $ES_{\alpha}$  decreases with  $\beta$ . For small  $\lambda$ , it tends to decrease with  $\beta$ , for large  $\lambda$  it can increase.

### Inference of $ES_{\alpha}$ Based on k-Record Values

Let  $X_1, X_2, ...$  be a sequence of independent and identically distributed (iid) random variables with cdf  $F_X(x)$  and pdf  $f_X(x)$ . Assuming that  $F_X(x)$  is continuous and non-degenerate, the observation  $X_i$  is termed an upper record value if it exceeds all previous observations, that is, if  $X_j >$  $max\{X_1, X_2, \dots X_{j-1}\}, j \ge 2$ . A similar definition applies to lower record values (Arnold, 2011). The concept of record values was first introduced by Chandler (1952). A major advantage of using record values is that they allow statistical inference to be made from fewer observations compared to using the entire sample. Since only the record values are required, this approach can lead to savings in time, cost, and effort. Consequently, record values and their theoretical properties have attracted considerable attention in many practical fields, including climate studies, natural disasters, economics, sports, and life-testing experiments. In practical applications, record data are observed rather infrequently, and the expected waiting time for each successive record beyond the first one is infinite. Indeed, in a random sample of size n, only about  $\log n$ records are typically observed. To address this limitation, Dziubdziela and Kopociński (1976) introduced the concept of k-record values as a generalization of the upper record values. The k-record process is constructed with respect to the  $k^{th}$  largest observation observed up to a given point. For the continuous case, let  $X_{i:n}$  denote the  $i^{th}$  order statistic in a random sample of size n. Then, for a fixed positive integer k, the sequence of k-record times  $T_{n(k)}$  can be defined accordingly (see Arnold et. Al., 2011) as  $T_{1(k)} = k$  and

$$T_{n(k)} = min\left\{j: j > T_{n-1(k)}, X_j > X_{T_{n-1(k)}-k+1:T_{n-1(k)}}\right\}$$

where n=2,3,... Thus, the sequence of upper k-record value is observed as  $U_{n(k)}=X_{T_{n(k)}-k+1:T_{n(k)}}$ . From the definition, it follows that the first k-record corresponds to the minimum observation within the finite sequence  $X_1,...,X_k$ ; that is,  $U_{1(k)}=X_{1:k}$ . When k=1, this formulation reduces to the classical upper record values.

Let assume  $U_{1(k)}, U_{2(k)}, \dots, U_{n(k)}$  be the first n, k-records from the Weibull distribution with parameters  $(\lambda, \beta)$ . Then, the likelihood function of the observed record values  $U_{i(k)}$  (i = 1, 2, ..., n) is obtained as

$$L(U|\lambda,\beta) = k^n (1 - F(U_n))^k \prod_{i=1}^n \frac{f(U_i)}{1 - F(U_i)},$$
 (5)

Then, replacing Equations (2) and (3) in (5) we obtain

$$L(U|\lambda,\beta) = \lambda^n \beta^n e^{(\beta-1)\sum_{j=1}^n \ln U_j - k\lambda U_n^{\beta}}$$
 (6)

The corresponding log-likelihood function is given by

$$\ell(U|\lambda,\beta) = n \ln \lambda + n \ln \beta - k\lambda U_n^{\beta} + (\beta - 1) \sum_{j=1}^{n} \ln U_j$$
 (7)

To obtain the MLEs of the parameters, denoted by  $\hat{\lambda}$  and  $\hat{\beta}$ , we should equate the partial derivates of  $\ell(U|\lambda,\beta)$  to zero with respect to  $\lambda$  and  $\beta$  respectively. Then we obtain, the MLE of  $\lambda$  and  $\beta$  as in the following.

$$\hat{\lambda} = \frac{n}{k U_{n(k)}^{\beta}}$$

where

$$\hat{\beta} = \frac{n}{n \log U_{n(k)} - \sum_{i=1}^{n} U_i}$$

Due to the invariance property of maximum likelihood estimators, the estimator of  $ES_{\alpha}$ , denoted by  $\widehat{ES}_{\alpha}$  is obtained by substituting the parameter

estimates—derived from the equalities above—into Equation (4). The resulting expression is given as follows

$$\widehat{ES}_{\alpha} = \frac{\widehat{\lambda}^{-1/\widehat{\beta}}}{1 - \alpha} \Gamma\left(1 + \frac{1}{\widehat{\beta}}, -\ln(1 - \alpha)\right)$$
 (8)

# Approximate Confidence Interval for $\widehat{ES}_{\alpha}$

Approximate confidence intervals (ACI) for  $\widehat{ES}_{\alpha}$  can be derived based on the asymptotic normality of the maximum likelihood estimators. The asymptotic covariance matrix necessary for this construction is obtained from the inverse of the expected Fisher information matrix.

$$I(\lambda,\beta) = -\begin{bmatrix} \frac{\partial^2 \ell(U|\lambda,\beta)}{\partial^2 \lambda} & \frac{\partial^2 \ell(U|\lambda,\beta)}{\partial \lambda \partial \beta} \\ \frac{\partial^2 \ell(U|\lambda,\beta)}{\partial \beta \partial \lambda} & \frac{\partial^2 \ell(U|\lambda,\beta)}{\partial^2 \beta} \end{bmatrix} = \begin{bmatrix} I_{11} & I_{12} \\ I_{21} & I_{22} \end{bmatrix}$$

Then, inverse of the Fisher information matrix for the observed sample gives the asymptotic variances as follows

$$\operatorname{Var}(\hat{\lambda}) \approx (I^{-1})_{11} = \frac{\frac{m}{\beta^2} + k\lambda C}{\frac{m}{\lambda^2} \left(\frac{m}{\beta^2} + k\lambda C\right) - (kB)^2}$$

$$\operatorname{Var}(\hat{\beta}) \approx (I^{-1})_{22} = \frac{\frac{m}{\lambda^2}}{\frac{m}{\lambda^2} \left(\frac{m}{\beta^2} + k\lambda C\right) - (kB)^2}$$

$$\operatorname{Cov}(\hat{\lambda}, \hat{\beta}) \approx (I^{-1})_{12} = (I^{-1})_{21} = -\frac{kB}{\frac{m}{\lambda^2} \left(\frac{m}{\beta^2} + k\lambda C\right) - (kB)^2}$$

where

$$A:=\mathbb{E}\left[U_n^\beta\right], B:=\mathbb{E}\left[U_n^\beta\ln\,U_n\right], C:=\mathbb{E}\left[U_n^\beta(\ln U_n)^2\right]$$

On the other hand,  $\widehat{ES}_{\alpha}$ , is asymptotically normal distributed with mean  $ES_{\alpha}$  and variance

$$\sigma_{ES_{\alpha}}^{2} = \sum_{j=1}^{2} \sum_{i=1}^{2} \frac{\partial ES_{\alpha}}{\partial \theta_{i}} \frac{\partial ES_{\alpha}}{\partial \theta_{j}} I_{ij}^{-1}$$

$$= \left(\frac{\partial ES_{\alpha}}{\partial \lambda}\right)^{2} I_{11}^{-1} + \left(\frac{\partial ES_{\alpha}}{\partial \beta}\right)^{2} I_{22}^{-1} + 2\left(\frac{\partial ES_{\alpha}}{\partial \lambda}\right) \left(\frac{\partial ES_{\alpha}}{\partial \beta}\right) I_{12}^{-1}$$

where  $(\theta = \lambda, \beta)$ ,  $s = 1 + 1/\beta$ ,  $q = -\ln(1 - \alpha)$  and

$$\frac{\partial ES_{\alpha}}{\partial \lambda} = -\frac{\lambda^{-1/\beta - 1}}{\beta (1 - \alpha)} \Gamma(s, q)$$

$$\frac{\partial ES_{\alpha}}{\partial \beta} = \frac{\lambda^{-1/\beta}}{(1 - \alpha)\beta^{2}} \left( \ln \lambda \Gamma(s, q) - \int_{q}^{\infty} t^{s - 1} \ln t e^{-t} dt \right)$$

Consequently, the  $100(1-\gamma)\%$  asymptotic confidence interval of  $ES_{\alpha}$  can be constructed by

$$\left(\widehat{ES}_{\alpha}, -z_{1-\frac{\gamma}{2}}\widehat{\sigma}_{ES_{\alpha}}, \widehat{ES}_{\alpha}, +z_{1-\frac{\gamma}{2}}\widehat{\sigma}_{ES_{\alpha}}\right)$$

where  $z_{\gamma}$  is the  $100\gamma^{th}$  percentile of standard normal distribution.

### **Simulation Studies**

In this section, we provide some simulation studies to evaluate the performances of the theoretical outcomes. In this purpose, we consider different confidence levels as  $\alpha=0.90$  and  $\alpha=0.95$ , respectively. We use two different sets of actual parameter values as  $(\lambda,\beta)=(2.50,1.50)$  and  $(\lambda,\beta)=(0.75,2.00)$ . We perform these plans for different number of k-record times. We choose different k values as (3,4) and record times (n) as (8,10,12,15). We perform simulations 1000 times and reported the point estimates  $\widehat{ES}_{\alpha}$  with mean squared errors (MSE). We also provide the average ACIs with their corresponding average lengths (AL). All computations are performed in R (R Core Team, 2023) software. The results are reported in Tables 1-2.

Our findings demonstrate three key patterns:

- 1. Expected shortfall values increase with higher confidence levels.
- **2.** Estimation accuracy improves with sample size, evidenced by reduced bias, lower MSE, and narrower confidence intervals.
- **3.** Smaller values k yield superior estimation performance, with  $\widehat{ES}_{\alpha}$  estimates closely approximating their true values.

α	k	n	$ES_{\alpha}$	$\widehat{ES}_{\alpha}$	MSE	ACI	AL
0.90	3	8	1.1936	1.1643	0.0801	0.6723;1.6564	0.9841
		10		1.1837	0.0626	0.7393;1.6281	0.8889
		12		1.1887	0.0551	0.7758;1.6016	0.8258
		15		1.2128	0.0499	0.8085;1.6170	0.8086
	4	8		1.1401	0.0960	0.6020;1.6783	1.0763
		10		1.1657	0.0676	0.7005;1.6309	0.9304
		12		1.1784	0.0521	0.7668;1.5900	0.8233
		15		1.1958	0.0418	0.8173;1.5742	0.7569
0.95	3	8	1.3588	1.2946	0.1139	0.7064;1.8828	1.1764
		10		1.3303	0.0826	0.8166;1.8440	1.0274
		12		1.3462	0.0663	0.8801;1.8123	0.9321
		15		1.3624	0.0584	0.9284;1.7965	0.8682
	4	8		1.2826	0.1437	0.6131;1.9520	1.3390
		10		1.3094	0.0960	0.7500;1.8688	1.1188
		12		1.3287	0.0719	0.8438;1.8136	0.9697
		15		1.3451	0.0552	0.9223;1.7679	0.8456

Tablo 1: Simulation results for  $\lambda = 2.5$ ,  $\beta = 1.5$ .

α	k	n	$ES_{\alpha}$	$\widehat{ES}_{\alpha}$	MSE	ACI	AL
0.90	3	8	2.0784	2.0290	0.1380	1.3937;2.6643	1.2706
		10		2.0561	0.1059	1.4867;2.6255	1.1387
		12		2.0777	0.0950	1.5323;2.6231	1.0907
		15		2.0883	0.0875	1.5604;2.6163	1.0560
	4	8		1.9969	0.1659	1.2997;2.6940	1.3943
		10		2.0277	0.1099	1.4315;2.6239	1.1924
		12		2.0471	0.0936	1.5091;2.5850	1.0759
		15		2.0727	0.0711	1.5802;2.5651	0.9849
0.95	3	8	2.2928	2.2055	0.1812	1.4673;2.9438	1.4765
		10		2.2420	0.1320	1.5928;2.8912	1.2984
		12		2.2645	0.1082	1.6765;2.8526	1.1762
		15		2.2895	0.0913	1.7393;2.8396	1.1003
	4	8		2.1837	0.2392	1.3359;3.0315	1.6956
		10		2.2207	0.1554	1.5171;2.9244	1.4073
		12		2.2493	0.1165	1.6360;2.8627	1.2266
		15		2.2689	0.0876	1.7325;2.8054	1.0729

**Tablo 2:** Simulation results for  $\lambda = 0.75$ ,  $\beta = 2$ .

# **Data Study (Actuarial Example)**

In this section, the healthcare charges dataset used in this study was obtained from the Kaggle repository, where it was initially uploaded by Miri Choi (2018) in Seoul, South Korea. We first fit the medical insurance costs incurred by the insured person by the Weibull distribution and evaluate the goodness of fit.

We first scaled data by dividing 10000 for better fitting. Then, we fit the data to the Weibull model defined Equations (2)-(3). We obtain the parameter estimations as  $\hat{\lambda} = 0.6678$  with standard error 0.0218 and  $\hat{\beta} = 1.1755$  with standard error 0.0242. The graphical presentation of the goodness of fit is shown in Figure 1. Figures are drawn using "fitdistrplus" package (Delignette-Muller and Dutang, 2015) in R software (R Core Team, 2023).

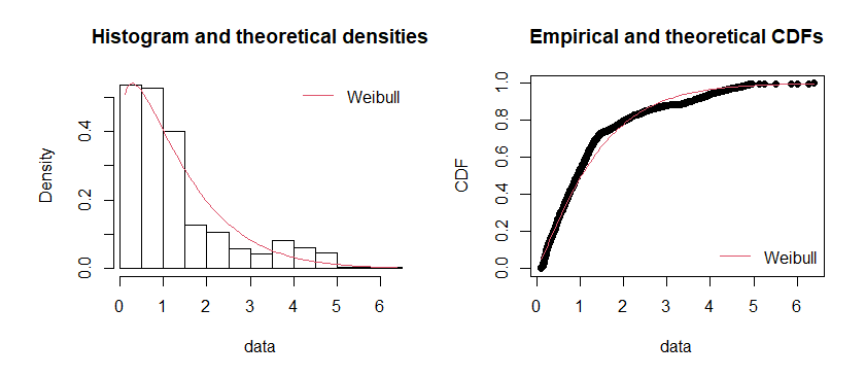


Figure 1: Graphical assessment of the Weibull distribution fit.

Histogram and theoretical density plot and empirical and theoretical cdfs plot show good fit of data to the Weibull distribution. Another important point this data consists of sufficient record points. Table (3) provides the record times of the scaled dataset based on different k values. Then, we calculated the  $\widehat{ES}_{\alpha}$  estimates for different confidence levels as  $\alpha = 0.90$ ,  $\alpha = 0.95$  and  $\alpha = 0.99$ , respectively. Thus, we obtain the ES estimates under different confidence levels using different number of record values. The results are reported in Table (4).

	0.173	0.445	1.688	2.198	2.781	2.892	3.684	3.770
k=2	3.871	3.961	3.977	4.817	4.882	4.889	5.119	5.857
	6.002	6.259						
	0.173	0.445	0.824	1.688	2.198	2.781	2.892	3.684
k=3	3.770	3.871	3.961	3.977	4.750	4.817	4.855	4.882
	4.889	5.119	5.514	5.857	6.002			
	0.173	0.387	0.445	0.728	0.824	1.688	2.198	2.781
k=4	2.892	3.684	3.770	3.871	3.961	3.977	3.984	4.358
K=4	4.729	4.750	4.817	4.852	4.855	4.868	4.882	4.889
	5.119	5.259	5.514	5.857				

Tablo 3: Record times in charges dataset.

α	k	n	$\widehat{ES}_{\alpha}$	ACI	AL
0.90	2	18	2.9023	1.4746;4.3300	2.8553
	3	21	3.4246	2.0863;4.7629	2.6766
	4	28	3.2957	2.1524;4.4390	2.2866
0.95	2	18	3.3615	1.8525;4.8706	3.0181
	3	21	3.9499	2.5303;5.3695	2.8392
	4	28	3.8146	2.5973;5.0319	2.4346
0.99	2	18	4.3572	2.6705;6.0439	3.3735
	3	21	5.0815	3.4433;6.7198	3.2765
	4	28	4.9385	3.5243;6.3527	2.8284

Tablo 4: Estimates based on charges dataset.

#### **Conclusions**

In this study, inference procedures for the ES under the Weibull distribution based on k-record values have been developed. The theoretical framework integrates record value theory with tail risk measurement, allowing efficient estimation of tail-dependent risk measures even when full random samples are not available. This provides a practical alternative for actuarial and financial applications where data collection is costly or restricted to extreme observations.

The MLEs of the Weibull parameters were derived from the likelihood function constructed on k-records, and the corresponding ACIs were obtained using the Fisher information matrix. Simulation experiments across various parameter configurations, confidence levels, and record sizes confirmed the reliability and robustness of the proposed estimators. The results showed that estimation accuracy improves with increasing record size and that smaller k values generally yield more efficient estimates. Furthermore, the expected

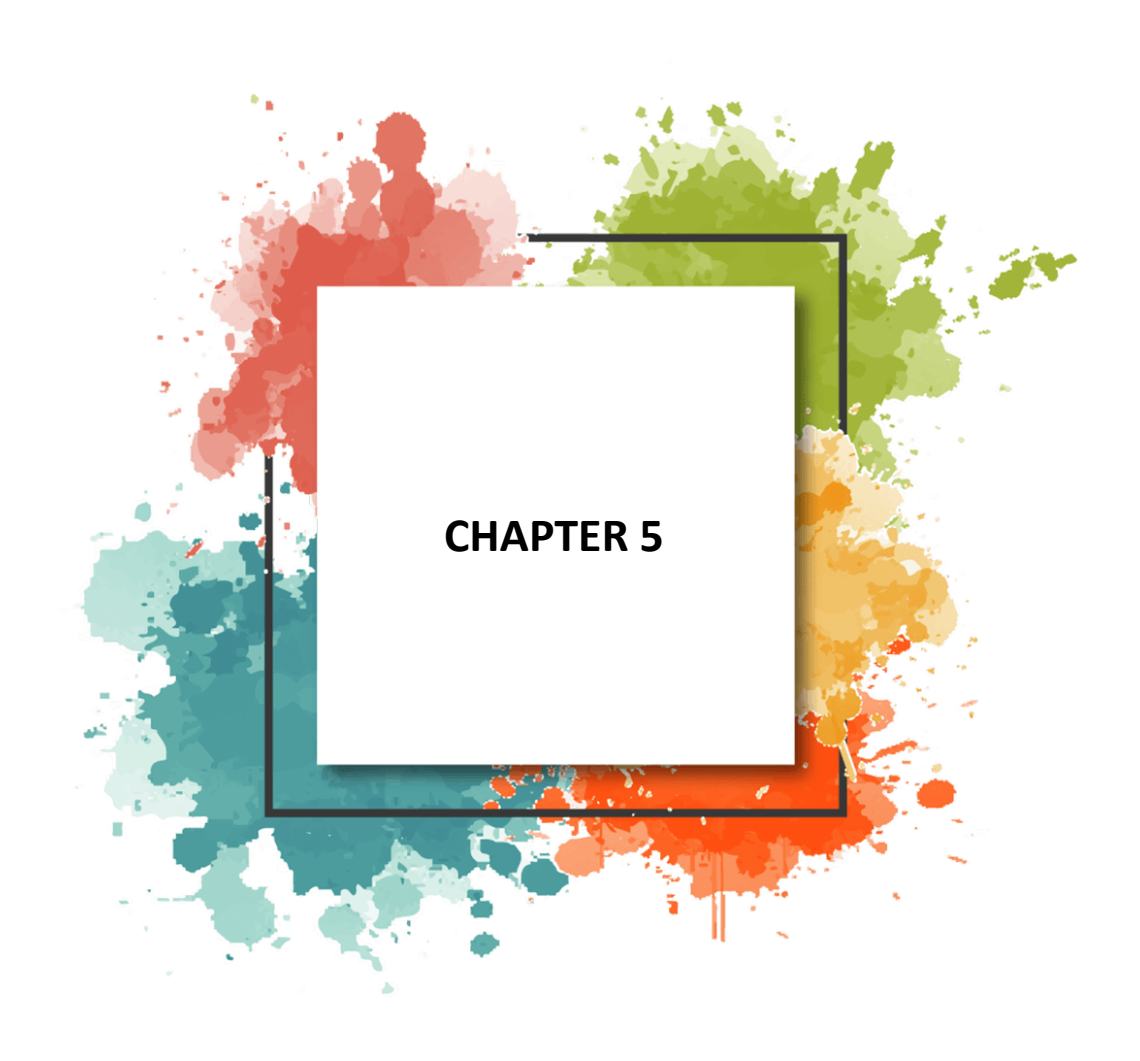
shortfall estimates increased with higher confidence levels, consistent with theoretical expectations.

The empirical application using a medical insurance cost dataset demonstrated that the Weibull model provides a satisfactory fit to real actuarial data. The ES estimates based on k-records successfully captured the tail behaviour of the data, indicating that the proposed inference procedure is suitable for assessing extreme loss events in insurance and financial risk contexts.

Overall, this research contributes to the literature by combining record theory and risk measurement, offering a flexible framework for tail risk estimation under incomplete data structures. Future work may extend this approach to other heavy-tailed distributions, dependent record structures, or Bayesian inference settings to further enhance the applicability of record-based ES estimation in risk management and actuarial practice.

# References

- Ahsanullah, M., Nevzorov, V. B., & Shakil, M. (2013). An Introduction to Records. Atlantis Press.
- Arnold, B. C., Balakrishnan, N., & Nagaraja, H. N. (1998). Records. John Wiley & Sons.
- Artzner, P., Delbaen, F., Eber, J. M., & Heath, D. (1999). Coherent measures of risk. Mathematical Finance, 9(3), 203–228.
- Acerbi, C., & Tasche, D. (2002). Expected shortfall: a natural coherent alternative to value at risk. Economic Notes, 31(2), 379–388.
- Balakrishnan, N., & Ahsanullah, M. (1994). Relations for single and product moments of record values from exponential distribution and some applications. Journal of Applied Statistical Science, 1(3), 261–272.
- Chandler, K. (1952). The distribution and frequency of record values. Journal of the Royal Statistical Society: Series B (Methodological), 14(2), 220-228.
- Choi, M. (2018). Healthcare insurance dataset. Kaggle. https://www.kaggle.com/datasets/mirichoi0218/insurance.
- Dhar, S. K., & Nagaraja, H. N. (2015). On k-record values and related statistics. Journal of Statistical Planning and Inference, 161, 63–76.
- Delignette-Muller, M. L., & Dutang, C. (2015). fitdistribus: An R package for fitting distributions. Journal of statistical software, 64, 1-34.
- Dziubdziela, W., & Kopociński, B. (1976). Limiting properties of the k-th record values. Applicationes Mathematicae, 15, 187-190.
- Embrechts, P., Klüppelberg, C., & Mikosch, T. (1997). Modelling Extremal Events for Insurance and Finance. Springer.
- Goovaerts, M. J., Kaas, R., & Dhaene, J. (2003). Risk measures, measures of risk, and insurance premium principles. Insurance: Mathematics and Economics, 33(1), 19–34.
- McNeil, A. J., & Frey, R. (2000). Estimation of tail-related risk measures for heteroscedastic financial time series: an extreme value approach. Journal of Empirical Finance, 7(3–4), 271–300.
- Nevzorov, V. B. (2001). Records: Mathematical Theory. American Mathematical Society.
- R Core Team (2023). R: A language and environment for statistical computing. R Foundation for Statistical Computing, Vienna, Austria. URL https://www.R-project.org/.
- Tasche, D. (2002). Expected shortfall and beyond. Journal of Banking & Finance,



# The Role of Dampening Solution in Offset Printing Technology: Its Effects On Print Quality and Productivity

Aslı Boztemir Tiftik<sup>1</sup>

#### 1. INTRODUCTION

Offset printing technology has long been, and continues to be, a foundational element of the printing industry, enjoying widespread use in modern applications. Its common selection for both commercial printing establishments and industrial manufacturing stems from compelling advantages like superior print fidelity, cost-effectiveness, and efficient operational workflows (Smith & Johnson, 2020). In offset lithography, a specially formulated fountain solution is employed to establish the critical balance between ink and water. The correct functioning of this system is vital for the proper operation of offset presses and the maintenance of consistent print quality (Harper & Wilson, 2019). The fountain solution is more than an auxiliary agent; it is an integral and indispensable component of the printing process.

The function of the fountain solution on the printing plate is of paramount importance. Specifically, its role in shielding non-image areas from ink and preserving their cleanliness is a major determinant in the consistency of print quality. By ensuring that ink is transferred exclusively to designated image areas, the fountain solution helps maintain sharp and clean printed output (Miller & Roberts, 2018). Attaining this equilibrium is the fundamental prerequisite for high-quality prints. Failure to do so can result in ink transferring to unintended non-image regions, causing degradation in print quality and the emergence of unwanted artifacts (Turner & Walker, 2017).

The chemical characteristics of the fountain solution are influential throughout the printing operation. Variables such as pH value, electrical conductivity, and water hardness can directly affect print outcomes. For example, precise pH adjustment can prolong the life of the printing plate, whereas excessively acidic or alkaline conditions may damage the plate surface (Smith & Johnson, 2020). Similarly, utilizing water with high conductivity or hardness can adversely impact the printing system's efficiency by disrupting the ink-water balance (Miller & Roberts, 2018).

-

 $<sup>^{\</sup>rm 1}$ İstanbul Üniversitesi-Cerrahpaşa, ORCID ID 0009-0006-2490-9624

Proper preparation of the fountain solution underpins the efficient operation of printing machinery. Consistently monitored fountain solution formulations foster stable printing processes and contribute to a safer working environment for operators. Keeping the fountain solution at appropriate pH, conductivity, and hardness levels enhances printing system efficiency and helps preserve print quality (Wang & Lee, 2021). Moreover, any imbalance related to the fountain solution can provoke technical issues during printing, potentially necessitating job reprints (Harper & Wilson, 2019).

The fountain solution's role extends beyond print quality, carrying significant environmental and economic implications. The adoption of eco-friendly fountain solution formulations can bolster sustainability within the printing sector. For instance, water reclamation strategies or the implementation of automated dosing systems can contribute to environmental protection and cost reduction (Green, 2022). Such innovations not only boost efficiency in the printing industry but also minimize its ecological footprint.

# 2. FUNDAMENTAL PRINCIPLES OF THE OFFSET PRINTING SYSTEM

The operational basis of offset printing is the mutual repulsion of oil and water. This system utilizes an offset printing plate characterized by a grained (micro-pitted) surface coated with a light-sensitive emulsion. Following exposure and development, the plate surface exhibits emulsified (image-receptive) areas and non-emulsified (water-receptive, non-image) areas. During the printing cycle, the plate first makes contact with dampening rollers. This interaction deposits a thin film of water onto the non-emulsified, non-image areas. Subsequently, when the plate engages with the ink rollers, the water-covered grained regions repel the oil-based ink. Conversely, the smooth-surfaced, emulsified image areas accept ink from the rollers. This mechanism allows the ink and water layers to coexist on the plate without intermingling, preparing them for transfer (Boztemir, 2013).

MürekkepÜnitesi
Mürekkep Kabul Eden Emülsiyonlu Alan
Mürekkep Merdanesi
Mürekkep Merdanesi
Mürekkebi İten Grenli
Alan

Nemlendirme Ünitesi

Baskı altı malzemesi

Nemlendirme
Merdanes

Image 1. Offset Printing System (Boztemir, 2013)

Achieving the correct ink-water balance necessitates the precise application of fountain solution. An excessive amount of fountain solution can impede proper ink distribution, resulting in a pale print. Conversely, an insufficient supply allows ink to migrate to non-image areas, leading to print defects like scumming or toning (Brown, 2020). The accurate metering of fountain solution is therefore a critical determinant in maintaining print quality (Green, 2022).

The chemical attributes of the fountain solution, including its pH value, conductivity, and hardness, also influence this equilibrium. Consequently, careful attention to these fountain solution-related parameters in offset presses plays a vital role in ensuring consistent print quality (Miller & Roberts, 2018).

#### 3. DEFINITION AND FUNCTION OF FOUNTAIN SOLUTION

In offset lithography, the ink-water balance stands as one of the most crucial parameters for achieving high-quality print results.

Conventional offset printing requires both printing ink and a fountain solution, typically a mixture of water and specific additives, to apply ink selectively to the printing plate. Initially, the printing plate is moistened by the fountain solution. Non-image areas readily accept this water, while image areas repel it. In the subsequent phase, ink is applied. The dampened sections of the plate reject the ink, whereas the dry, image-bearing areas accept it. For this process to function correctly, the water must possess specific characteristics, which are imparted through carefully prepared mixtures and additives. This specially treated water, enhanced with additives for printing suitability, is known as the fountain solution.

The precision with which the fountain solution ratio is adjusted during printing directly correlates with the perfection of the print outcome. Improper adjustment can lead to numerous negative consequences. These may include faintness in the printed image, a reduction in halftone dot size, excessive ink consumption resulting in toning (ink adhering to non-image areas), diminished color intensity, and over-dampening of the paper stock, which can cause structural distortions (Boztemir, 2013).

The fountain solution aids in confining ink transfer exclusively to the intended areas, thereby ensuring the sustainability of print quality (Wilson & Thompson, 2021).

By preventing ink from bleeding or spreading to non-image areas, the fountain solution obviates such undesirable outcomes (Green, 2022). Additionally, this fluid helps prevent the plate surface from overheating. Since temperature increases during printing can lead to significant degradation in print quality, the fountain solution's cooling effect helps maintain plate surface stability. Achieving this delicate balance makes it possible to secure high-quality results throughout the printing run.

The correct application of fountain solution also contributes to overall stability in printing machinery. It supports the smooth functioning of the mechanical systems within the presses. A continuously monitored and correctly formulated fountain solution enhances the efficiency of the printing process and helps create a safer operational environment (Harper & Wilson, 2019). Precise adjustment of fountain solution properties such as pH value, hardness level, and conductivity directly impacts print quality. Therefore, monitoring and, when necessary, adjusting the fountain solution are fundamental requirements for the efficient operation of printing machines (Smith & Johnson, 2020).

Regular maintenance and diligent management of the fountain solution are of considerable importance for preserving print quality. Ideal fountain solution formulations deliver optimal performance during every printing operation, which helps prevent issues in printing machinery and averts quality loss. Furthermore, the adoption of environmentally friendly fountain solution formulations and automated dosing systems offers substantial benefits in terms of sustainability while concurrently boosting efficiency in printing processes (Green, 2022). Such innovations can contribute to cost reduction and the minimization of environmental impacts within the printing sector.

# 4. CHEMICAL PROPERTIES OF FOUNTAIN SOLUTION

For the fountain solution to perform effectively, its chemical composition must be precisely regulated. A paramount factor is the pH value, which should ideally be maintained within the range of 4.8 to 5.5. When the fountain solution operates within this specified pH range, it helps prevent corrosion on the printing plate, thereby extending its operational life. pH values that are excessively low can lead to abrasion of the plate surface, while high pH levels can disrupt the inkwater balance, adversely affecting print quality (Miller & Roberts, 2018). Consistent monitoring of the fountain solution's pH level, with interventions as needed to meet the correct criteria, is crucial for printing process efficiency.

Conductivity, measured in microsiemens per centimeter ( $\mu$ S/cm), is another vital property indicating the concentration of ions within the fountain solution. High conductivity often suggests an excessive quantity of additives, which can result in a decline in print quality. The optimal conductivity value generally lies between 800 and 1500  $\mu$ S/cm. Elevated conductivity values can negatively influence water quality and lead to imbalances in ink receptivity. Consequently, the conductivity of the fountain solution should be regularly checked in printing machines, and corrective actions implemented when necessary (Turner & Walker, 2017).

Water hardness also significantly influences the chemical characteristics of the fountain solution. Hard water, rich in ions like calcium and magnesium, can lead to the formation of deposits within the press over time. Such build-up diminishes the efficiency of printing machinery and necessitates more frequent maintenance. Therefore, water softening is of great importance. The softening process, particularly by removing calcium and magnesium ions, inhibits deposit formation. Moreover, maintaining water hardness at a specific level is essential for the system's proper functioning, typically aimed between 100–150 mg/L (equivalent to approximately 5.6-8.4 °dH, though direct conversion can vary based on units used for mg/L source) (Brown, 2020). The use of water softening systems is instrumental in preventing these potential problems.

The chemical properties of the fountain solution—pH, conductivity, and hardness—not only directly affect print quality but also have environmental implications. For instance, high conductivity and hardness can contribute to the generation of environmentally detrimental waste. This has spurred an increasing search for eco-friendly solutions within the printing industry. Environmentally conscious fountain solution formulations often involve minimal additive use and incorporate biodegradable compounds. Such formulations lessen the

environmental footprint of the printing process while concurrently enhancing efficiency (Adams & Zhao, 2022). Furthermore, the integration of environmentally sensitive water treatment and recycling systems in printing facilities enables the reuse of wastewater, thereby curtailing resource consumption.

To ensure consistent print quality, the chemical composition of the fountain solution must be continuously monitored. Regular analyses permit the tracking of the water's pH value, hardness, conductivity, and other constituents. These monitoring systems help prevent erroneous print outcomes and facilitate more efficient printing processes. Moreover, technological advancements, including digital measuring devices, allow for more precise and rapid management of fountain solution parameters (Martin & Clark, 2021). Such developments in the printing industry ensure the ongoing improvement of print quality.

# 5. ADDITIVES USED FOR FOUNTAIN SOLUTION

Fountain solution formulations extend beyond pure water, incorporating various chemical additives designed to improve print quality. These additives fulfill numerous roles, from adjusting the fountain solution's pH to reducing its surface tension. Acids introduced into the fountain solution lower the pH level, which protects the printing plate surface and ensures that ink adheres only to the intended image areas. Weak acids, such as phosphoric and citric acid, are commonly employed because they facilitate precise pH control and contribute to extending the lifespan of the printing plate (Miller & Roberts, 2018). Failure to manage pH can lead to high levels that disrupt the ink-water balance, negatively impacting print quality.

Buffer solutions represent another crucial category of additives. These substances help stabilize the pH of the fountain solution, preventing deviations that could compromise print quality. An unstable pH can lead to color distortions, issues with ink receptivity, and undesirable contamination on the plate surface during printing. Therefore, buffer solutions ensure the chemical stability of the fountain solution, thereby maintaining consistent print quality (Harper & Wilson, 2019). Buffers used in fountain solutions create an equilibrium between acidic and basic components, allowing the solution to remain stable over extended periods.

In essence, a buffer agent is a vital additive that maintains a constant pH value in the fountain solution. It typically comprises an acid and its conjugate salt. The pH value and conductivity are influenced by the dosage of this buffer agent (Boztemir, 2013).

Surfactants (surface-active agents) are also key additives. They enable the water to spread more effectively over the plate surface by reducing surface tension. This promotes even water distribution, ensuring ink transfers only to the image areas. However, the overuse of surfactants can lead to foaming, which can introduce undesirable effects into the printing process. Consequently, these substances must be used judiciously to prevent excessive foam generation (Turner & Walker, 2017). Surfactants also modify the water's viscosity, contributing to more efficient water distribution during printing.

Biocides (antibacterial agents) and chelating agents are other important additives. Biocides prevent microbial contamination of the fountain solution, keeping the water cleaner for longer durations. This is critically important for maintaining system stability, especially during extended print runs. Chelating agents, conversely, bind metal ions present in the water, thereby preventing the formation of deposits and contamination. These additives enhance the overall quality of the fountain solution, ensuring the efficient and long-term operation of printing machinery (Jones & Wilson, 2020).

# 6. EFFECT OF FOUNTAIN SOLUTION ON PRINT QUALITY

In offset printing, a harmonious interaction between ink and water on the plate is essential. This compatibility, achieved at the point of ink and water meeting during printing, depends not only on the ink's characteristics but also on the properties of the water used and the fountain solution concentrate.

The recommended ideal hardness for water in offset printing ranges between 8-12 °dH (German degrees of hardness). If the available water is harder, it should be treated, and its hardness adjusted to the desired level using suitable printing auxiliaries.

Within the offset printing system, as the pH of the dampening water trends towards more acidic values, it can progressively weaken halftone dots. To mitigate such losses, the pH of the dampening water during printing should be consistently maintained between 4.8 and 5.3.

Fountain solution concentrates, which impart various beneficial properties to the printing water, are indispensable for achieving optimal print results. The use of these concentrates, containing a diverse array of chemical substances such as acids, bases, inorganic salts, glycols, surfactants, corrosion inhibitors, and biocides, positively influences the printing outcome.

Employing fountain solution facilitates more efficient printing through ideal wetting; optimal wetting of the non-image areas of the printing plate is achieved

by rapidly establishing a perfect ink-water balance with minimal water (Boztemir, 2013).

The fountain solution not only shields the printing plate from ink and foreign contaminants but also plays a pivotal role in the continuity and stability of print quality. In the offset system, the correct equilibrium of water and ink is the most fundamental requirement for quality printing. While the fountain solution keeps the printing surface clean, it also enhances process efficiency by maintaining this crucial ink-water balance. Preserving this balance ensures the long-term healthy operation of printing machines and minimizes printing errors (Wang & Lee, 2021).

Achieving the correct ink-water balance, a primary factor influencing print quality, is paramount. Excessive fountain solution can hinder proper ink spread, leading to pale and indistinct images. Conversely, insufficient water can cause ink to transfer to unintended non-image areas, resulting in contamination. Such issues negatively affect print quality and reduce machine efficiency. Operators who correctly manage the amount of fountain solution help prevent printing defects (Brown, 2020).

The lifespan of the printing plate is directly contingent on the chemical properties and formulation of the fountain solution. Utilizing an appropriate pH value and correct additives extends plate life and improves print quality. Conversely, issues like pH imbalance or high conductivity can lead to corrosion on the plate surface. This corrosion causes a decline in print quality and may necessitate frequent plate replacement, which in turn increases production costs and adversely affects printing process efficiency (Miller & Roberts, 2018).

Proper management of the fountain solution enhances not only print quality but also the efficiency of the printing press. A well-formulated fountain solution mixture provides stability throughout the printing process and prevents fluctuations in print quality. Excessively acidic or alkaline fountain solutions can lead to frequent malfunctions or increased maintenance needs in printing machines, elevating operational costs and reducing process efficiency. For this reason, the chemical components of the fountain solution must be regularly monitored and adjusted (Green & Walker, 2020).

The consistency of print quality is directly linked to the chemical control of the fountain solution and optimal formulations. The fountain solution maintains the ink-water balance, ensuring the printing plate surface functions efficiently. When correct formulations are employed, contamination of non-image areas on the plate with ink is prevented, yielding high print quality. This control is particularly important for large-volume printing operations, as it ensures consistently high-quality output (Jones & Thompson, 2021).

The influence of fountain solution on print quality is a significant consideration in offset printing systems. Effective management of the fountain solution, maintenance of the ink-water balance, and protection of the plate surface are all necessary for a high-quality and efficient printing process. Operators who continuously monitor this balance ensure the efficient operation of printing machinery and the consistency of print quality (Turner & Walker, 2017).

# 7. PROBLEMS AND SOLUTION PROPOSALS

# 7.1. pH Imbalance

In offset printing, the pH level of water (where 'p' denotes potential or power, and 'H' signifies Hydrogen ions) indicates the acidity or alkalinity of the medium. On the pH scale, values from 0 to 7 are acidic, and 7 to 14 are alkaline (Uğur, 2007).

It is a measure of the acidity or alkalinity of an aqueous solution. A pH of 7 is neutral. Solutions with a pH below 7 are acidic, and those above 7 are alkaline. Treated fountain solution typically has a pH between 6.5 and 7. However, various printing studies and experiments indicate that optimal dampening in offset printing, leading to high-quality prints, is achieved with water having a pH between 4.8 and 5.3. This specific range is attained by adding additives to the fountain solution (Boztemir, 2013).

A pH imbalance in the fountain solution is a frequent issue in offset printing. The pH level directly impacts both the printing plate and ink characteristics. When the pH deviates from the ideal 4.8-5.5 range, corrosion can occur on the plate surface, and the proper distribution of ink can be compromised. Imbalances stemming from excessively acidic (low pH) or alkaline (high pH) water can cause numerous problems.

# *If the fountain solution is overly acidic:*

- It can etch or irritate the surface of the aluminum printing plate.
- It may cause halftone dots to shrink, leading to a loss of tonal value.
- As the irritated plate surface binds less water, toning (ink adhering to non-image areas) can occur.
  - Acids can react with driers in the ink, impeding oxidative drying.

# *If the fountain solution is overly alkaline:*

- Fats (fatty acids) in the ink can be dissolved by the alkali, leading to saponification (formation of fatty acid salts).
- Since saponified molecules have components that attract both water and ink, the interfacial tension between water and ink is significantly reduced.
- Ink and water can partially mix, leading to emulsification (often termed 'scumming' or 'greasing'). Halftone dots may enlarge, and non-image areas can become toned (Boztemir, 2013).

The solution to these issues involves regular pH monitoring and, when necessary, rebalancing using pH buffer solutions. Maintaining a stable pH not only preserves print quality but also extends printing plate life. pH measuring devices are essential for this control, and frequent measurements can help identify factors causing pH instability. Additionally, using pH-adjusting chemicals in manufacturer-recommended quantities prevents the creation of an overly acidic or alkaline environment.

Another factor in achieving pH balance is the water's inherent composition. Dissolved minerals or chemical contaminants can lead to pH instability. Water purification and monitoring are necessary to prevent this. Furthermore, operator training on the correct use of pH regulators is important for consistent results and preventing quality loss (Turner & Walker, 2017; Green & Wilson, 2020).

# 7.2. High Conductivity of Fountain Solution

Conductivity is a measure of a substance's ability to conduct electricity. For aqueous solutions, it is typically measured in microSiemens per centimeter  $(\mu S/cm)$ . Pure water contains very few ions and is a poor electrical conductor; ions are the charge carriers. The higher the ion concentration in water, the higher its conductivity.

Measuring conductivity serves as a method to control the dosage of fountain solution additives. As the additive concentration increases, conductivity generally rises proportionally. Unlike pH, there isn't a universally ideal conductivity value, but a range of approximately 800-1500  $\mu$ S/cm is often considered acceptable as a guideline (Boztemir, 2013).

High conductivity, resulting from an excessive concentration of ions in the fountain solution (often due to too many additives or the use of hard water), can directly impair print quality. It can hinder the proper spreading of ink on the plate

and cause printing errors. Specifically, high conductivity can make the ink overly fluid, leading to issues like ink slippage or fading during printing. This may compel the press operator to make constant adjustments, reducing production efficiency.

To resolve this, fountain solution with high conductivity must be brought within ideal levels. Installing water softening systems is highly beneficial, as these systems regulate water hardness and ion levels, thereby reducing conductivity and ensuring stable press operation. Additionally, using the correct proportions of additives can address excessive conductivity. Therefore, adhering to manufacturer-recommended chemical quantities and avoiding over-dosing is crucial.

Furthermore, frequent changes of the water in printing machines can prevent prolonged use of high-conductivity water. Using such water not only affects print quality but can also accelerate wear on machine parts. Regular water changes, keeping it fresh, can lead to long-term improvements in both print quality and machine longevity (Harper & Wilson, 2019; Smith & Johnson, 2020).

# 7.3. Foaming

Foaming is typically caused by an excessive amount of surfactants in the fountain solution. While surfactants ensure even spreading of the solution on the plate, their overuse leads to foam formation on the water surface. Foaming can result in undesirable consequences such as splashing within the press, uneven water distribution, and printing defects. Foam can prevent proper water contact with the plate, disrupting the ink-water balance and degrading print quality. It can also cause mechanical problems, blockages, and increased maintenance.

To address foaming, surfactant dosage must be carefully controlled, adjusting amounts based on specific formulations and printing conditions. The use of antifoaming additives (defoamers) can also be effective in eliminating excess foam by helping it dissipate quickly and aiding even water spread. Beyond reducing surfactant use, identifying and eliminating other factors contributing to foaming during printing is also important.

Minimizing foaming requires regular cleaning of printing machines and attention to water cleanliness. Monitoring the quality of water used can help prevent foam formation, as clean, pure water can reduce unwanted surfactant reactions. Such measures enable more efficient press operation while maintaining high-quality print results (Miller & Roberts, 2018; Green, 2022).

#### 7.4. Hardness of Fountain Solution

Water is classified as soft or hard based on the concentration of magnesium and calcium salts. A common unit of measurement is the 'German degree of hardness' (°dH), with a typical measurement range of 0-40 °dH. If one liter of water contains 10 mg of Calcium Oxide (dissolved or ionic), its hardness is 1 German degree (1°dH). Note that 1 °dH (German) = 1.781 °fH (French) = 17.8 ppm (US, typically as CaCO<sub>3</sub> equivalent).

The ideal hardness for offset fountain solution is generally considered to be between 7-12 °dH. If the hardness is 15 °dH or higher, magnesium and calcium in the solution can react with fatty acids in the printing ink, forming soapy (alkaline) deposits. This can cause several problems:

- These alkaline formations can accept both water and ink, leading to non-image areas (toned areas) filling in with ink.
- They can fill the pores on ink roller surfaces, causing them to become glazed and impairing good ink transfer.
- They can accumulate on dampening rollers, leading to their deterioration. They may also settle on the blanket surface, causing it to retain too much water and, consequently, transfer ink poorly.
- This can lead to excessive ink spread (emulsification causing the image to 'open up') on the paper.
  - These negative effects intensify as water hardness increases.
- Conversely, water hardness below 3 °dH can lead to rusting and contamination of rollers.

Therefore, the hardness of water intended for offset printing should be adjusted, typically by adding purified water, to fall within the 7 to 12 °dH range, and this level should be regularly monitored (Boztemir, 2013).

#### 8. FOUNTAIN SOLUTION AND PRODUCTIVITY

The correct application of fountain solution is a significant factor directly influencing the productivity of offset printing machines. Appropriate chemical composition of the water used in the printing process allows machines to operate continuously and without issues. The use of incorrect components or excessive water can disrupt the ink-paper balance, negatively affecting print quality. This scenario leads to printing errors and material waste, thereby increasing operational costs (Öztürk, 2020).

Homogeneous distribution of water can enhance the speed of printing machines and reduce printing times. Insufficient water quantity or improper water components can impede ink transfer, thus lowering printing speed. Conversely, effective water management enables machines to operate at higher speeds, thereby increasing production capacity and leading to an upturn in overall output. Furthermore, efficient water use helps optimize ink consumption, resulting in less material wastage during the printing process (Yılmaz, 2021).

Another element contributing to enhanced productivity is the precise adjustment of the fountain solution's pH level. When the pH level is excessively acidic or alkaline, distortions in print quality occur, which can prolong the printing process and escalate production costs. Consequently, the correct pH value is a parameter that directly affects both print quality and production speed. With technological advancements, automated monitoring and adjustment of these parameters optimize the efficiency of printing machines (Çelik, 2019).

#### 9. ENVIRONMENTAL AND ECONOMIC

The judicious management of fountain solution is critically important for environmental sustainability. Reducing water consumption and facilitating water recycling directly contributes to the conservation of water resources. Minimizing the volume of water used, especially in industrial printing machinery, promotes the efficient utilization of this vital resource. These practices help diminish environmental impacts while also aiding in the preservation of natural resources. Additionally, recycling used water reduces the quantity of wastewater generated, thereby minimizing adverse environmental effects (Öztürk, 2020).

Another significant environmental factor related to fountain solution management is the use of eco-friendly chemicals. Traditional chemicals can degrade water quality and contribute to environmental pollution. Therefore, the adoption of biodegradable and environmentally sound chemicals should be actively encouraged. Eco-friendly chemicals reduce waste volumes, protecting the ecological balance. Furthermore, the use of such chemicals supports long-term environmental sustainability because they readily decompose in nature and leave a minimal impact on the ecosystem (Yılmaz, 2021).

From an economic standpoint, the proper management of fountain solution directly influences business costs. Ensuring the water used in printing machines is mixed with the correct components and that appropriate adjustments are made increases efficiency and reduces expenditures. Incorrect water components and excessive water use can lead to printing errors and material loss, thereby increasing waste rates and, consequently, operational costs. Efficient water use

optimizes these costs, providing businesses with long-term economic advantages (Celik, 2019).

Furthermore, managing environmental and economic impacts assists businesses in complying with sustainability policies. Particularly in the current climate, environmentally conscious consumers and business partners increasingly prefer eco-friendly production processes. In this context, environmentally sound water management practices can enhance a business's brand value and provide a competitive edge. Economically, eco-friendly methods also offer long-term benefits through lower energy and material consumption (Çelik, 2019).

# 10. ADVANCED TECHNOLOGIES IN FOUNTAIN SOLUTION MANAGEMENT

In recent years, numerous advanced technologies have emerged in fountain solution management, significantly boosting the efficiency of printing machines. Digital monitoring systems enable real-time tracking of parameters such as water pH level, temperature, and hardness. These systems continuously assess water quality and automatically make necessary adjustments based on the printing machine's operational conditions. This ensures water quality is maintained at an optimal level, leading to improved print quality and reduced error rates (Yılmaz, 2021).

Smart sensors, integrated with these digital monitoring systems, track all fountain solution parameters with greater precision. These sensors detect the water's chemical composition, pH level, and factors like temperature in real-time, transmitting immediate feedback to the printing machine. This allows users to intervene rapidly in case of any anomalies. Additionally, smart sensors ensure that water is mixed with the correct components, which prevents errors and losses in the printing process (Öztürk, 2020).

Automated dosing systems represent another key technological advancement. These systems ensure that water is accurately mixed with the appropriate chemical components. The system automatically controls the proportional mixing of substances added to the water, eliminating human error and minimizing the margin of error in water preparation, thereby helping to maintain stable print quality. Moreover, correct dosing optimizes chemical and water consumption, offering both environmental and economic advantages (Yılmaz, 2021).

Energy saving is a further significant benefit of these technologies. Digital monitoring and automatic dosing systems render water management more

efficient, thereby reducing the energy consumption of printing machines. The correct and efficient operation of these systems ensures that water and chemicals are used only in the required amounts, resulting in lower energy consumption and reduced operating costs. Furthermore, thanks to these technologies, printing machines can operate without problems for longer durations, thus also reducing maintenance costs (Çelik, 2019).

The application of advanced technologies not only increases efficiency but also supports environmental sustainability. It aids in achieving environmental objectives such as more efficient use of water resources, reduction of waste, and increased recycling rates. Minimizing environmental impacts, particularly in the printing sector, provides businesses with a competitive advantage and contributes to the development of eco-friendly production processes. These technologies have become an indispensable component of sustainable production (Çelik, 2019).

#### 11. CONCLUSION

In offset printing systems, the fountain solution plays an indispensable role in maintaining print quality consistency and ensuring the efficiency of the production process. By establishing the correct equilibrium between ink and water, the fountain solution enables the smooth execution of printing. This balance can only be preserved through appropriate chemical content and regular maintenance. Even minor alterations in fountain solution quality can lead to significant declines in print quality and inefficient machine operation. Consequently, the fountain solution must be meticulously formulated and diligently monitored.

The chemical characteristics of the fountain solution are direct determinants of printing process success. Variables such as pH value, conductivity, and hardness allow for the anticipation of potential technical problems during printing. Therefore, printing operators must possess comprehensive knowledge about fountain solution and effectively apply this knowledge during operations. Prudent management of the fountain solution ensures high and consistent print quality.

The efficiency of printing machinery is contingent upon the correct management of the fountain solution. Regular maintenance, preservation of chemical balance, and the use of appropriate additive quantities ensure system longevity. Well-designed fountain solution formulations not only improve print quality but also reduce production costs. In this context, operator training is of great importance for the proper management of the fountain solution.

Looking ahead, the widespread adoption of environmentally friendly fountain solution formulations and automated dosing systems will foster more efficient and sustainable printing processes. Such innovations will curtail energy and water consumption in the printing sector while minimizing environmental impact. These advancements, which will also yield economic benefits, will enable the printing industry to operate with greater efficiency and effectiveness.

In summary, fountain solution is not merely a technical element in offset printing systems but a critical factor that dictates quality. Therefore, investments in fountain solution management are essential for consistently upholding high print quality and for the efficient operation of production processes. This management approach, when combined with modern technologies, will guide the printing sector towards a more environmentally friendly and sustainable future. The development of advanced technologies in fountain solution management in recent years has already enhanced the efficiency of printing machines.

#### REFERENCES

- [1] ADAMS, R., & ZHAO, Q. (2022). Environmental Impact Of Water-Based Solutions In Offset Printing, Green Printing Technology, 11(2), 34-47.
- [2] BROWN, C. (2020). Printing Press Optimization And Water Balance İn Printing Processes. Journal Of Industrial Printing, 22(5), 45-56.
- [3] ÇELİK, M., (2019). Ofset Baskı Teknolojilerinde Kalite Kontrol (2. Baskı), Baskı Yayıncılık, Istanbul.
- [4] GREEN, L. (2022), Water Management İn Modern Printing, Journal Of Print Technology, 15(4), 112-125.
- [5] GREEN, L., & WALKER, S. (2020), The İmportance of Water Management in High-Volume Printing, Journal of Print Quality, 28(2), 99-111.
- [6] HARPER, B., & WİLSON, T. (2019), Water-Based Technologies in Offset Printing, Paper & Print, 42(1), 52-66.
- [7] JONES, M., & WİLSON, T. (2020). Additives in Offset Printing: Enhancing Water Properties, Journal of Print Innovation, 19(3), 125-138.
- [8] JONES, M., & THOMPSON, R. (2021), Ensuring Consistency in Offset Printing: The İmpact of Water Management, PrintTech Research, 33(6), 49-63.
- [9] MARTÍN, T., & CLARK, E. (2021), Digital Monitoring of Water Properties in Offset Printing, Advanced Print Technology, 40(4), 88-102.
- [10] MİLLER, J., & ROBERTS, L. (2018), Chemical Influences in Printing Processes, Journal of Printing Science, 35(2), 112-130.
- [11] ÖZTÜRK, S., *Baskı Makineleri ve Çevresel Etkileri*, Yüksek Yayıncılık, Ankara, 2020.
- [12] SMİTH, R., & JOHNSON, P. (2020), *Principles of Offset Printing: A Comprehensive Guide*, Printing Technology Press.
- [13] TURNER, P., & WALKER, S. (2017), Offset Printing Technology: Fundamentals and Processes, Printing Journal, 25(3), 77-89.
- [14] YILMAZ, F., Ofset Baskı Sistemleri: Teknolojik Gelişmeler ve Verimlilik (1st Ed.), Endüstriyel Yayınlar, Izmir, 2021.
- [15] WANG, S., & LEE, H. (2021). The Role of Water in the Offset Printing Process, PrintTech Journal, 18(4), 75-88.
- [16] BOZTEMİR, A., Karton Etiket Üretiminde Standardizasyon Süreçlerinin Uygulanması, Marmara University Institute of Science, Department of Printing Education, Master's Thesis, Istanbul, 2013
- [17] UĞUR, E., Renk Bilgisi ve Renk Yönetimi, Kuşbakışı Yayınevi, Istanbul, 2007

Spanish Case. Netherlands: Springer.



# On Pseudo-Slant Submanifolds of Kähler-Norden Manifolds

# Süleyman Dirik<sup>1</sup> & Ramazan Sarı<sup>2</sup>

#### 1. Introduction

In [4], B.-Y. Chen proposed the notion of slant submanifolds within the framework of almost Hermitian manifolds. A submanifold is said to be slant if the angle  $\theta$  formed between IX and the tangent bundle is constant for every tangent vector field X. Such submanifolds constitute an intermediate class between complex submanifolds ( $\theta = 0$ ) and totally real submanifolds ( $\theta = \frac{\pi}{2}$ ). Since their introduction, slant submanifolds have been extensively investigated, yielding a substantial body of results and a wide range of examples. In addition, several generalizations of this concept have been developed, notably the classes of semi-slant, bi-slant, and generic submanifolds.

Research on slant submanifolds has also been broadened to encompass both odd-dimensional structures and semi-Riemannian manifolds.

Let (M, J, g) be a manifold endowed with a (1,1)-tensor field J satisfying  $J^2 =$ +I and a metric q. Different cases arise according to the specific compatibility relations between I and g.

- $I^2 = -I$  and g(JX, JY) = g(X, Y), (M, J, g) is an almost complex manifold.
- $I^2 = -I$  and g(IX, IY) = -g(X, Y), (M, J, g) is a Norden manifold.
- $I^2 = I$  and g(IX, IY) = g(X, Y), (M, I, g) is an almost product manifold.
- $J^2 = I$  and g(JX, JY) = -g(X, Y), (M, J, g) is an almost paracomplex manifold.

The class of Norden manifolds was originally introduced by A.P. Norden under the name B-manifolds [10], and in some references they are also referred to as anti-Kähler manifolds [3].

The notion of slant submanifolds in the setting of almost product manifolds was introduced by B. Sakin [14]. Subsequently, the first two authors examined

<sup>&</sup>lt;sup>1</sup> Prof., Amasya University, Orcid: 0000-0001-9093-1607

<sup>&</sup>lt;sup>2</sup> Assoc.Prof., Amasya University, Orcid: 0000-0002-4618-8243

curves as examples of slant submanifolds [2] and initiated the investigation of slant submanifolds within almost para-complex manifolds [1]. The aim of this paper is to extend this line of research by providing a definition of pseudo-slant submanifolds in the context of Kähler Norden manifolds.

The structure of the paper is organized as follows: the preliminary section reviews the fundamental concepts and background related to Kähler Norden manifolds and their submanifolds. Subsequently, pseudo-slant submanifolds within the context of a Kähler Norden manifold are formally defined and their key properties are characterized.

# 2.Preliminers

Let  $(\overline{M}, J)$  be an almost complex manifold of dimension dim $(\overline{M})$ =2n. A metric g on  $\overline{M}$  is called a Norden metric if the almost complex structure J acts as an anti-isometry on the tangent bundle, that is,

$$I^2 = -I$$
 and  $g(IX, IY) = -g(X, Y)$  (2.1)

for all vector fields X, Y on  $\overline{M}$ . Such a manifold is referred to as an almost complex manifold with Norden metric (or Norden manifold) and is also known in the literature as an almost complex manifold with B-metric [3, 8, 9, 11]. It is said to be Kähler-Norden or anti-Kähler if, in addition,  $\overline{V}J = 0$ . From (2.1) it is deduced.

$$g(JX,Y) = g(X,JY)$$
 [12]. (2.2)

Let M be a submanifold of  $(\overline{M}, J, g)$ . Where g induced metric on M. Furthermore, let  $\overline{V}$  and  $\overline{V}^{\perp}$  be the induced connections on TM and  $T^{\perp}M$  of M, respectively. The Gauss and Weingarten formulas for this setting are expressed as follows:

$$\tilde{V}_X Y = V_X Y + \sigma(X, Y) \tag{2.3}$$

and

$$\tilde{\nabla}_X V = -A_V X + {\nabla}_X^{\perp} V, \tag{2.4}$$

for all  $X, Y \in \Gamma(TM), V \in \Gamma(T^{\perp}M)$ .

The second fundamental form  $\sigma$  and the shape operator  $A_V$  are connected by the following relationship.

$$g(A_V X, Y) = g(V, \sigma(X, Y))$$
(2.5)

for all  $X, Y \in \Gamma(TM)$ ,  $V \in \Gamma(T^{\perp}M)$ . The mean curvature vector H of M is given by

$$H = \frac{1}{2m} \sum_{i=1}^{2m} \sigma(e_i, e_i)$$
 (2.6)

Here  $\dim(M) = 2m$ ,  $sp\{e_1, e_2, \dots, e_{2m}\}$  is a local orthonormal frame of M.

let M be a submanifold of (M, J, g). The submnifold M is said to be totally umbilical if the second fundamental form  $\sigma$  satisfies

$$\sigma(X,Y) = g(X,Y)H,\tag{2.7}$$

for all vector fields X, Y tangent to M, here H is the mean curvature vector. A submnifold M is said to be totally geodesic if the second fundamental form  $\sigma = 0$ , and the manifold M is said to be minimal if the mean curvature vector H = 0.

let M be a submanifold of (M, J, g). Then for any  $X \in \Gamma(TM)$ , we get

$$JX = TX + NX, (2.8)$$

In this context, TX represents *the* tangent part, while NX denotes the normal part of  $\varphi X$ .

Similary for  $V \in \Gamma(T^{\perp}M)$ , we get

$$JV = tV + nV, (2.9)$$

In this context, tV represents the tangent part, while nV denotes the normal part of  $\varphi V$ .

Let M be a submanifold of Kähler-Norden  $(\overline{M},J,g)$  . Then for any  $X \in \Gamma(TM)$ , we get

$$J^{2}X = JTX + JNX = T^{2}X + NTX + tNX + nNX = -X$$

here

$$T^2X + tNX = -X$$

and

$$NTX + nNX = 0.$$

On the other hand, let M be a submanifold of Kähler-Norden  $(\overline{M},J,g)$ . Then for any  $V\in \Gamma(T^\perp M)$ , we get

$$J^{2}V = JtV + JnV = TtV + NtV + tnV + n^{2}V = -V$$

SO

$$TtV + tnV = 0$$

and

 $NtV + n^2V = -V.$ 

**Proposition 2.1** let M be a submanifold of Kähler-Norden manifold  $(\overline{M}, J, g)$ . Then we have

$$g(TX,Y) = g(X,TY), (2.10)$$

$$g(nW, V) = g (2.11)$$

$$g(NX,V) = g(X,tV) \tag{2.12}$$

for any  $X, Y \in \Gamma(TM)$  and for any  $W, V \in \Gamma(T^{\perp}M)$ .

From (2.1), by using (2.8) and (2.9), we obtain

$$g(JX,JY) = g(TX + NX,TY + NY) = g(TX,TY) + g(NX,NY) = -g(X,Y)$$

Thus,

$$g(TX, TY) = -g(X, Y), \ g(NX, NY) = 0,$$
 (2.13)

for any  $X, Y \in \Gamma(TM)$ .

$$g(JV,JW) = g(tV + nV,tW + nW) = g(tV,tW) + g(nV,nW) = -g(V,W)$$

Thus,

$$g(nV, nW) = -g(V, W), g(tV, tW) = 0$$
 (2.14)

for any W,  $V \in \Gamma(T^{\perp}M)$ .

Therefore, (T, g) and (n, g) forms a Kähler-Norden structure on M.

where the covariant derivatives of the tensor fields T, N, t and n are defined as follows:

$$(\nabla_X T)Y = \nabla_X TY - T\nabla_X Y, \tag{2.15}$$

$$(\nabla_X N)Y = \nabla_X^{\perp} NY - N\nabla_X Y, \tag{2.16}$$

$$(\nabla_X t)V = \nabla_X tV - t\nabla_Y^{\perp} V \tag{2.17}$$

and

$$(\nabla_X n)V = \nabla_X^{\perp} nV - n\nabla_X^{\perp} V \tag{2.18}$$

for any  $X, Y \in \Gamma(TM)$ , for any  $W, V \in \Gamma(T^{\perp}M)$ .

let M be a submanifold of Kähler-Norden manifold  $(\overline{M}, J, g)$ . Through direct calculations, the following formulas are obtained:

$$(\nabla_X T)Y = A_{NY}X + t\sigma(X, Y) \tag{2.19}$$

and

$$(\nabla_X N)Y = n\sigma(X, Y) - \sigma(X, TY). \tag{2.20}$$

Similary, for any  $V \in \Gamma(T^{\perp}M)$ , we obtain

$$(\nabla_X t)V = A_{nV}X - TA_VX \tag{2.21}$$

and

$$(\nabla_X n)V = -\sigma(tV, X) - NA_V X. \tag{2.22}$$

Corollary 2.2 let M be a submanifold of Kähler-Norden manifold  $(\overline{M},J,g)$ . If M iare  $\phi$  – invariant and J –anti– invariant submanifold , the following properties are satisfied: ,

If M is J- invariant	If M is J-anti-invariant
Submanifold	submanifold
N = 0	T=0,
$(\nabla_X T)Y = 0,$	$(\nabla_X N)Y = -n\sigma(X,Y),$
$(\nabla_X n)V = 0$	$(\nabla_X t)V = A_{nV}X,$
$n\sigma(X,Y) = \sigma(X,TY)$	$A_{NY}X = -t\sigma(X,Y)$
$A_{nV}X = TA_{V}X$	$A_{NY}Z = -A_{NZ}Y$

for any  $X, Y, Z \in \Gamma(TM)$ , for any  $V \in \Gamma(T^{\perp}M)$ .

# 3. Slant Submanifolds of Kähler-Norden Manifolds

Some characterizations of slant submanifolds in a Kähler-Norden manifold have been provided.

**Definition 3.1.** A submanifold M is called slant if the angle  $\theta(x)$  between JX and the tangent space  $T_xM$  is constant, independent of the choice of the point  $x \in M$  and the tangent vector  $X \in T_xM$ . In this context, invariant and anti-invariant submanifolds appear as particular cases of slant submanifolds with slant angle  $(\theta = 0)$  and  $(\theta = \frac{\pi}{2})$ , respectively. A slant submanifold is referred to as a proper slant submanifold when it is neither invariant nor anti-invariant [18].

Let M be a slant submanifold of an anti-Hermitian manifold  $\overline{M}$ . For such a submanifold, we have

$$JT_{x}M\subseteq T_{x}^{\perp}M, \quad \forall x\in M$$

where J denotes the structure tensor of  $\overline{M}$ . Consequently, the normal space can be decomposed as

$$T_x^{\perp}M = JT_xM) \oplus \mu$$
,

where  $\mu$  is the orthogonal complementary subbundle of *JTM* in the normal bundle  $T^{\perp}M$ 

**Theorem 3.2.** Let M be a submanifold of a Kähler-Norden manifold  $\overline{M}$ . M is considered a slant submanifold if and only if there exists a constant  $\lambda \in [-1,0]$  such that:

$$T^2 = \lambda I \tag{3.1}$$

and

$$J^2 = \frac{1}{\lambda} T^2 \tag{3.2}$$

where T denotes the tangential component of the almost complex structure and  $\lambda = -cos^2\theta$ 

with  $\theta$  being the slant angel of M [18].

**Lemma 3.3.** Let (M, g) be a slant submanifold of a Kähler-Norden manifold  $(\overline{M}, J, g)$ . Then, we have

$$g(TX, TY) = -\cos^2\theta g(X, Y) \tag{3.3}$$

and

$$g(NX, NY) = -\sin^2\theta g(X, Y). \tag{3.4}$$

for all  $X, Y \in \Gamma(TM)$ .

Proof. From (2.10) and (3.1), we can conclude that

$$g(TX,TY) = g(X,T^2Y) = \lambda g(X,Y) = -\cos^2\theta g(X,Y)$$

The equations in (2.1) and (2.8) result in

$$g(NX, NY) = -g(X, Y) - g(TX, TY)$$
$$= -g(X, Y) + \cos^2\theta g(X, Y)$$

$$= -\sin^2\theta g(X,Y) [18].$$

# 4.Pseudo-Slant Submanifolds of Kähler-Norden Manifolds

Some characterizations of pseudo- slant submanifolds in a Kähler manifold have been provided

**Definition 4.1.** Let M be a submanifold of a Norden manifold  $(\overline{M}, J, g)$ . M is pseudo-slant submanifold if there exist two orthogonal distributions  $D_{\theta}$  and  $D^{\perp}$ , exist on M such that

(1) The tangent bundle TM has an orthogonal direct sum decomposition expressed as

$$TM = D^{\perp} \oplus D_{\Theta}$$
,

- (2)  $D^{\perp}$  is anti-invariant, which means that  $JD^{\perp} \subset T^{\perp}M$ ,
- (3)  $D_{\theta}$  is a slant,  $\theta \neq \frac{\pi}{2}$ , implying that the angle between  $D_{\theta}$  and  $J(D_{\theta})$  remains constant [19].

**Remark4.2.** Let us assume that M is a pseudo slant submanifold of a Kähler-Norden manifold  $(\overline{M}, J, g)$ . Let  $p = \dim(D^{\perp})$  and  $q = \dim(D_{\theta})$  we can distinguish the following six cases:

- 1. If q = 0, M is anti-invariant submanifold.
- 2. If p = 0 and  $\theta = 0$ , then M is invariant submanifold.
- 3. If p = 0 and  $\theta \in \left(0, \frac{\pi}{2}\right)$ , then M is classified as proper slant submanifold.
- 4. If  $\theta = \frac{\pi}{2}$ , M is anti-invariant submanifold
- 5. If  $p \neq 0$  and  $q\neq 0$  with  $\theta = 0$ , then M is a semi-invariant.
- 6. If  $p \neq 0$  and  $q\neq 0$  with  $\theta \in \left(0, \frac{\pi}{2}\right)$ , then M is considered pseudo-slant submanifold.

Let  $\mu$ , represent the orthogonal complement of JTM in  $T^{\perp}M$ . In this case,  $T^{\perp}M$  can be expressed as the following decomposition:

$$T^{\perp}M = JTM \oplus \mu = ND^{\perp} \oplus ND_{\theta} \oplus \mu, \ ND_{\theta} \perp ND^{\perp}$$
 [19].

**Definition 4.3.** Let (M, g) be a submanifold of a a pseudo-slant submanifold Kähler-Norden manifold  $(\overline{M}, J, g)$ . Denote by  $\sigma$  the second fundamental form of M. The submanifold M is called  $D_{\theta}$ -geodesic if

$$\sigma(X,Y)=0$$
, for any  $X,Y\in\Gamma(D_{\theta})$ , and  $D^{\perp}$ -geodesic if 
$$\sigma(Z,U)=0$$
, for any  $Z,U\in\Gamma(D^{\perp})$ ,

Furthermore, if the mixed component of the second fundamental form vanishes, that is,

$$\sigma(X, U) = 0$$
, for any  $X \in \Gamma(D_{\theta})$  and  $U \in \Gamma(D^{\perp})$ ,

then the submanifold M is referred to as a mixed geodesic submanifold.

**Theorem 4.4.** Let (M, g) be a pseudo-slant submanifold Kähler-Norden manifold  $(\overline{M}, J, g)$ . A normal vector field n is parallel with respect to the normal connection, i.e  $(\nabla n = 0)$ . if and only if the shape operator A satisfies

$$A_U t V + A_V t U \in \Gamma(T^{\perp}M)$$
, for any  $V, U \in \Gamma(T^{\perp}M)$ .

In particular, if the tangential component vanishes, then

$$A_UtV + A_VtU = 0.$$

**Proof.** Suppose that the normal vector field n is parallel, i.e.  $\nabla n = 0$ . From relations (2.12) and (2.22), we obtain:

$$0 = g(\sigma(X, tV) + NA_V X, U)$$

$$= g(\sigma(X, tV), U) + g(A_V X, tU)$$

Using the relation between the second fundamental form  $\sigma$  and the shape operator A, we obtain

$$0 = g(A_U tV, X) + g(A_V tU, X) = g(A_U tV + A_V tU, X)$$

for any  $U, V \in \Gamma(T^{\perp}M)$  and for any  $X \in \Gamma(TM)$ .

Hence, either  $A_U tV + A_V tU = 0$  (if it lies in the tangent bundle) or  $A_U tV + A_V tU \in \Gamma(T^{\perp}M)$  (if it lies in the normal bundle).

Conversely, if the condition  $A_UtV + A_VtU \in \Gamma(T^{\perp}M)$  holds for any  $U, V \in \Gamma(T^{\perp}M)$ , then the same computation as above shows that

$$g(\sigma(X,tV),U)+g(A_VX,tU)=0$$

which directly implies that  $\nabla n = 0$ . Thus, the claim follows

**Theorem 4.5.** Let (M, g) be a pseudo-slant submanifold Kähler-Norden manifold  $(\overline{M}, I, g)$ . In this case,  $D^{\perp}$  is integrable if and only if

$$(\nabla_X T)Y = (\nabla_Y T)X$$
, for all  $X, Y \in \Gamma(D^{\perp})$ ,

where T denotes the tangential component of the almost complexs structure J on M.

**Proof.** Let  $X, Y \in \Gamma(D^{\perp})$ . From relation (2.19), we obtain

$$(\nabla_X T)Y = A_{NY}X + t\sigma(X, Y)$$

Replacing *X* by *Y* in the above equation, we have

$$(\nabla_Y T)X = A_{NX}Y + t\sigma(Y, X)$$

where *A* is the shape operator and  $\sigma$  is the second fundamental form of *M* in  $\overline{M}$ 

On the other hand, The distribution  $D^{\perp}$  is integrable if and only if the Lie bracket [X,Y] lies in  $\Gamma(D^{\perp})$ . This condition is equivalent to the symmetry of the covariant derivative of T on  $D^{\perp}$ . i.e.,

$$(\nabla_{\mathbf{X}} \mathbf{T}) \mathbf{Y} = (\nabla_{\mathbf{Y}} \mathbf{T}) \mathbf{X}$$
, for all  $\mathbf{X}, \mathbf{Y} \in \Gamma(\mathbf{D}^{\perp})$ ,

Hence, the integrability of  $D^{\perp}$  is exactly characterized by the condition above.

Remark 4.6. The condition

$$(\nabla_X T)Y = (\nabla_Y T)X$$
, for all  $X, Y \in \Gamma(D^{\perp})$ ,

provides a complete characterization of the integrability of the anti-invariant distribution  $D^{\perp}$ . Geometrically, this means that the action of the tangential part T of the almost complex structure J behaves symmetrically on the distribution  $D^{\perp}$  equivalently, the vanishing of the skew-symmetric component of  $\nabla T$  on  $D^{\perp}$  ensures that the Lie bracket of any two vector fields in  $D^{\perp}$  remains in  $\Gamma(D^{\perp})$ .

This condition is analogous to the well-known Frobenius integrability criterion, and it coincides with similar results obtained for invariant and slant distributions in the context of almost Hermitian and Norden geometry.

**Theorem 4.7.** Let (M, g) be a pseudo-slant submanifold of a Kähler-Norden manifold  $(\overline{M}, J, g)$ . If the normal bundle N is parallel, then, M can be classified as either a mixed geodesic submanifold, an anti-invariant submanifold of  $\overline{M}$ .

**Proof**. Assume that the normal bundle N is parallel if and only if t is parallel, If t is parallel, then  $\nabla t = 0$ . For all  $X \in \Gamma(D_{\theta}), Z \in \Gamma(D^{\perp}), V \in \Gamma(T^{\perp}M)$ . We can conclude this from (2.5), (2.10), (2.11) and (2.21).

$$0 = A_{nV}X - TA_{V}X$$

$$= g(A_{nV}X - TA_{V}X, Z)$$

$$= g(\sigma(X, Z), nV) - g(TA_{V}X, Z)$$

$$= g(\sigma(X, Z), nV) - g(\sigma(X, TZ), V)$$

$$= g(n\sigma(X, Z), V) - g(\sigma(X, TZ), V),$$

Thus, we have

$$n\sigma(X,Z) = \sigma(X,TZ)$$

for  $Z \in \Gamma(D^{\perp})$ , we have TZ = 0. Therefore, it follows that:

$$n\sigma(X,Z)=0$$

By replacing X with TX in the above equation, we obtain

$$n\sigma(TX,Z)=0.$$

By replacing X with TX in the above equation and using (3.1), we have

$$n\sigma(T^2X, Z) = n\sigma(\lambda X, Z) = n\lambda\sigma(X, Z) = -\cos^2\theta n\sigma = 0.$$

Therefore, one of the following holds

- 1)  $\sigma = 0$ , in which case M is mixed geodesic submanifold,
- 2)  $\theta = \frac{\pi}{2}(\lambda = -\cos^2\theta = 0)$  corresponding to an anti invariant submanifold,

Hence, the classification of M follows from the parallelism of the normal bundle.

**Theorem 4.8**. Let (M, g) be a totally umbilical pseudo-slant submanifold of a Kähler-Norden manifold  $(\overline{M}, J, g)$ . If the normal bundle N is parallel, then, M can be classified as either a minimal submanifold, an anti-invariant submanifold, or an invariant submanifold of  $\overline{M}$ .

**Proof.** Let M be a totally umbilical pseudo-slant submanifold of a Kähler-Norden manifold  $(\overline{M}, J, g)$  with parallel normal bundle N. Parallel of N implies that the tangential part t of J is parallel  $(\nabla t = 0)$ , so the tangent distribution is invariant under J.

Let  $X \in \Gamma(D_{\theta}), Y \in D^{\perp}, W \in \Gamma(T^{\perp}M)$ . We can conclude this from (2.5), (2.10), (2.11) and (2.21).

$$A_{nW}X - TA_WX = 0,$$

Taking the inner product with *Y*, it follows that

$$g(n\sigma(X,Y),W)-g(\sigma(X,TY),W)=0.$$

Since  $Y \in \Gamma(D^{\perp})$  implies TY = 0, we obtain

$$n\sigma(X,Y)=0.$$

By replacing X with TX in the above eq. we get

$$n\sigma(TX,Y)=0.$$

Because M is totally umbilical submanifold, from (2.7) we have

$$ng(TX,Y)H = 0.$$

where H is the mean curvature vector. Then from (3.1)

$$ng(T^2X,Y)H = n\lambda g(X,Y)H = 0$$

Hence, one of the following cases occurs:

- 1) H = 0, in which case M is minimal submanifold.
- 2)  $\theta = \frac{\pi}{2}(\lambda = -\cos^2\theta = 0)$  corresponding to an anti invariant submanifold.

Therefore, the classification of *M* follows.

**Theorem 4.9.** Let (M, g) be a pseudo-slant submanifold of a Kähler-Norden manifold  $(\overline{M}, I, g)$ . Asume that

$$g(\sigma(X, Y), JU) = 0$$
 for any  $X, Y \in \Gamma(D_{\theta})$  and  $U \in \Gamma(D^{\perp})$ .

Than the distribution  $D_{\theta}$  —integrable, and the leaves of  $D_{\theta}$  are geodesic in M.

**Proof.** Let (M, g) be a pseudo-slant submanifold of a Kähler-Norden manifold  $(\overline{M}, J, g)$ . For all  $X, Y \in \Gamma(D_{\theta})$  and  $U \in \Gamma(D^{\perp})$ , by the Gauss formula we have

$$\tilde{\nabla}_X Y = \nabla_X Y + \sigma(X, Y).$$

Taking the inner product with JU

$$g(\sigma(X,Y),JU) = g(\tilde{\nabla}_X Y - \nabla_X Y,JU).$$

Since  $\tilde{\nabla}I = 0$ , we get

$$g(\sigma(X,Y),IU) = g(I\tilde{V}_XY,U) = g(\tilde{V}_XIY,U).$$

 $U \in \Gamma(D^{\perp})$  and  $JD^{\perp} \subset T^{\perp}M$ , it follows that

$$g(\sigma(X,Y),JU) = g(\nabla_X JY + \sigma(X,JY),U) = g(\nabla_X JY,U) = g(\nabla_X Y,NU).$$

Thus the condition  $g(\sigma(X,Y),JU)=0$  implies  $[X,Y] \in \Gamma(D_{\theta})$ , so the leaves of  $D_{\theta}$  are geodesic in M.

**Theorem 4.10.** Let M be a pseudo-slant submanifold in a Kähler-Norden manifold  $(\widetilde{M}, g, J)$ . Then the anti-invariant distribution  $D^{\perp}$  is integrable if and only if

$$A_{NZ}U = 0$$
, for all  $Z, U \in \Gamma(D^{\perp})$ .

where *A* denotes the shape operator.

**Proof.** Since *M* is a pseudo-slant submanifold, for all  $Z, U \in \Gamma(D^{\perp})$ , we have TZ = TU = 0, by using (2.15)

$$T([Z, U]) = 0$$
 if and only if  $A_{NZ}U = A_{NU}Z$ .

On the other hand from the Gauss and Weingarten formulas, for all  $X \in \Gamma(TM)$ .

$$g((\nabla_X T)Z, U) = g(A_{NZ}X, U) + g(t\sigma(X, Z), U) = 0, \tag{4.1}$$

where  $t\sigma$  denotes the tangential component of the second fundamental form.

If (4.1) vanishes, then by the symmetry of the shape operator we obtain

$$g(A_{NZ}U, X) = 0$$
, for all  $X \in \Gamma(TM)$ ,

which implies

$$A_{NZ}U=0.$$

Conversely, suppose  $A_{NZ}U=0$ , for all  $Z,U\in\Gamma(D^{\perp})$  then for any  $X\in\Gamma(TM)$ ,

$$g(t\sigma(X,Z),U)=g(\sigma(X,Z),NU)=g(A_{NU}Z,X)=0$$

Moreover using (2.19) and the relation (2.10) we have

$$g((\nabla_Z T)U, X) = -g(\nabla_Z U, TX) = 0$$
, for any  $X \in \Gamma(D_\theta)$ .

Hence

$$\nabla_z U \in \Gamma(D^\perp)$$
,

which yields

$$[Z,U] \in \Gamma(D^{\perp}),$$

Thus, the distribution D<sup>1</sup> is integrable. This completes the proof

**Theorem 4.11.** Let M be a pseudo-slant submanifold in a Kähler-Norden manifold  $(\widetilde{M}, g, J)$ . If the normal component N is parallel on the slant distribution  $D_{\theta}$ , then either

- 1) M is a  $D_{\theta}$  -geodesic submanifold, or
- 2) The second fundamental form  $\sigma(X,Y)$  is an eigenvector of  $n^2$  with eigenvalues  $-\cos^2\theta$ .

Ispat: Let M be a pseudo-slant submanifold of  $(\widetilde{M}, g, J)$ . For any  $X \in D_{\theta}$ , we decompose

$$JX = TX + NX$$

where TX is tangential and NX is normal. By the definition of pseudo-slant submanifold, the tangential part satisfies

$$T^2X = \lambda X$$
,  $\lambda = -\cos^2\theta$ .

Now assume that the normal component N is parallel on  $D_{\theta}$ . Then, for all  $X, Y \in D_{\theta}$  we have

$$\nabla_X^{\perp} NY = N \nabla_X Y. \tag{4.2}$$

On the other hand, by the Weingarten formula

$$\tilde{\nabla}_X NY = -A_{NY}X + {\nabla_X^{\perp}}NY.$$

Using (4.2), we get

$$\tilde{\nabla}_X NY = -A_{NY}X + N\nabla_X Y$$

Projecting onto the normal bundle yields

$$\sigma(X,Y)=N\nabla_XY.$$

if  $\sigma(X,Y)$ , then from (3) show that  $\nabla_X Y \in TM$  for all  $X,Y \in \Gamma(D_\theta)$  Thus the leaves of the distribution  $D_\theta$  are totally geodesic in M, and thus, M is  $D_{\theta}$ -geodesic submanifold.

If  $\sigma(X,Y) \neq 0$ , then by the pseudo-slant condition and (3,1) we deduce that  $n^2\sigma(X,Y)=\lambda \sigma(X,Y)$ ,  $\lambda=-cos^2\theta$ .

Thus,  $\sigma(X,Y)$  is an eigenvector of  $n^2$  with the required eigenvalues. This completes the proof.

**Conclusion**: In this study, we investigate pseudo-slant submanifolds within the framework of a Kähler–Norden manifold, focusing on their distinctive geometric properties. These submanifolds exhibit remarkable characteristics, particularly in the interaction between their tangent spaces and the structure of the ambient manifold.

#### References

- [1] P. Alegre and A. Carriazo. Slant Submanifolds of Para-Hermitian Manifolds. Mediterr. J. Math. (2017) 14, 1-14.
- [2] P. Alegre and A. Carriazo. Curves as slant submanifolds of an almost product Riemannian manifold. Turk. J. Math. (2024) 48, 701-712.
- [3] A. Borowiec and M. Francaviglia and I. Volvovich. Anti-K"ahlerian manifolds. Differential Geometry and its Applications, 12 (2000), 281–289.
- [4] B.-Y. Chen. Slant inmersions. Bull. Austral. Math. Soc. 41 (1990), 135-147.
- [5] B.-Y. Chen and O. Garay. Classification of quasi-minimal surfaces with parallel mean curvature vector in pseudo-Euclidean 4-space E42. Results Math. 55 (2009), 23-38.
- [6] B.-Y. Chen and I. Mihai. Classification of quasi-minimal slant surfaces in Lorentzian complex space forms. Acta Math. Hungar. 122 (2009), 307-328.
- [7] F. Etayo and R. Santamar'ıa. ( $J^2 = \mp I$ )-metric manifolds. Publ. Math. Debrecen. 57/3-4 (2000), 435-444.
- [8] G.T. Ganchev and A.V. Borisov. Note on the almost complex manifolds with a Norden metric. C.R.Acad. Bulgarie. 39 (1986), 31-34.
- [9] G. Ganchev and K. Gribachev and V. Mihova. B-connections and their conformal invariants on conformally Kähler manifolds with B-metric. Publ. de L'Inst. Math. 42 (56) (1985), 107–121.
- [10] A.P. Norden. On a class of four-dimensional A-spaces. Izv. Vys s. U cebn. Zava ested. Matematika. 4 (1960),145-157.
- [11] R. Castro, L.M. Hervella and E.G. Rio. Some examples of almost complex manifolds with Norden metric. Riv. Mat. Univ. Parma (4). 15 (1989), 133-141.
- [12] B.K. Gupta and B.B: Chaturvedi. On a slant submanifold of a Kähler-Norden manifold. J. Tensor Soc. 16 (2022), 71-80.
- [13] V. Ayhan and S.P. Perktas. Slant submanifolds of almost poly-Norden Riemannian manifolds. Int. J. Maps Math. 6(2023), no. 1, 22-36.
- [14] B. Sahin. Slant submanifolds of an almost product Riemannian manifold. J. Korean Math. Soc. 43 (2006), No. 4, 717-732.
- [15] K. Olszak, On the Bochner conformal curvature of Kaehler-Norden manifolds, Central European Journal of Mathematics, CEJM 3, (2005) ,2, 309-317.

- [16] E. Karataş, S. Zeren, and M. Altın, Geometric Analysis of Riemannian Submersions Curvature Tensors and Total Umbilic Fibers," Konuralp Journal of Mathematics, vol. 12 (2024), 2, 158 171,
- [17] S. Dirik, and R. Sari, Contact Pseudo-Slant Submanifolds of Lorentzian Para Kenmotsu Manifold. Journal of Engineering Research and Applied Science, *12*(2023), 2, 2301-2306.
- [18] J. L. Cabrerizo, A. Carriazo, L. M, Fernandez, M. Fernandez, Slant Submanifolds in Sasakian manifolds, Glasgow Math, J. 42(2000), 125-138
- [19] V. A. Khan, M. A. Khan, Pseudu-slant submanifolds of a sasakian manifold, India J. Pure Appl., 38(2007),31-42